SNYMAN, JOHANNA ELIZABETH WILHELMINA

MASS EXTINCTION ON THE PERMIAN - TRIASSIC BOUNDARY: GEOLOGICAL EVIDENCE FROM THE KAROO SUPERGROUP

MSc **UP** **1995**

Mass extinction on the Permian - Triassic boundary: geological evidence from the Karoo Supergroup

by

Johanna Elizabeth Wilhelmina Snyman

Thesis submitted in partial fulfilment of the requirements
for the degree of
MASTER OF SCIENCE
in the Faculty of Science,
University of Pretoria
Pretoria

September 1995

Aan Derik en Danielle

A fire-mist and a planet
A crystal and a cell,
A jelly-fish and a saurian,
And caves where the cave-men dwell;
Then a sense of law and beauty,
And a face turned from the clod -
Some call it Evolution,
And others call it God.

W.H. Carruth : Each in his own tongue.

ABSTRACT

This work comprises a study of the sedimentary rocks and petrified wood found across the Permian-Triassic boundary. The study area is situated in the northeastern Orange Free State, near the towns Harrismith and Senekal, South Africa.
The aim of the study is to determine a possible reason for the mass extinction at the Permian-Triassic boundary by investigating the relevant lithostratigraphic units.

The lithostratigraphy across the Permian-Triassic boundary consists of the Beaufort Group, which forms part of the Karoo Supergroup. The Permian-Triassic boundary occurs at the contact between the Harrismith Member (at the top) and the Schoondraai Member (at the base) of the Normandien Formation. Two reptile biozones, which form part of the biostratigraphy of the Beaufort Group, can be related to the Harrismith and Schoondraai Members. The Schoondraai Member is equivalent to the *Dicynodon - Theriognathus* Assemblage Zone and the Harrismith Member to the *Lystrosaurus - Procolophon* Assemblage Zone.

Six lithofacies are recognised from the Schoondraai Member and five lithofacies from the Harrismith Member. Mudstones provide evidence of suspension settling of fine material in a low energy system. This fine material was probably deposited on a floodplain. Fine sandstone interbedded with the mudrock points to a fluctuation in energy levels, most probably due to pronounced seasonality. Moderate to well sorted sandstones were more effectively transported and it is proposed that they were fluvial channel deposits, which tend to be upward-fining. A trend of declining energy levels upwards in the succession can be observed from the Schoondraai Member to the Harrismith Member. The palaeoenvironment appears to have become more arid with time.
Petrographic studies of the sandstones show a red pigment (hematite) that covers the sand grains. This can indicate a warm climate, for brown limonite alters to red hematite relatively rapidly in warm and dry conditions. No shattered mineral grains, shock lamellae in quartz nor small shatter cones on the clasts, which could be indicative of impact metamorphism, could be observed. The source area of the sandstones was

probably granitic. The sandstones are classified as feldspathic arenites.

The mineralogy of the clay fraction shows the presence of quartz, plagioclase, smectite, illite and chlorite. No glass shards, cristobalite and/or laumontite, which would indicate a probable volcanic source of the clay minerals, and no potassium feldspar, were observed. The sediments were therefore not related to volcanic ash layers, but were rather detrital, terrestrial sediments. The diagenetic environment was most likely alkaline.

The geochemistry of the mudrocks shows a slight enrichment of SiO_2, Al_2O_3, TiO_2, CaO, K_2O and Na_2O, and a slight depletion of MgO and Fe_2O_3, across the Permian-Triassic boundary. The TiO_2/Al_2O_3 ratios, as well as the CIA-values of the mudrocks point to ordinary or "typical shales" rather than altered volcanic ash layers. Cr/Zr ratios suggest a granitic source area with few or no contributions from ultramafic rocks. Palaeosalinity indicators such as the Rb/K ratio may indicate a brackish water to marine transition, but due to a limited number of samples and no evidence of tidal activity from the sedimentological data, care should be taken when interpreting these results. Analyses for platinum-group elements indicate values below the respective detection limits.

The petrified wood was studied macroscopically as well as microscopically. The woods all belong to the class Gymnospermae. No angiosperm woods were found. The trunks were found in fine-grained sandstone or *in situ* in weathered soil. Only some *in situ* petrified logs have roots embedded in a clay layer. The presence of prominent growth rings indicates a seasonal control. Analysis of these growth rings shows that the trees grew under limited to favourable climatic conditions. The width of the rings from both assemblage zones indicates that the growth rates of the trees were fast.

The petrifying mineral in all the specimens is silica (quartz), but high concentrations of zinc and iron also occur. The concentrations of zinc and iron increases upwards in the succession across the Permian-Triassic boundary. This iron enrichment can probably be linked to oxidation of the iron due to a palaeoenvironment that became more arid.

The results from this study point to a gradual change of climatic conditions across the Permian-Triassic boundary, rather than an abrupt change due to volcanic activity or an asteroid impact.

UITTREKSEL

Die studie behels 'n ondersoek van die sedimentêre gesteentes en versteende hout wat gevind word in die omgewing van die Perm-Trias grens. Die studiegebied is geleë in die noordoos Vrystaat naby die dorpe Harrismith en Senekal, Suid-Afrika.
Die doel van die studie is om 'n moontlike verklaring vir die massa-uitsterwing by die Perm-Trias grens te verkry deur die betrokke litostratigrafiese eenhede te ondersoek. Die litostratigrafie by die Perm-Trias grens vorm deel van die Beaufort Groep, Karoo Supergroep. Die Perm-Trias grens kom voor op die kontak tussen die boonste Harrismith Lid en die onderste Schoondraai Lid, wat deel uitmaak van die Normandien Formasie. Twee reptielbiosones wat deel uitmaak van die biostratigrafie van die Beaufort Groep kan gekorreleer word met die Harrismith en Schoondraai Lede. Die Schoondraai Lid korreleer met die *Dicynodon - Theriognathus* Versamelsone en die Harrismith Lid met die *Lystrosaurus - Procolophon* Versamelsone.

Ses litofasies is herkenbaar in die Schoondraai Lid en vyf in die Harrismith Lid. Die modderstene dui op suspensie uitsakking van fyn materiaal in 'n lae-energie sisteem. Hierdie fyn materiaal is waarskynlik afgeset op 'n vloedvlakte. Fynkorrelrige sandsteenlagies word ook afgewissel met moddersteenlagies wat dui op 'n fluktuasie in energievlakke, waarskynlik toegeskryf aan 'n seisoenale invloed. Medium tot goed gesorteerde sandstene is doeltreffend vervoer en is waarskynlik fluviale kanaalafsettings wat neig om opwaarts fynwordend te wees. Die afgeleide energievlakke neem opwaarts af in die opeenvolging vanaf die Schoondraai Lid tot en met die Harrismith Lid. Waarskynlik het die omgewing droër geword met verloop van tyd.
Petrografiese studies van die sandstene toon 'n rooi pigment (hematiet) wat die korrels bedek. Dit kan 'n aanduiding wees van 'n warm klimaat, omdat bruin limoniet redelik vinnig verander na rooi hematiet in warm en droë toestande. Geen versplinterde korrels, skoklamelle in kwarts of klein skokkeëls op die klaste, wat as aanduidings van skokmetamorfose beskou kan word, kon opgemerk word nie. Die brongebied van die sandstene was heelwaarskynlik granities. Die sandstene word geklassifiseer as veldspatiese areniete.

Die mineralogie van die klei-fraksie toon die teenwoordigheid van kwarts, plagioklaas, smektiet, illiet en chloriet. Geen glasskerfies, kristobaliet en/of laumontiet, wat 'n aanduiding kan wees dat die kleie 'n vulkaniese bron kan hê, is opgemerk nie. Die sedimente verteenwoordig dus nie vulkaniese aslagies nie, maar eerder detritale, terrestriële sedimente. Die diagenetiese omgewing was heelwaarskynlik alkalies.

Die geochemie van die modderstene toon 'n effense verryking van SiO_2, Al_2O_3, TiO_2, CaO, K_2O and Na_2O, en 'n effense verarming van MgO and Fe_2O_3 oor die Perm-Trias grens. Die TiO_2/Al_2O_3 verhoudings, sowel as die CIA-indeks dui daarop dat die modderstene geklassifiseer kan word as gewone of "tipiese skalies" eerder as verweerde vulkaniese aslagies. Cr/Zr verhoudings dui op 'n granitiese brongebied met min of geen bydrae vanaf ultramafiese gesteentes. Paleosaliniteitsaanwysers soos die Rb/K-verhouding dui op 'n moontlike oorgang van brakwater na 'n mariene omgewing, maar as gevolg van 'n beperkte aantal monsters en geen aanduidings van gety-aktiwiteit in die sedimentologiese data nie, moet hierdie resultate versigtig geïnterpreteer word. Die platinum-groep element analises toon waardes onderkant die betrokke deteksiegrense.

Die versteende hout is makroskopies sowel as mikroskopies bestudeer. Die hout behoort tot die klas Gymnospermae. Geen angiosperm-hout is gevind nie. Die boomstamme is gevind in fynkorrelrige sandsteen of in *in situ* verweerde grond. Slegs 'n paar *in situ* boomstamme met wortels in 'n kleilaag is gevind. Die teenwoordigheid van groeiringe dui op seisoenaliteit. Groeiringanalises toon aan dat die bome in beperkte tot gunstige klimaatstoestande gegroei het. Die wydte van die groeiringe van beide versamelsones dui op 'n vinnige groeitempo van die bome.

Die versteningsmineraal in al die houtmonsters is silika (kwarts), maar hoë konsentrasies van sink en yster kom ook voor. Die konsentrasie van die sink en yster neem toe opwaarts in die opeenvolging oor die Perm-Trias grens. Hierdie ysterverryking kan waarskynlik gekoppel word aan die oksidasie van die yster as gevolg van 'n omgewing wat mettertyd droër geword het.

Die resultate van hierdie studie dui op 'n geleidelike klimaatsverandering oor die Perm-Trias grens, eerder as 'n skielike verandering as gevolg van vulkaniese aktiwiteit of 'n asteroidimpak.

TABLE OF CONTENTS

CHAPTER 4. THE GEOLOGY ASSOCIATED WITH THE PERMIAN-TRIASSIC BOUNDARY: THE NORMANDIEN FORMATION 28

LIST OF FIGURES

LIST OF TABLES

CHAPTER 1. INTRODUCTION

The disappearance and/or reduction in diversity of many life-forms from the fossil record at the Permian-Triassic boundary (± 230 Ma), as well as at the Cretaceous-Tertiary boundary (± 65 Ma), gave rise to the hypothesis of mass extinction. The mass extinction at the Permian-Triassic boundary was even more severe than that at the Cretaceous-Tertiary boundary (Gould, 1977; Raup, 1979; Clark *et al.*, 1986). Over the years many hypotheses have been put forward to account for this mass extinction, but two stand out.

The Asteroid Impact Hypothesis (Alvarez *et al.*, 1980) suggests that the biotic catastrophe resulted from the impact of an asteroid, some 6 to 14 kilometres in diameter, with the earth. This produced a dust cloud that obscured the sun and stopped photosynthesis for several years, so that the extermination of many organisms occurred. This dust, which should be distinguishable by its relatively high concentration of iridium and other platinum group elements, settled and became incorporated into marine and terrestrial sediments. Extinction is regarded to have been essentially geologically instantaneous (Clemens, 1981). Although this hypothesis specifically refers to the extinction at the Cretaceous-Tertiary boundary, it has also been invoked to explain the extinction at the Permian-Triassic boundary (Asaro *et al.*, 1982; Sun *et al.*, 1984; Xu *et al.*, 1985).

The Climatic Change Hypothesis, suggests that the extinction took place due to changes in oceanographic, atmospheric or climatic conditions (Dickins, 1983). The extinction is regarded to have been spread over tens or hundreds of thousands of years, a geologically short, but biologically significant period of time (Clemens, 1981).

Although mass extinction probably cannot be linked to volcanic eruptions on their own, they may have had a significant effect on plant metabolism and therefore also on the fauna which depends on the vegetable matter as a food source. The presence of volcanic ash beds and volcanic fragments in the Karoo Supergroup has been reported by several authors (Martini, 1974; Elliot and Watts, 1975; Ho-Tun, 1979; Keyser, 1983;

Keyser and Zawada, 1988; McLachlan and Jonker, 1990).

The aim of this study is to determine a possible reason for the mass extinction at the Permian-Triassic boundary in a chosen study area of the Karoo Supergroup in South Africa by investigating the relevant lithostratigraphic units with respect to:

* The anatomy (and possibly taxonomy) of the petrified wood embedded in the sandstone and mudrock;
* geochemical characteristics and
* the possible presence of volcanic ash beds.

1.1 FOSSIL WOOD: GENERAL CONSIDERATIONS

Evidence from terrestrial plants is particularly critical because plants form the base of the terrestrial food chain. Massive disruptions of the earth's vegetation by an extraterrestrial impact, for example an asteroid, would have a notable effect on the land fauna (Hickey, 1981). The growth ring patterns in petrified wood may show a sudden disruption possibly due to an asteroid impact, or a gradual change possibly due to climatic changes.

In vascular plants the principal water-conducting tissue is the xylem and the main food-conducting tissue is the phloem. Together these two tissues are called the vascular tissue and they form a continuous vascular system through the branches, stem and root of the plant. A distinction is made between primary vascular tissue which governs length growth, and secondary vascular tissue which governs the increase in thickness. This increase in thickness results from the activity of the vascular cambium by which secondary xylem or wood is formed.

Two distinct systems of cells occur in wood:

(1) The axial (longitudinal or vertical) system consists of cells or files of cells with their long axes parallel to the length of the stem.

(2) The radial (transverse, horizontal or ray) system has cells or files of cells orientated perpendicular to the axis of the stem, parallel to the radii of the circular cross-section.

The tracheary elements are the most specialized cells of the xylem. Their function is to conduct water and its dissolved substances (Table 1). They are elongated and non-living at maturity. They have secondarily thickened lignified walls and a variety of pits. There are two kinds of tracheary cells, namely the tracheids with tapering ends and the vessel members. The latter are not present in the Gymnosperms. In the tracheids, the passage of water from cell to cell occurs mainly through pitpairs in which the pit membranes are highly permeable to aqueous solutions. The secondary walls of tracheids have simple and bordered pits, the arrangement and number of which are highly variable. The bordered pitpairs of conifers are large, particularly in the early wood (Esau, 1977).

TABLE 1. The principal cell types of the secondary xylem (Esau, 1977).

CELL TYPES	PRINCIPAL FUNCTION
AXIAL SYSTEM:	
Tracheary elements:	
Tracheids	Conduction of water
Vessel members	
Fibers:	
Fiber-tracheids	
Libriform fibers	Support; sometimes storage
Parenchyma cells	Storage, healing, origin of structures
RAY SYSTEM:	
Parenchyma cells (Tracheids in some conifers)	Storage and translocation of ergastic substances

Growth increments of trees may be affected by water supply, atmospheric humidity, day length, mineral nutrients, temperature, light and force of gravity. The activity of the vascular cambium in laying down the current season's growth increment, is primarily controlled by growth hormones. These hormones are produced in the young leaves and shoots at the crown of the tree (Larson, 1964). The climate acts directly on the crown of the tree, controlling both the production of carbohydrate as raw material and the formation of growth hormones which govern the thickness and character of the secondary wood laid down (Denne, 1976).

The mechanism that initiates the growth of new leaves is not triggered by the ambient temperature, water availability or the rate of photosynthesis, but by photoperiodism, that is the change in day length. The amount of both early wood and late wood is controlled by the environment to which the crown of the tree is exposed. With the lengthening of the day during spring, the cambium is stimulated for optimal growth and the large cells of the early wood are formed. As the days become shorter during autumn, the stimulation of the cambium decreases and the small, dense cells of the late wood are formed. The early and late wood cells therefore differ in terms of colour change, wall thickness and radial diameter of the tracheids. These differences give rise to clearly visible ring boundaries (See also Fig. 25).

From the record of fossil wood it is clear that at any time in the past a given species of tree would have been adapted to its environment with regard to climate and photoperiod. A change of climate would presumably be slow enough for the species to adapt to the new conditions. If the species did not adapt, it would be ousted by competition. The presence of growth rings in wood shows the response of the tree to the normal climatic periodicity and also photoperiodism (Creber and Chaloner, 1984a).

Growth rings occur in the branches and trunk of the tree and are displayed as a banded structure in cases where growth took place in moderate latitudes, reflecting the seasonal growth. Trees from a tropical environment with a high humidity, show indefinite growth rings or no rings at all (Chaloner and Creber, 1973), whereas trees from a more arid environment show very prominent growth rings.

The growth rings (as seen on a transverse section), represent a sequence of "growth layers". Each growth layer consisting of large and small cells, can be the result of growth in one season, but environmental conditions can trigger the formation of more than one growth layer in one season. Therefore, it is more correct to use the term growth ring than annual ring.

The relative proportions of early and late wood depend on environmental conditions. Intraseasonal or "false" growth rings occur when the growing season is interrupted by late frost, spells of drought or when the trees lose their leaves due to fire or insect activity. Damaged cells in the early wood can be an indicator of late frost. In such traumatic conditions, most conifers develop a band of "traumatic resin canals" which protects the tree against the frost and helps to heal damaged tissue (Chaloner and Creber, 1973).

Fossil wood is fairly abundant in the geological record from the Devonian to Recent. Because wood is so resistant, it is readily fossilized by different methods:
petrification (that is replacement by siliceous, calcareous or pyritic material); coal formation and charcoalification by partial combustion (Creber and Chaloner, 1984a).

For preservation and fossilization, decay of the wood should be prevented. This can take place where fine sediment accumulates rapidly and buries the plant material, as in small bays or aggrading rivers. Burial of the wood by volcanic ash would also enhance the possibility of preservation. Low oxygen levels and high concentrations of toxic humic substances also prevent decay.
Petrification is the most important mechanism of fossilization from the point of view of anatomical study of the material and can be divided into five stages (Scurfield and Segnit, 1984):

* Entry of inorganic matter (most commonly silica) in solution or as a colloid into the wood.
* Penetration of cell walls by the mineralising solution.
* Progressive dissolution of cell walls and concomitant build-up of a mineral framework which maintains the dimensional stability of the original wood.

* Deposition of mineral material in cell cavities and voids created in intercellular regions.
* Final lithification involving loss of water, perhaps polymorphic transformation (eg. of one form of silica to another), pseudomorphic replacement and/or recrystallization.

The source of the silica can be either volcanic ash or geothermal water (Arnold, 1947). In the Karoo rocks the source was probably volcanic ash (Martini, 1974; Elliot and Watts, 1975; Ho-Tun, 1979; Keyser, 1983; Keyser and Zawada, 1988; McLachlan and Jonker, 1990). The weathering of porous, unstable glassy volcanic ash is much faster than the weathering of a massive, crystalline rock. In the former, the silica is available rapidly (Murata, 1940). Meteoric water percolating through the ash bed dissolves the silica and high concentrations of silica occur in solution or as a colloid in the ground water.

As mentioned before, the wood will be silicified if it is buried in volcanic ash or sediments rich in volcanic ash under conditions of minimum decay. The silicification of wood by silica-bearing magmatic water, which migrates upwards through faults and openings, is still uncertain (Murata, 1940).
Cryptocrystalline silica like agate, chalcedony and jasper, as well as opal occur in silicified wood (Arnold, 1947). Only the cryptocrystalline and amorphous silica preserve the tissue in its original form and even small crystals can deform the structure. A positive correlation seems to exist between the crystallinity of the silica in silicified wood and its age; the older the silica, the more crystalline it becomes (Scurfield and Segnit, 1983; Stein, 1983; Dr. D. Bühmann, pers. comm., 1995).

1.2 GEOCHEMICAL CONSIDERATIONS

Dust derived from an extraterrestrial impact and subsequently incorporated into sediments should result in an enrichment in platinum group elements (iridium, osmium, platinum, rhodium, palladium, rutherium) in these sediments. The earth's crust and upper mantle are usually depleted in platinum group and other siderophile elements compared with chondritic meteorites (Alvarez *et al.*, 1980). Typical continental crustal

iridium concentrations are ± 50pg/g (Fremer and Presley, 1984).

Acid volcanic material has a high concentration of Cs, Hf, Ta, Th, U, Pb, Sn, B, Y and Be and a low TiO_2/Al_2O_3 (<0.02) ratio. The TiO_2/Al_2O_3 ratio in typical shales may range from 0.035 to 0.05. The concentrations of Ti, Cr, V, Ni, Co, Cu and Mn in acid volcanic rocks are also low relative to those of basic volcanic material (Spears and Kanaris-Sotiriou, 1979; Clark *et al.*, 1986).

1.3 THE PRESENCE OF VOLCANIC ASH

Bentonite is an altered volcanic ash. The presence of the pure clay mineral smectite and the absence of discrete illite, are typical of bentonite. Discrete illite and mixed-layered smectite/illite represent altered volcanogenic material that has been partially illitized by mild burial diagenesis. Illite and kaolinite can also, of course, be detrital (Rampino, 1982).

The presence of cristobalite (high temperature silica) indicates that the clay minerals were formed by *in situ* weathering of volcanic ash (McLachlan and Jonker, 1990). The formation of laumontite as a product of the diagenetic alteration of fine-grained or glassy volcanic debris is well known. Laumontite-rich sedimentary rocks in the Karoo Supergroup (Fuller, 1971; Elliot and Watts, 1974) could therefore indicate an admixture of volcanic debris, and that volcanic activity must have been of an explosive type (Fuller, 1971).

CHAPTER 2. METHODS OF INVESTIGATION

2.1 FIELD WORK

In order to be able to relate the botanical characteristics of the petrified wood to the Permian-Triassic boundary, only specimens for which the stratigraphic position is known were investigated. For this reason, an area in the northeastern Orange Free State where this boundary is well known from biostratigraphical evidence (Broom, 1906; Watson, 1914; Kitching, 1970; Keyser and Smith, 1978, 1979), was selected. (Figs. 1 and 2).

Apart from the relevant topocadastral sheets (2929 CD Verkykerskop; 2729 DC Mont Pelaan; 2829 AB Groothoek; 2829 BA Santiago; 2829 AD Van Reenen; 2729 CA Rietkuil; 2827 BC Senekal; 2827 AD Rietspruit), aerial photographs at a scale of 1 : 30 000 were also used to locate outcrop areas. At suitable localities in the study area, lithostratigraphic profiles showing the major lithofacies were compiled in order to infer palaeoenvironmental conditions during deposition of the sedimentary rocks.

Fossil wood that was strictly *in situ* was collected from sandstone and mudrock across the Permian-Triassic boundary (Figs. 3a and b). Fossil wood in the Senekal district was collected from the Katberg Formation. The Katberg Formation is considered to be equivalent to the Verkykerskop Formation in the Harrismith area (Groenewald, 1984), and therefore part of the *Lystrosaurus - Procolophon* Assemblage Zone (Hiller and Stavrakis, 1984). No wood was found in the Harrismith Member (Normandien Formation) or the Verkykerskop Formation (*Lystrosaurus Procolophon* Assemblage Zone) in the Harrismith area.
At the same time, the rocks across the boundary were sampled for petrographical, mineralogical and geochemical investigation.

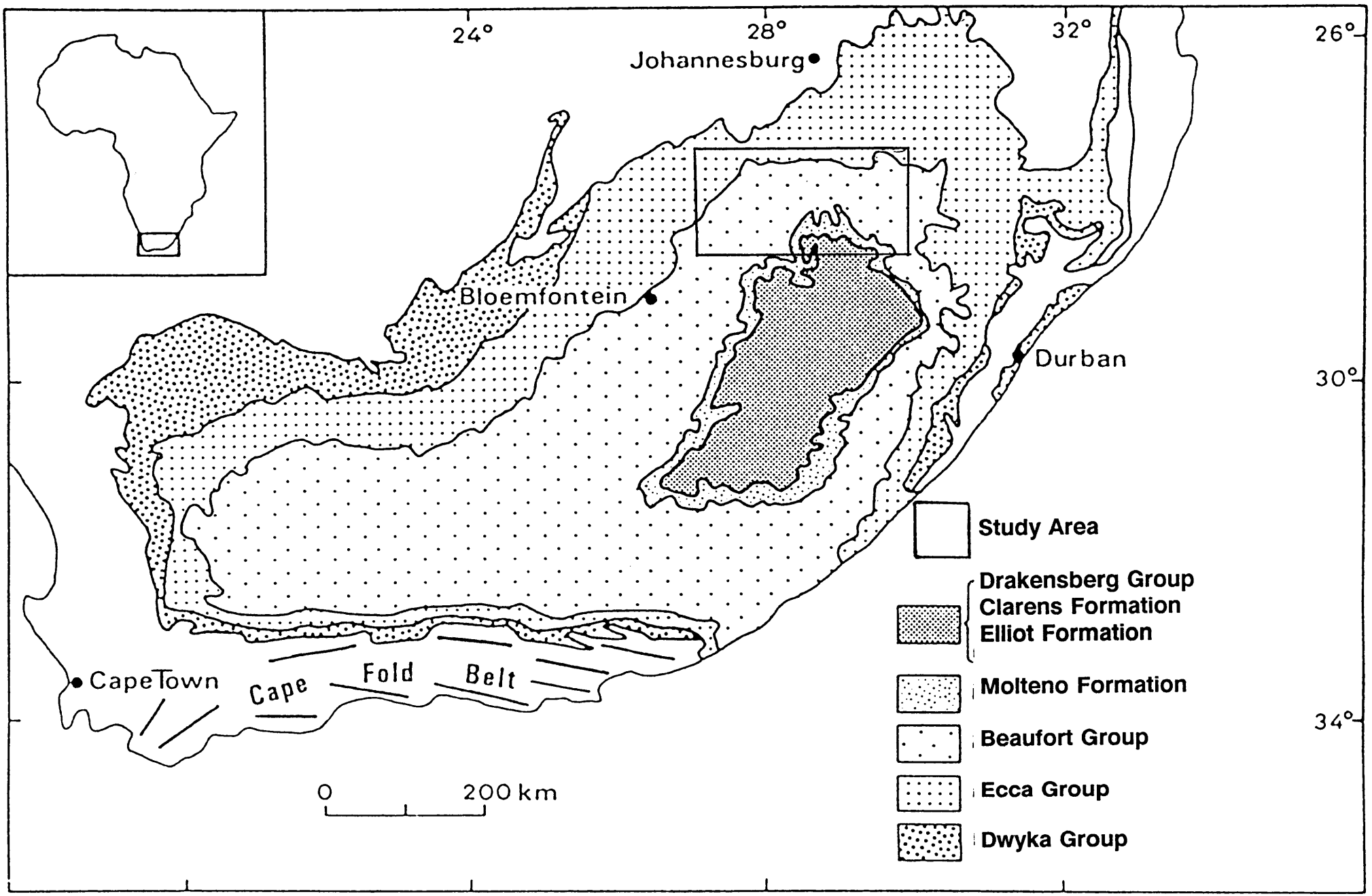

FIGURE 1. Generalised geological map of the Karoo Basin. (Based on published South African Geological Survey maps)

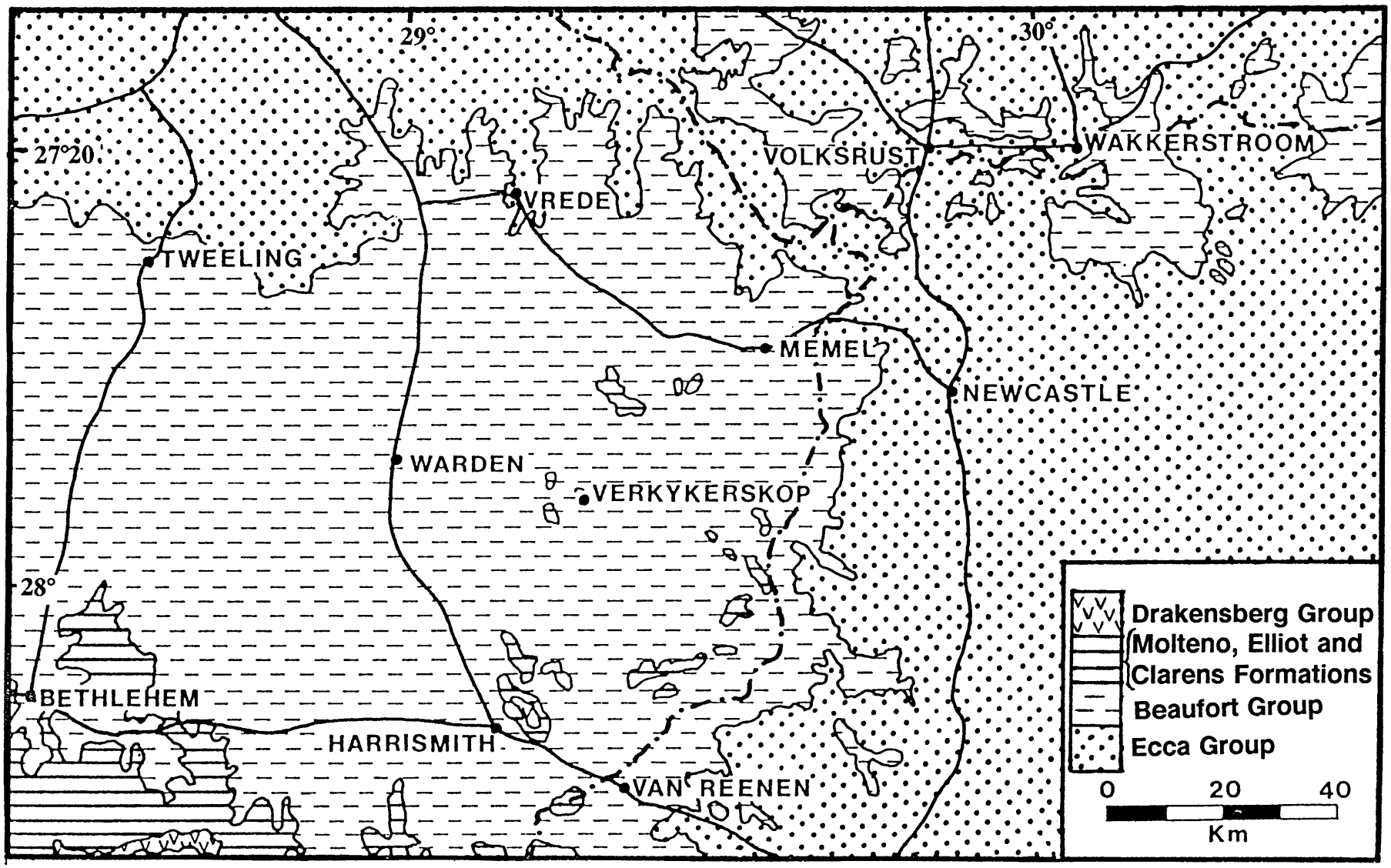

FIGURE 2a. Locality and geological map of the Harrismith study area

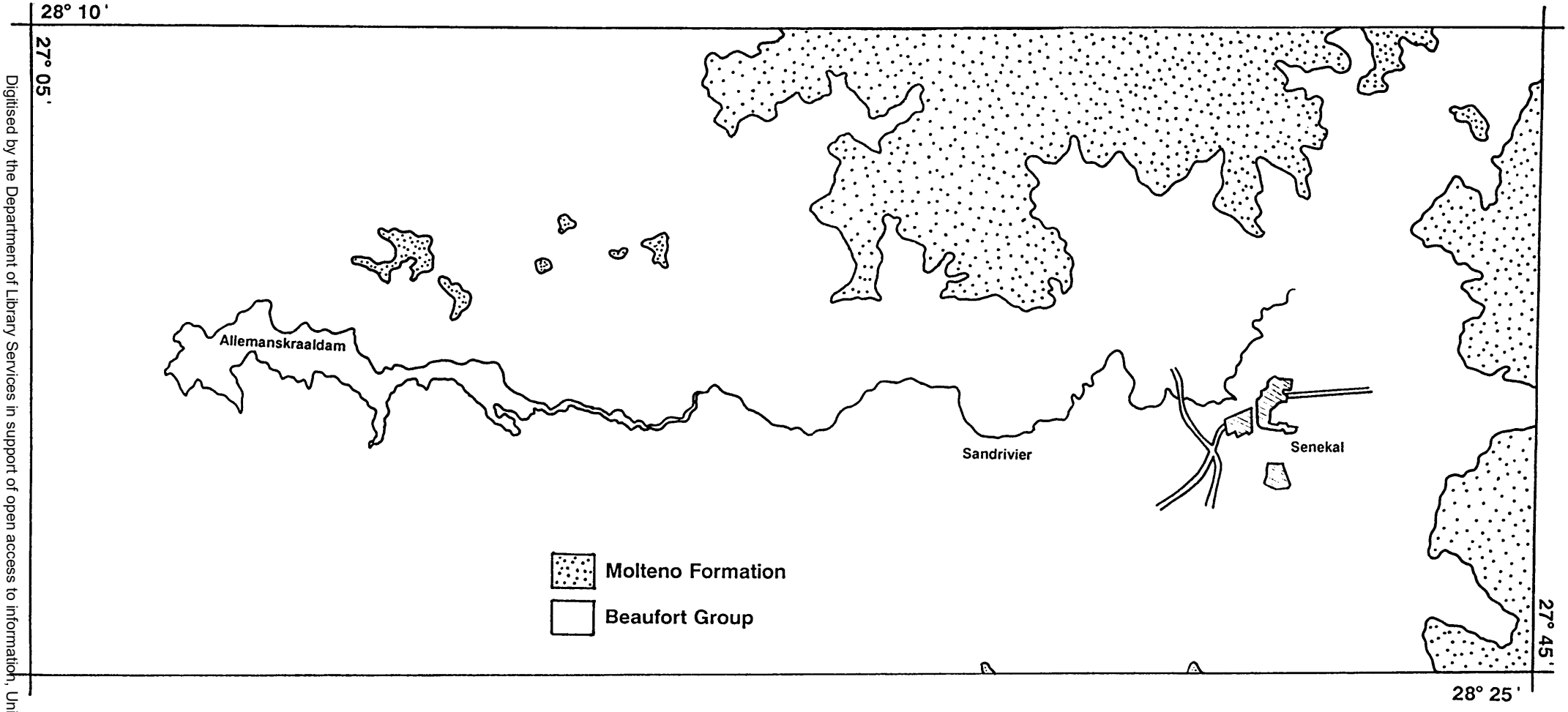

FIGURE 2b. Locality and geological map of the Senekal study area

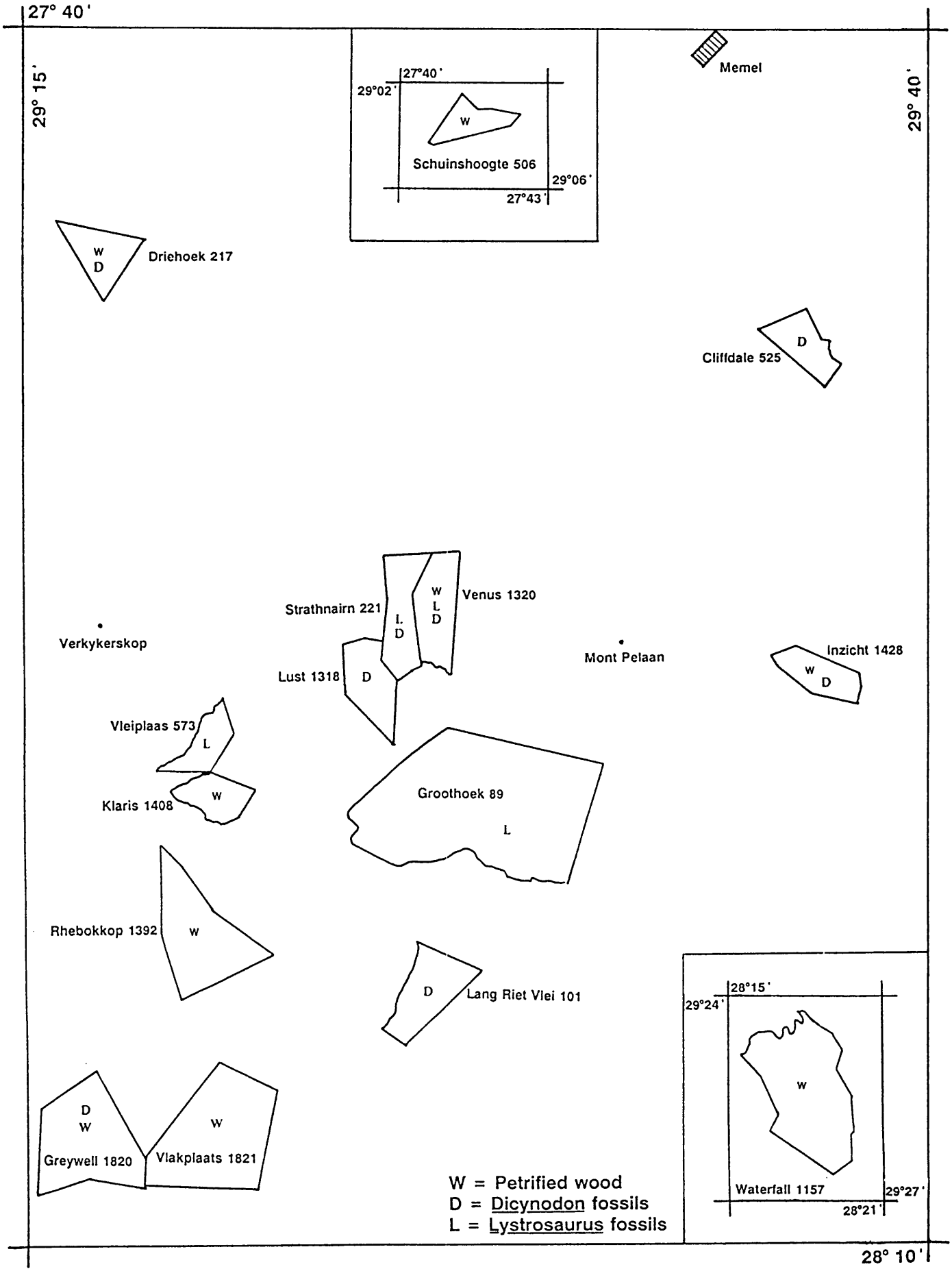

FIGURE 3a. Locations of fossils and fossil wood collected in the Harrismith district.

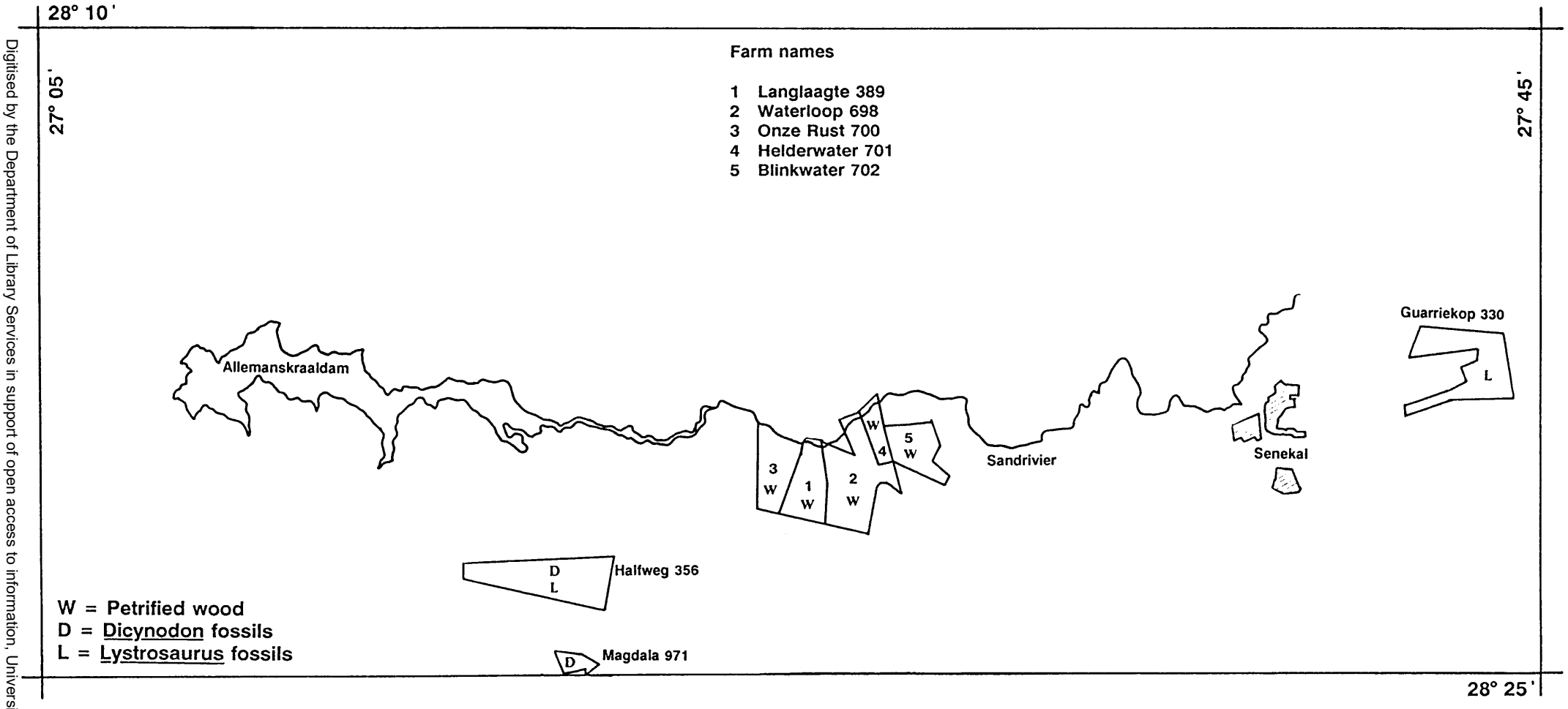

FIGURE 3b. Locations of fossils and fossil wood collected in the Senekal district.

2.2 LABORATORY METHODS

2.2.1 Fossil wood

Polished thin-sections (30µm thick) of the wood were prepared in cross-section, perpendicular to the long axis of the stem, and also in longitudinal radial and longitudinal tangential sections (Figs. 4 and 5). These three directions are required to form an idea of the three-dimensional shape of the cells. Polished thin-sections reveal greater anatomical detail, especially if oil-immersion objectives are used at high magnification. The sections were investigated at 25x, 100x, 250x and 400x magnification by means of a petrographic microscope.

2.2.2 Petrography

The mineralogical composition and textures of the different rocks were investigated by means of a petrographic microscope from 30µm thick, polished thin-sections. In many cases this was supplemented by X-ray diffraction and energy dispersive analysis of X-rays (EDAX), also used to identify the replacement minerals in the petrified wood.

The mineralogical composition (clay mineralogy) of the samples was determined by means of an X-ray diffractometer at the Council for Geoscience, South Africa by Dr. D. Bühmann. The samples were crushed, ground and then pressed into sample holders. Analyses were performed with a Philips diffractometer operated at 40 kV and 30 mA. The radiation used was Co K_α with a secondary graphite monochromator. X-ray diffraction traces were recorded from 2° to 75° 2θ at a speed of 1° per minute. The X-ray traces were matched with those of the Data Book of the Joint Committee on Powder Diffraction Standards (1986), as well as with the PDF-2 Database of the International Centre for Diffraction Data.

To determine the replacement minerals, petrified wood thin-sections were submitted to analysis by EDAX spectrometry (model 901A) working at 1740 volts.

Reddish-black minerals and greyish-black minerals in the petrified wood thin-sections were studied and identified by means of a Leica 440i Stereoscan scanning electron microscope (SEM). The analyses were carried out by Mrs. E. Hattingh of the Council for Geoscience of South Africa.

The quartz crystallinity index (Q.C.I.) was determined to show the variations of this index in the wood specimens. It was done at the Council for Geoscience by Dr. D. Bühmann according to the procedure of Murata and Norman (1976). Quantitative measurements of the degree of resolution of the 68°2θ quintuplet, which is a set of well-developed peaks in well-crystallised quartz, was carried out. The values were scaled by an arbitrary factor yielding a crystallinity index of 10.0 for a standard, using the peak height ratio of the [212] peak at 67.74°2θ above background. The radiation used by Murata and Norman (1976) is Cu K_{α}. The radiation used at the Council for Geoscience is Co K_{α}. Although the same procedure is used, the quintuplet will therefore be situated at 80° - 82°2θ (Co K_{α}). The standard material used was crystals of clear quartz from Pietersburg, South Africa with an index of 10. The X-ray diffraction traces were obtained from the powdered Pietersburg standard, whereas the traces of the petrified wood were obtained from thin-sections. X-ray diffraction analyses on powders nearly always give better results than analyses carried out on thin-sections.

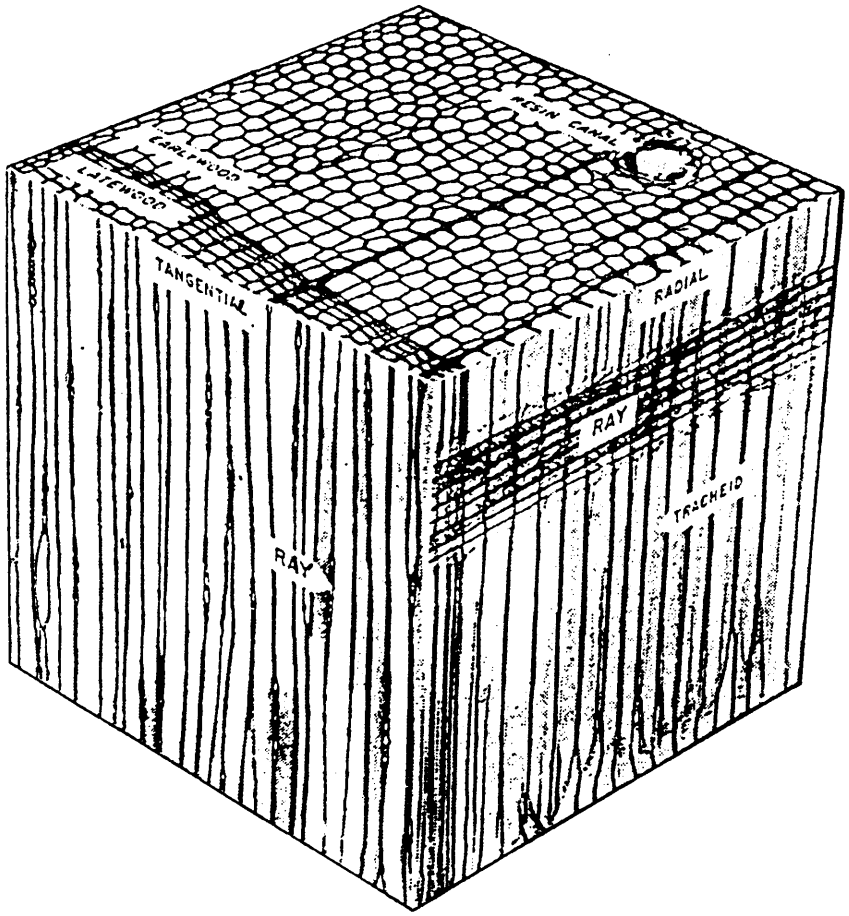

FIGURE 4. A schematic block diagram illustrating the three different cut sections in wood (Panshin & de Zeeuw, 1970).

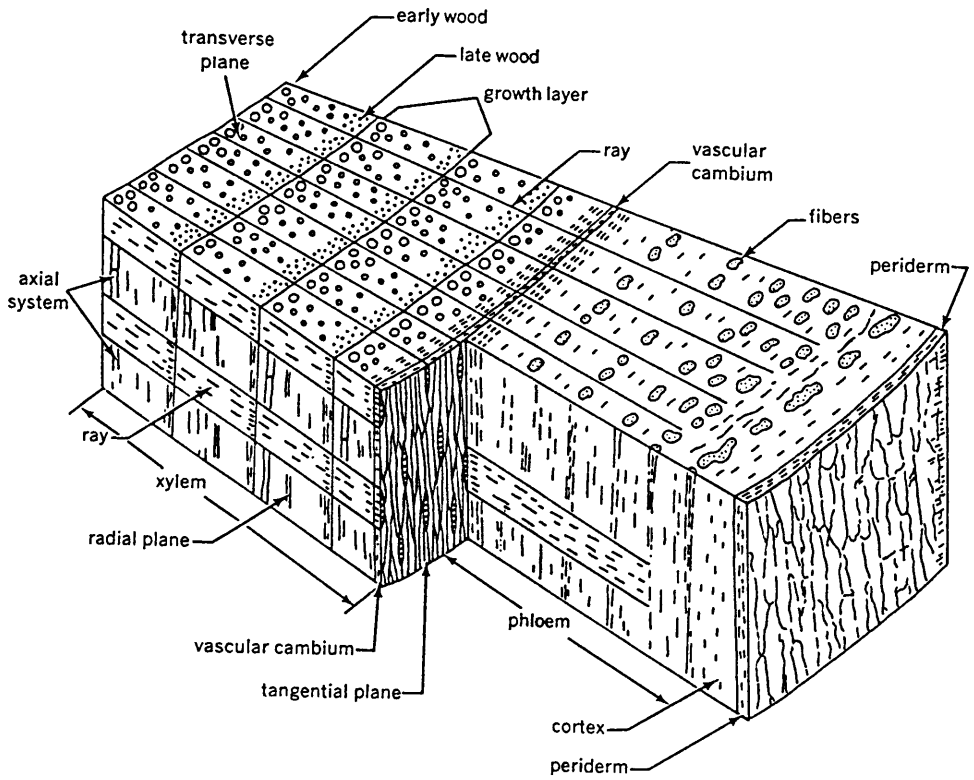

FIGURE 5. A block diagram illustrating basic features of secondary vascular tissue (Esau, 1977).

2.2.3 Geochemistry

The major element and common trace element rock analyses were carried out at the Council for Geoscience using X-ray fluorescence (XRF) techniques. The **major elements** were analysed (with a Sc anode side window X-ray tube) using the procedure of Norrish and Hutton (1969) and values were expressed as weight per cent oxide. Analyses were preformed using the K_α line. Na_2O was analyzed on pressed powder briquettes. Free water and water of crystallisation, as well as carbonate carbon and organic carbon were analysed by means of infrared absorption spectroscopy.
All **trace element analyses** were carried out on pressed powder briquettes using a Rh anode side window X-ray tube. The K_α spectral line was used for analyses of most trace elements, but an L spectral line was used for the analyses of Ba, W, Pb, Th and U. For elements with wavelengths shorter than the Fe-K-absorption edge, the mass absorption coefficients were determined from the Rh K_β Compton peak. The mass absorption coefficients for elements with wavelengths which fall on the long wavelength side of the Fe absorption, were calculated from the major element analysis, using the values for elemental mass absorption coefficients from Heinrich (1986). International rock, soil and sediment standards were used for the calibrations.

The XRF major element analysis was done by Mrs. H.C.C. Cloete and the trace element analysis by Mr. J.H. Elsenbroek.

Platinum-group elements (PGE) were determined at the Schonland Research Centre for Nuclear Physics, University of the Witwatersrand, by means of neutron activation analysis (NAA) techniques.

The analysis comprises the following steps:

(a) Preparing and crushing of samples,
(b) Preconcentration of PGE by nickel sulphide fire-assay,
(c) Acid dissolution of the assay button to leave a PGE sulphide residue which can be filtered, and
(d) Irradiation and gamma spectrometric analysis of the residue.

Few reference materials are available to use as PGE standards. The only available geological reference material for all six PGE's is the South African Bureau of Standards Pt ore SARM-7 and an in-house standard, Wits-1 (Tredoux, 1990). SARM-7 is a composite of mineralized Merensky Reef and barren anorthosite from the Bushveld Complex (Steele *et al.*, 1975). To achieve a range of concentrations which is more representative of PGE levels in basic and ultrabasic rocks, solid dilutions (dilutant is extra-pure silica powder) of 1:10, 1:20 and 1:40 of SARM-7 as standards were employed. Wits-1 is a komatiite which has an undifferentiated and fairly uniform PGE distribution. It was collected south of Barberton. The komatiites in this area are not mineralized (Naldrett and Campbell, 1982) and low concentrations (<15ppb) of the PGE and Au were expected. Blank samples (B1, B2 and B3) were also prepared. 50g of pure silica powder was used instead of the 50g of rock sample powder. Blanks are used to test or monitor the purity of the reagents. Nickel carbonate always contains traces of PGE (McDonald, 1993).

Preconcentration of the PGE and gold (Au) is done to collect the precious metals from a large mass of molten sample material (fire-assay). The procedure used in this study is called the Nickel Sulphide (NiS) Fire Assay. NiS was used as a collector for the PGE. Normally 50g of rock sample is used, but with samples which may contain very low concentrations of PGE, two assay buttons are combined during filtering. This leads to double the amount of PGE residue on the filter paper. Therefore, the analytical peaks from the residue are more prominent relative to background noise during gamma counting. Corrections are done by dividing the final concentrations by two.
The powdered rock samples were melted in a clay assay crucible at 1000°C using a mixture of sodium carbonate, borax, nickel carbonate and sulphur. Two immiscible melts were produced, a borosilicate melt and a dense NiS melt. The latter melt extracted the PGE and Au from the silicate.

Acid dissolution was done by adding 500ml of 35.4% HCl to each button in a glass beaker. Dissolution of the buttons takes 8 to 12 hours on a hot plate. After dissolution, the beakers were removed and cooled quickly with damp towels. These quickly cooled samples were then **filtered** under vacuum through micropore filter papers which

trapped the PGE. They were then dried in a desiccator before irradiation.

Irradiation was carried out in the Pneumatic Facility of the SAFARI-1 reactor operated by the Atomic Energy Corporation of South Africa at Pelindaba. The samples were irradiated for 12 hours. The samples are allowed to decay for 6 hours after irradiation and then counted for 1 hour to determine the ^{109}Pd activity. After 6 days counts were done for ^{199}Au (Pt) and ^{198}Au (2 hours per sample) and after 20 days for ^{103}Ru, ^{192}Ir and ^{191}Os (3 hours per sample).

The peak areas of the gamma rays obtained by the samples were compared with calibration curves and the PGE concentrations calculated. The values from the standards and blanks were used in the preparation of the calibration curves for the samples. A summary of the analytical procedures of the NiS-NAA employed by McDonald (1993) is shown in the following diagram:

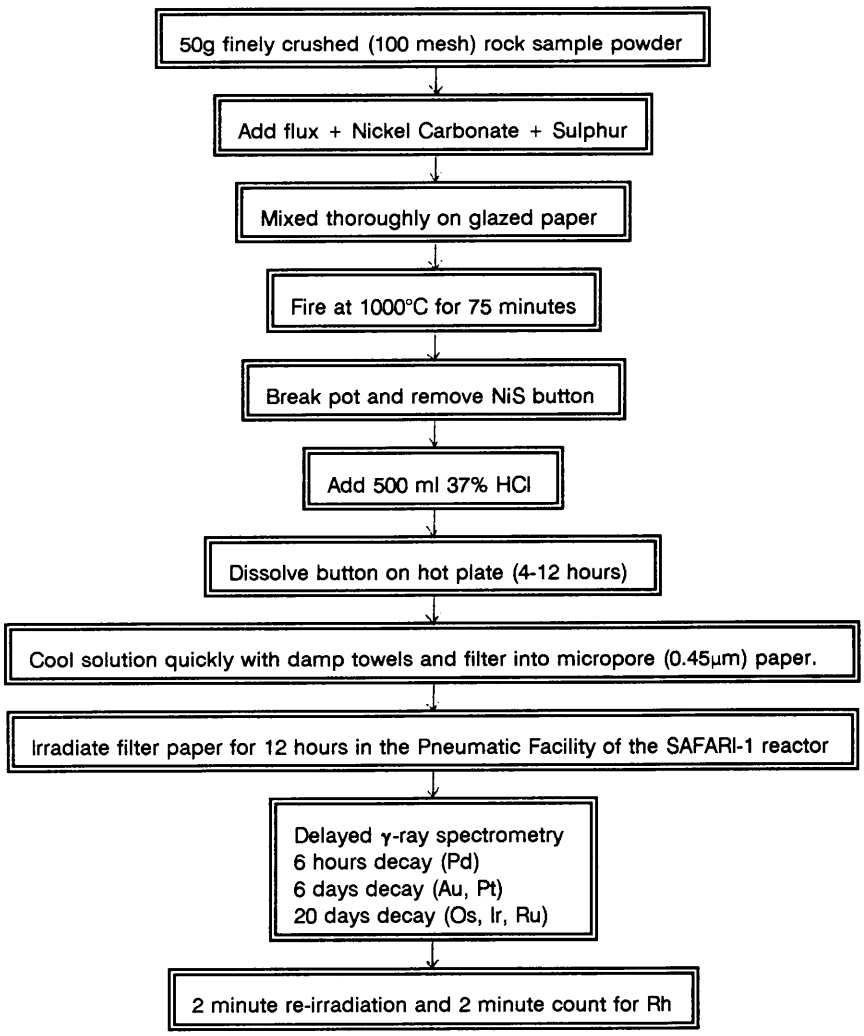

The **^{13}C organic data** can be useful in identifying the stratigraphic position of the Permian-Triassic boundary in South Africa. In addition, these isotopic values give valuable insights into palaeoclimatic processes. Plants assimilate carbon from atmospheric carbon dioxide (CO_2) by one of the following photosynthetic ways (Deines, 1980). These pathways differ in the number of carbon atoms in the first-formed intermediate compounds (Bassham, 1971).

(1) C_3 (Calvin-Benson or non-Kranz cycle) - modern plants

(2) C_4 (Hatch-Slack or Kranz cycle) - tropical grasses

(3) CAM (Use both the C_3 and C_4 pathways) - xeric-adapted flora

According to Deines (1980) and Hoefs (1987) the $\delta^{13}C$ values for the C_3 plants range from about -23 to -34 per mil, whereas the $\delta^{13}C$ values for the C_4 plants range from -6 to -23 per mil.

The different pathways for fixing the CO_2 result in the plants having different isotopic compositions (Deines, 1980). Plants from the Permian only used the C_3 - pathway of fixing atmospheric CO_2 (Ehleringer *et al.*, 1991). Because of this, it can be assumed that isotopic shifts of the organic matter are due to primary effects such as p_{CO2}, climate, plant species, etc. An increase in p_{CO2} decreases $\delta^{13}C$ and an increase in dryness results in an increase of $\delta^{13}C$ of plants (Tieszen, 1991).

Decreasing organic $\delta^{13}C$ values are associated with colder climates and increasing $\delta^{13}C$ values with warmer climates (Faure, 1993). Environmental factors such as water stress increases the $\delta^{13}C$ values in plants (Tieszen, 1991).

The oxidation of terrestrial carbon will decrease the $\delta^{13}C$ values in rivers flowing into the sea. It also results in an increase in atmospheric CO_2 causing a greenhouse effect and an increase of atmospheric temperatures accompanied by continental aridity (Faure, 1993). These factors may affect terrestrial and marine life causing extinction OR reduction in species.

The $^{13}C/^{12}C$ ratios are reported in δ - notation, as per mil (‰) deviations from the $^{13}C/^{12}C$ ratio of the PDB standard:

$$\delta^{13}C_{sample} = \frac{(^{13}C/^{12}C_{sample} - {}^{13}C/^{12}C_{standard})}{^{13}C/^{12}C_{standard}} \times 1000$$

The PDB standard is calculated from carbon dioxide which is prepared from a Cretaceous belemnite *Belemnitella americana*, from the Peedee Formation of South Carolina.

An attempt was made to determine the $\delta^{13}C$ across the Permian-Triassic boundary. Unfortunately, the organic carbon values obtained from the samples were very low. Four of the samples do not contain any organic C. The values for the rest of the samples range from 0.017% to 0.805% organic C (Table 9). Because of these low concentrations of organic carbon in the sediments and the obvious erratic values which would result (Dr. K. Faure, pers. comm., 1995), it was decided not to determine $\delta^{13}C$.

CHAPTER 3. GENERAL GEOLOGY

In this study strata of the Beaufort Group, which is part of the Karoo Supergroup (approximate age ranging from 300 Ma to 180 Ma)(SACS, 1980), are examined. The general stratigraphy of the Karoo Basin (Fig. 1) is shown in Table 2.

In the study area (Fig. 2), the rocks of the Karoo Supergroup are essentially horizontal, with a dip of 1° to 3° to the south. Groenewald (1984) reported local dips of up to 7° where the sedimentary rocks have been disturbed by dolerite intrusions, but such high dips have not been observed in the present study.

3.1 LITHOSTRATIGRAPHY

The lithostratigraphical subdivision in the study area (Table 3) is essentially that of SACS (1980), slightly modified on the basis of previous work by SOEKOR (1966 - 1976) who launched aerial photographic geological mapping projects in the area (Czaky and Wachsmuth, 1971; Bars and Roux, 1972; Bars, 1973; Sieswerda, 1974; Cadle and Proedrou, 1975; Bars and Guillebert, 1976). Groenewald (1984) also made certain modifications to the detailed lithostratigraphic division of the Beaufort Group in the northeastern Orange Free State.

The topography in the area is closely related to the lithostratigraphy, and Groenewald (1984) used the topography to recognise the larger lithostratigraphic units and also to distinguish two formations in the Beaufort Group.
The topography can be divided into four plateaus:
The escarpment of plateau 1 (upper) is formed by Witkoppe (2336m above sea level), Kranskop and Tafelkop. This plateau itself consists of Clarens sandstone and Drakensberg lava.
Plateau 2 consists of sandstone of the Verkykerskop Formation (Beaufort Group) (Table 3).

Plateau 3 consists of the Normandien Formation (Beaufort Group).
Plateau 4 is underlain by sedimentary rocks of the Ecca Group.

The Schoondraai Member (sandstone and mudrock) of the Normandien Formation (Table 3) is easily recognized in the field, because it forms prominent cliffs in the southern and eastern parts. To the west the outcrops become scarce.
The Harrismith Member (yellow-green mudrock) seldom outcrops, but is recognized by a zone of negative topographic weathering between the overlying Verkykerskop Formation and the underlying Schoondraai Member (Groenewald, 1984).

TABLE 2. Generalised stratigraphy of the Karoo Basin (SACS, 1980).

NAME OF GROUP/FORMATION	PROMINENT LITHOLOGY
Drakensberg Group	Basalt
Clarens Formation	Sandstone
Elliot Formation	Mudrock
Molteno Formation	Sandstone
Beaufort Group	Sandstone and Mudrock
Ecca Group	Sandstone and Mudrock
Dwyka Group (basal)	Diamictite

TABLE 3. Stratigraphy and lithology of the Beaufort Group, Karoo Supergroup

(thick black line indicates the approximate position of the Permian-Triassic boundary)

MAIN KAROO BASIN (SACS 1980)			STUDY AREA (GROENEWALD 1984)	
STRATIGRAPHY		**LITHOLOGY**	**STRATIGRAPHY**	**LITHOLOGY**
TARKASTAD SUBGROUP			TARKASTAD SUBGROUP	
Burgersdorp Formation		Mudrock interbedded with fine-grained sandstones	Driekoppen Formation	Red mudrock with interbedded minor sandstone
Katberg Formation		Fine- to medium-grained sandstone, subordinate mudrocks	Verkykerskop Formation	Coarse- to fine-grained feldspathic sandstone, conglomerate with manganiferous and ferruginous matrix
ADELAIDE SUBGROUP			**NORMANDIEN FORMATION**	
	Palingkloof Member	Shale with thin sandstone intercalations	Harrismith Member	Red, purple and yellow mudrock
BALFOUR FORMATION	Elandsberg Member	Mudrock	Schoondraai Member	Coarse- to fine-grained sandstone with carbonate concretions
	Barberskrans Member	Sandstone	Rooinek Member	Coarse-grained feldspathic sandstone
	Daggaboersnek Member Oudeberg Member	Mudrocks Sandstone	Frankfort Member	Interbedded dark-grey mudrock and coarse-grained sandstone

3.2 BIOSTRATIGRAPHY

Broom (1906) originally proposed a six-fold biostratigraphic zonation of the Beaufort Series. Kitching (1970) proposed a new biostratifigraphy for the Beaufort Series, without linking it to any lithological subdivision. Johnson and Keyser (1976) linked the biostratigraphic subdivision of Kitching to the various formations of the Beaufort Group (SACS, 1980). More recently, Rubidge *et al.* (1991) published a revised version of the reptilian biostratigraphy of the Permian-Triassic Beaufort Group (Table 4).

The biostratigraphy of the Beaufort Group is very important in this study. These biozones are shown in Fig. 6. The Permian-Triassic boundary is believed to be situated between the *Dicynodon - Theriognathus* Assemblage Zone and the overlying *Lystrosaurus - Procolophon* Assemblage Zone in the Beaufort Group (SACS, 1980). Both assemblage zones are present in the Harrismith area. The reptilian biostratigraphy in relation to the lithostratigraphy of the Beaufort Group is shown in Table 4.

The lower boundary of the *Dicynodon-Theriognathus* Assemblage Zone is marked by the first occurrence of *Dicynodon lacerticeps* and of *Theriognathus (Whaitsia)*. This zone is characterized by the abundant presence of therapsid genera (Reptilia, Synapsida).The genus *Dicynodon* is a medium to large sized herbivorous, mammal-like reptile. The average skull length is between ten and forty centimetres. The therocephalian *Theriognathus (Whaitsia)* is restricted to this assemblage zone. Fossils occur in mudrock horizons. The age of this biozone is Late Permian (Rubidge *et al.*, 1991).

The base of the *Lystrosaurus - Procolophon* Assemblage Zone can be correlated with the contact between the Adelaide Subgroup and the Tarkastad Subgroup of the Beaufort Group. The zone is characterized by the first occurrence of the genera *Lystrosaurus* (Reptilia) and *Procolophon*. This biozone does not contain any *Dicynodon lacerticeps* reptile fossils. Other genera that occur in this biozone include *Lydekkerina* and *Thrinaxodon*. The fossils occur in mudrock sequences between major and minor channel sandstones. The age of the biozone is Early Triassic (Rubidge *et al.*, 1991).

TABLE 4. Relationship between the biostratigraphy and lithostratigraphy of the Beaufort Group (After SACS 1980 and Rubidge *et al.*, 1991)

LITHOSTRATIGRAPHIC UNITS						BIOSTRATIGRAPHY	
PERIOD	**GROUP**	**SACS 1980 SUBGROUP (Sg) FORMATION (Fm) MEMBER (Mbr)**		**GROENEWALD 1984 SUBGROUP (Sg) FORMATION (Fm) MEMBER (Mbr) (Study area)**		**KEYSER and SMITH (1978-1979) ASSEMBLAGE ZONES**	**RUBIDGE *et al.* (1991) ASSEMBLAGE ZONES**
TRIASSIC	BEAUFORT	TARKASTAD SG	Burgersdorp Fm	TARKASTAD SG	Driekoppen Fm	*Kannemeyeria-Diademodon*	*Cynognathus-Diademodon* (Kitching J.W.)
			Katberg Fm		Verkykerskop Fm	*Lystrosaurus-Thrinaxodon*	*Lystrosaurus-Procolophon* (Groenewald G.E. & Kitching J.W.)
225 Ma			Palingkloof Mbr, Balfour Fm		Harrismith Mbr		
PERMIAN	BEAUFORT	ADELAIDE SG	Lower part of Balfour Fm	NORMANDIEN FM	Schoondraai Mbr	*Dicynodon lacerticeps-Whaitsia*	*Dicynodon-Theriognathus* (Kitching J.W.)
			Middleton Fm		Rooinek Mbr	*Aulacephalodon-Cistecephalus*	*Aulacephalodon-Cistecephalus* (Smith R.M.S. & Keyser A.W.)
					Frankfort Mbr	*Tropidostoma-Endothiodon*	*Tropidostoma-Endothiodon* (Smith R.M.S & Keyser A.W.)
			Koonaap Fm			*Pristerognathus-Diictodon*	*Pristerognathus-Diictodon* (Smith R.M.S & Keyser A.W.)
						Dinocephalian	*Tapinocephalus-Bradysaurus* (Smith R.M.S & Keyser A.W.)
			Abrahamskraal Fm				*Eodicynodon-Tapinocaninus* (Rubidge B.S.)

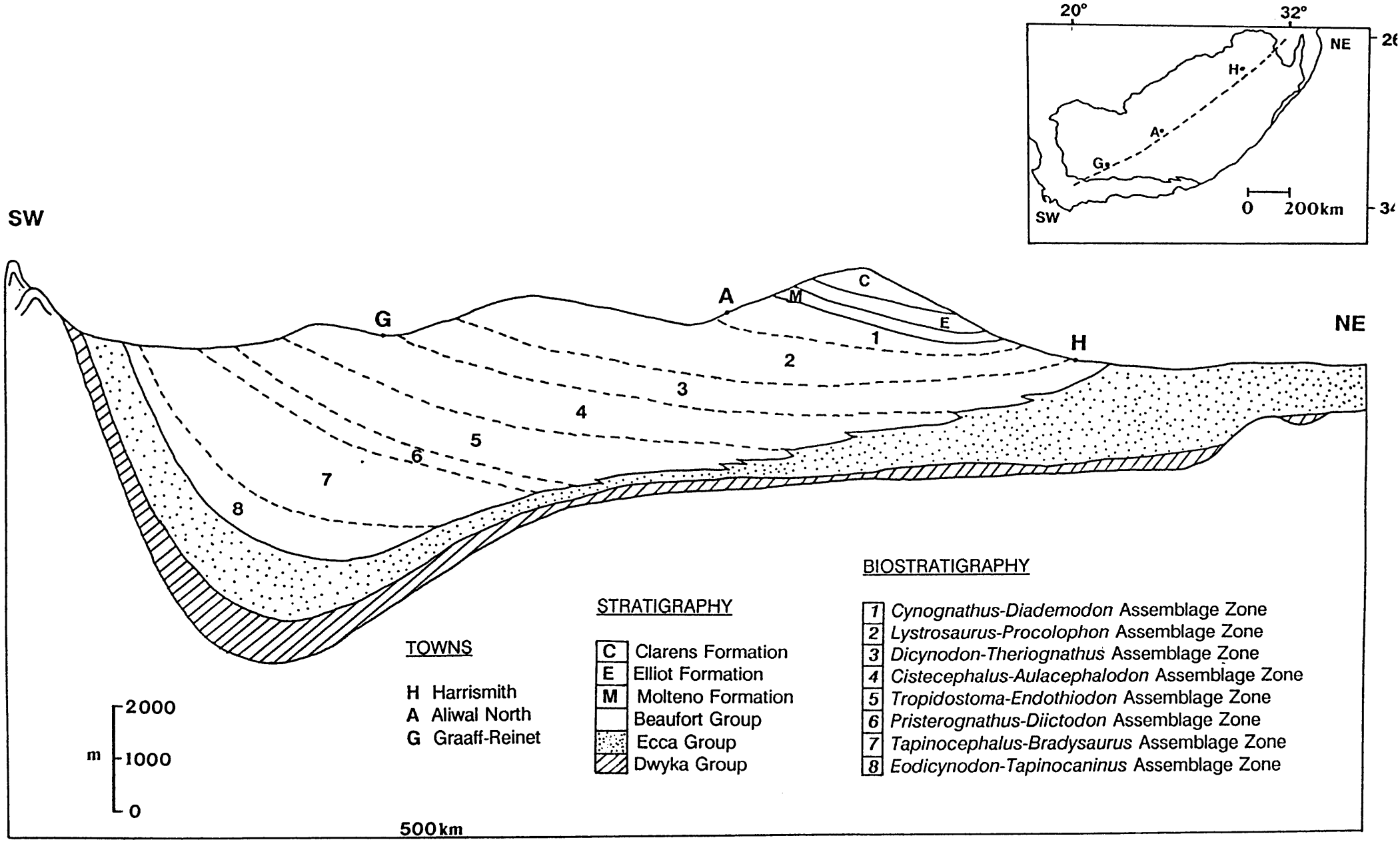

FIGURE 6. A schematic southwest - northeast section through the Karoo Basin to show the distribution of the biozones of the Beaufort Group. (Drawing after Dr. B.S. Rubidge, 1990).

CHAPTER 4. THE GEOLOGY ASSOCIATED WITH THE PERMIAN-TRIASSIC BOUNDARY: THE NORMANDIEN FORMATION

4.1 SEDIMENTOLOGY

4.1.1 Lithofacies and profiles of the sedimentary rocks

The Permian-Triassic boundary in the study area lies in the Normandien Formation (Table 3), approximately at the transition between the Schoondraai and Harrismith Members (Groenewald, 1984). Relationships between various lithologic units (ie. sedimentary lithofacies) within this formation should therefore provide palaeoenvironmental information on the late Permian and early Triassic.

Palaeoenvironmental studies rely on the subdivision of the lithostratigraphy into lithofacies (Turner, 1977). The term "facies" is defined as "any areally restricted part of a designated stratigraphic unit which exhibits characters significantly different from those of other parts of the unit" (Blatt *et al.*,1972, p.186). The term facies is thus used for sedimentary rocks that show similar characteristics, regardless of age differences. The same lithofacies may be found at different levels within the same stratigraphic unit.

The characteristics that were used to divide a stratigraphic unit into lithofacies were grain size, sedimentary structures, contacts between lithofacies, the colour of sedimentary rocks and the thickness of beds. Table 5 shows the characteristics of the lithofacies in the Schoondraai Member, and Table 6 those of the Harrismith Member. The lithofacies of the Schoondraai and Harrismith Members were studied separately from each other to determine, if possible, a separate (and possibly unique) palaeoenvironment for each of these members, situated on either side of the Permian-Triassic boundary.
The total thickness of the Schoondraai Member is about 11.50m and the total thickness of the Harrismith Member is approximately 9.90m in the study area.
The Udden-Wentworth grain size classification (Pettijohn *et al.*, 1972) was used for the sedimentary rocks.

4.1.1.1 The Schoondraai Member: facies and representative vertical profile

The Schoondraai Member can be divided into 6 lithofacies (Table 5):

1. Micaceous mudrock lithofacies
2. Massive mudrock lithofacies
3. Interbedded mudrock and sandstone lithofacies
4. Flat-bedded sandstone lithofacies
5. Massive sandstone lithofacies
6. Cross-bedded sandstone lithofacies

A representative profile, illustrating vertical facies relationships of the Schoondraai Member, is shown in Fig. 7.

1. MICACEOUS MUDROCK LITHOFACIES

This lithofacies consists of a light grey micaceous mudrock with horizontal lamination. The thickness is up to about 90 centimetres. Sharp upper and lower contacts are present.

2. MASSIVE MUDROCK LITHOFACIES

The thickness of this lithofacies varies from 10 centimetres to about 1 metre. Medium-grained, brown sandstone lenses are present locally in this lithofacies. The example in Fig. 7 is 1 meter wide and 3.5 centimetres thick with a sharp erosive contact. Calcareous concretions are also present in this lithofacies (Fig. 8). Fractures in the concretions are sometimes filled with calcite. This lithofacies contains reptile fossils (Fig. 9), as well as leaf imprints. Unfortunately, the embedded fossil is not very clear due to the subtle colour contrast between the fossil and the mudrock. Sharp contacts are present at the top and bottom of the facies.

TABLE 5. The characteristic lithofacies of the Schoondraai Member.

FACIES	LITHOLOGY	STRUCTURES	INFERRED DEPOSITIONAL PROCESSES
1.	Micaceous mudrock	Horizontal laminae	Suspension settling
2.	Massive mudrock	Massive	Bioturbation, diagenesis or rapid deposition of sediment
3.	Interbedded mudrock and sandstone	Bedding	Traction sedimentation alternating with suspension sedimentation
4.	Flat-bedded sandstone	Planar bedding	Traction sedimentation; upper flow regime plane bed sedimentation
5.	Massive sandstone	Massive	Rapid deposition of sediment, or due to weathering, diagenesis or bioturbation
6.	Cross-bedded sandstone	Planar cross-bedding	Migration of small, straight-crested aqueous dunes

LEGEND OF LITHOFACIES PROFILES

LITHOLOGY/FACIES

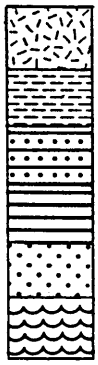

Micaceous mudrock

Massive mudrock

Interbedded mudrock and sandstone

Flat-bedded sandstone

Massive sandstone

Cross-bedded sandstone

COLOUR

LB Light brown

B Brown

LG Light grey

G Grey

RB Reddish brown

YG Yellowish green

CYCLES

Upward fining

Upward coarsening

THICKNESS

mm Millimetres

m Metres

GRAIN SIZE OF SANDSTONES

Fine	0.15mm - 0.2mm
Medium	0.3mm - 0.4mm
Coarse	0.6mm - 0.8mm

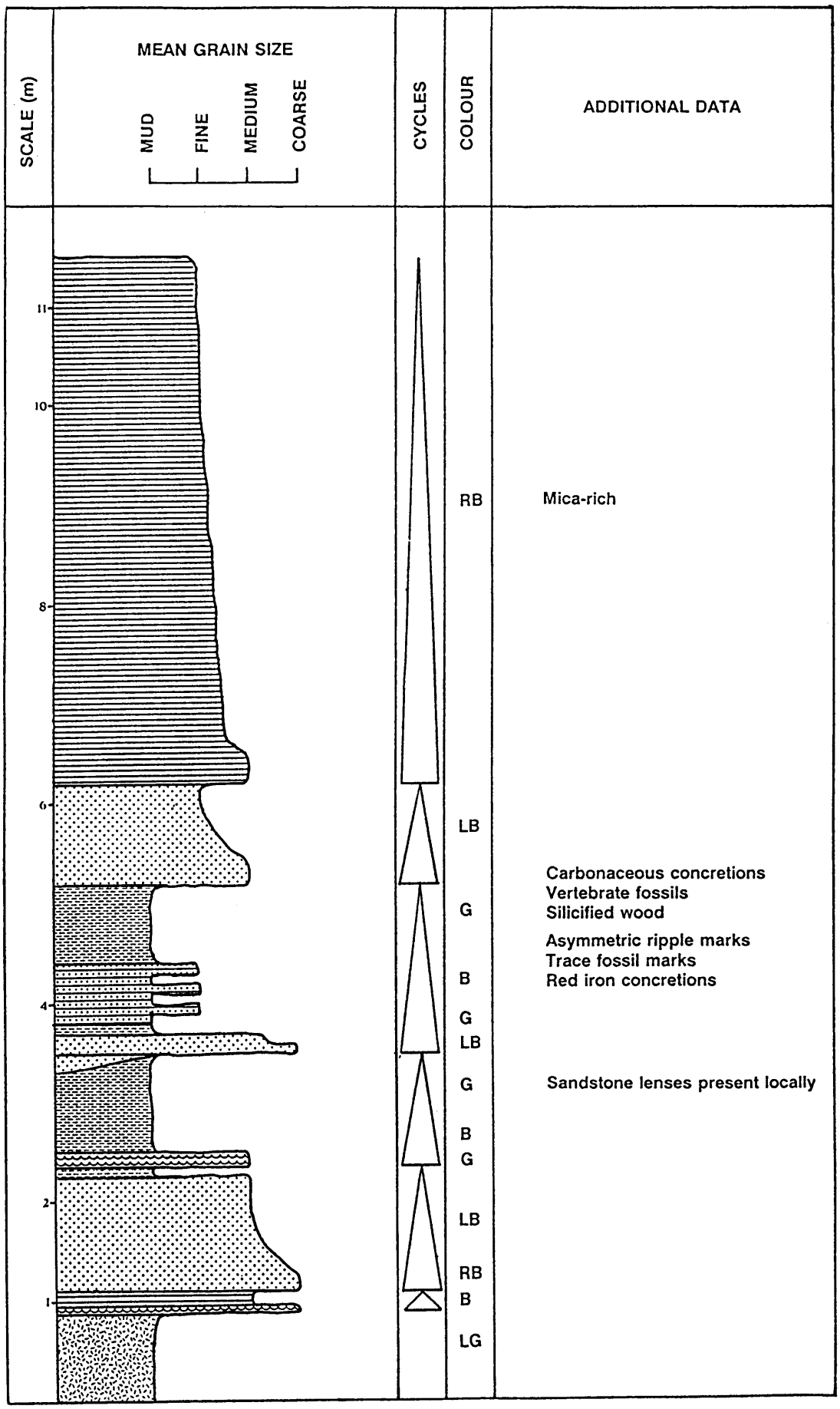

FIGURE 7. A lithostratigraphic profile of the Schoondraai member.

FIGURE 8. Calcareous concretions (indicated by arrows) present in lithofacies 2.

FIGURE 9. The front limb of a *Dicynodon lacerticeps* in mudrock of almost the same colour (lithofacies 2)

3. INTERBEDDED MUDROCK AND SANDSTONE LITHOFACIES

Comprises of interbedded fine-grained, brown sandstone and greyish mudrock (Fig. 10), with up to eight sets of sandstone and mudrock interbeds in field outcrops. The bed thicknesses of the mudrock vary from approximately 3 to 7 centimetres and the sandstone bed thicknesses from 5 to 20 centimeteres. Asymmetric ripple-marks are found in the sandstone, with horizontal fossil traces (Fig. 11) and red concretions (Fig. 12). Reptile fossils and silicified wood are also found in this lithofacies. The thickness of the lithofacies is up to 60 centimetres and the upper and lower contacts are sharp.

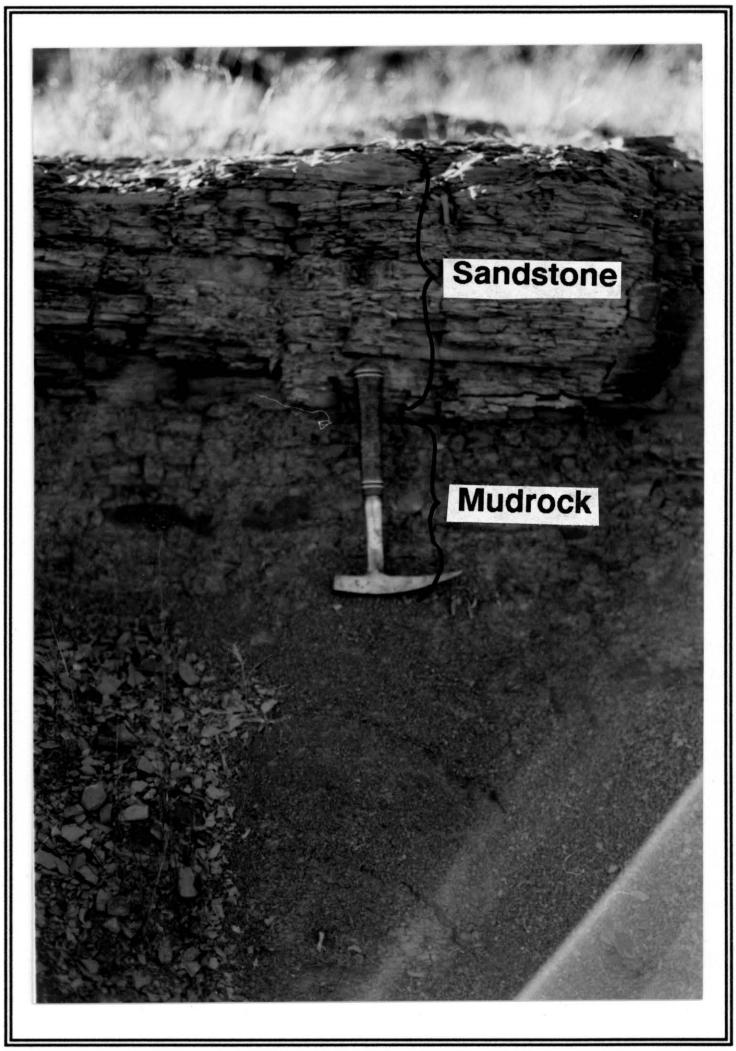

FIGURE 10. Interbedded fine sandstone and mudrock of lithofacies 3.

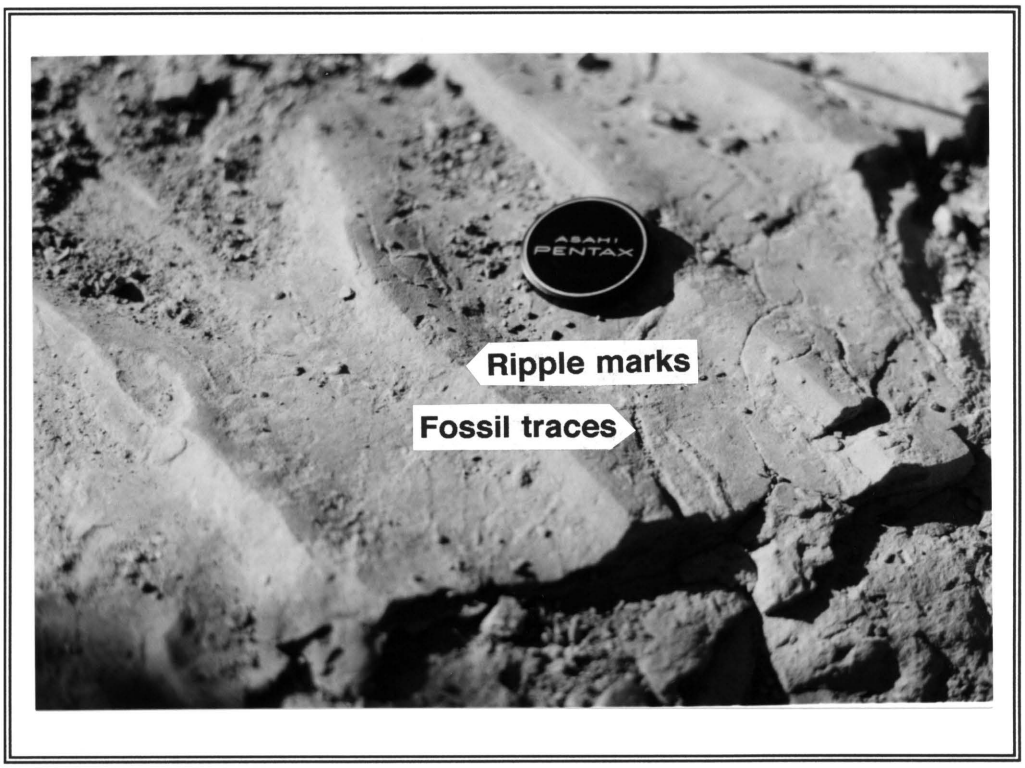

FIGURE 11. Asymmetric ripple marks and fossil traces in fine-grained sandstone of lithofacies 3.

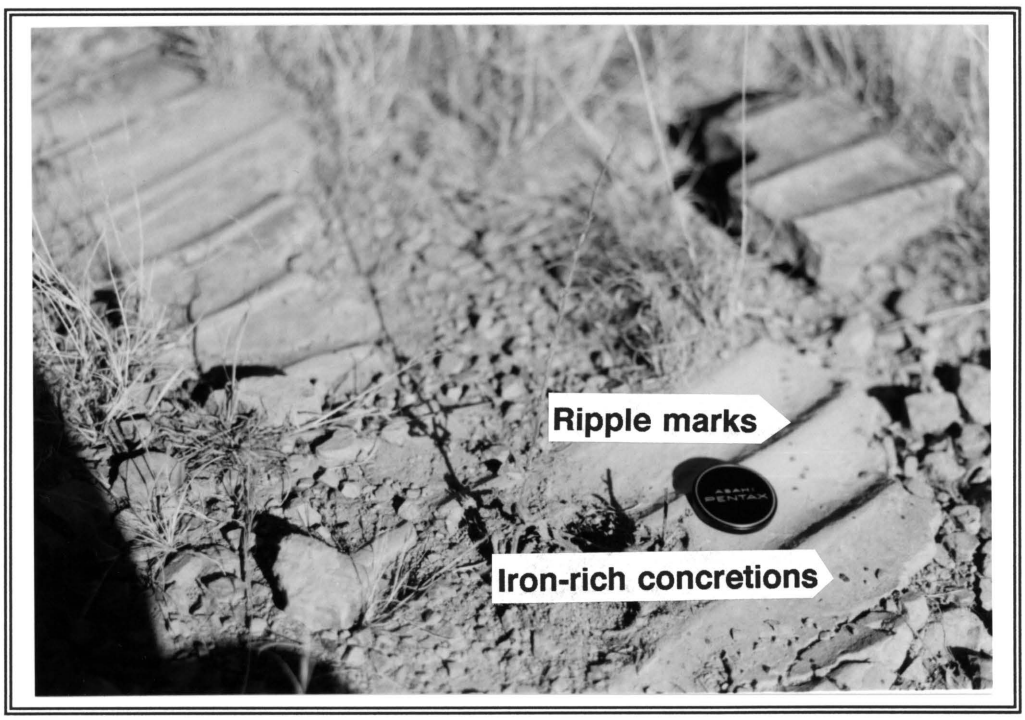

FIGURE 12. Asymmetric ripple marks with iron-rich concretions (goethite) of lithofacies 3.

4. FLAT-BEDDED SANDSTONE LITHOFACIES

This medium- to fine-grained, flat-bedded sandstone lithofacies is reddish-brown in colour. Horizontal sandstone laminae thickness is 10mm or less. The thickness of the facies in field outcrops varies from 14 centimetres to 1 metre. The lithofacies is micaceous at some localities. Sharp contacts are present at the top and bottom.

5. MASSIVE SANDSTONE LITHOFACIES

The lithofacies consists of medium- to coarse-grained, massive, light brown sandstone. The thickness of the facies ranges from 17 centimetres to about 1 metre. The contacts at the top and bottom are sharp.

6. CROSS-BEDDED SANDSTONE LITHOFACIES

These medium- to coarse-grained, well sorted sandstones have a brown colour. Planar, low angle cross-bedding is present. Set thicknesses range from 3 to 8 centimeteres with the thicknesses of the laminae 10 mm and less. The thickness of the facies varies from 5 to 15 centimetres. The upper and lower contacts are sharp.

4.1.1.2 The Harrismith Member: facies and representative vertical profile

The Harrismith Member is divided into 5 lithofacies (Table 6):

1. Massive mudrock lithofacies
2. Interbedded sandstone and mudrock lithofacies
3. Flat-bedded sandstone lithofacies
4. Cross-bedded sandstone lithofacies
5. Massive sandstone lithofacies

A representative lithofacies profile of the Harrismith Member is shown in Fig 13.

1. MASSIVE MUDROCK LITHOFACIES

This massive mudrock lithofacies has a yellowish-green colour. Iron concretions, most probably goethite, are also present. The thickness of this lithofacies varies from 1 metre to 2 metres. The upper and lower contacts are sharp.

2. INTERBEDDED MUDROCK AND SANDSTONE LITHOFACIES

Analogous to lithofacies 3 of the Schoondraai Member. Horizontal laminae occur as well. The thickness of the lithofacies is approximately 2.1 metres. The upper and lower contacts are sharp.

3. FLAT-BEDDED SANDSTONE LITHOFACIES

This lithofacies consists of brown, fine-grained, flat-bedded sandstone. Bed thickness varies from approximately 1 centimeter to 5 centimeters. The thickness of the facies is about 50 centimetres. The contacts at the top and bottom are sharp.

4. CROSS-BEDDED SANDSTONE LITHOFACIES

Analogous to lithofacies 6 of the Schoondraai Member, with small-scale, low angle cross-bedding. Set thicknesses range from 3 to 5 centimeteres with the thicknesses of the laminae 5mm and less. The thickness of the lithofacies ranges from approximately 20 centimetres to 1 meter. Sharp top and bottom contacts are present.

5. MASSIVE SANDSTONE LITHOFACIES

This fine-grained sandstone lithofacies is characterized by its reddish-brown colour. The thickness of the facies is up to 15 centimetres. The lower and upper contacts are sharp.

TABLE 6. The characteristic lithofacies of the Harrismith Member.

FACIES	LITHOLOGY	STRUCTURES	INFERRED DEPOSITIONAL PROCESSES
1.	Massive mudrock	Massive	Bioturbation, diagenesis or rapid deposition
2.	Interbedded mudrock and sandstone	Bedding	Traction sedimentation alternating with suspension sedimentation
3.	Flat-bedded sandstone	Planar bedding	Traction sedimentation; upper flow regime plane bed sedimentation
4.	Cross-bedded sandstone	Planar cross-bedding	Migration of small, straight-crested aqueous dunes
5.	Massive sandstone	Massive	Rapid deposition, diagenesis, weathering or bioturbation

LEGEND OF LITHOFACIES PROFILES

LITHOLOGY/FACIES

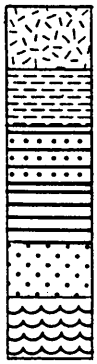

Micaceous mudrock

Massive mudrock

Interbedded mudrock and sandstone

Flat-bedded sandstone

Massive sandstone

Cross-bedded sandstone

COLOUR

LB Light brown

B Brown

LG Light grey

G Grey

RB Reddish brown

YG Yellowish green

CYCLES

Upward fining

Upward coarsening

THICKNESS

mm Millimetres

m Metres

GRAIN SIZE OF SANDSTONES

Fine	0.15mm - 0.2mm
Medium	0.3mm - 0.4mm
Coarse	0.6mm - 0.8mm

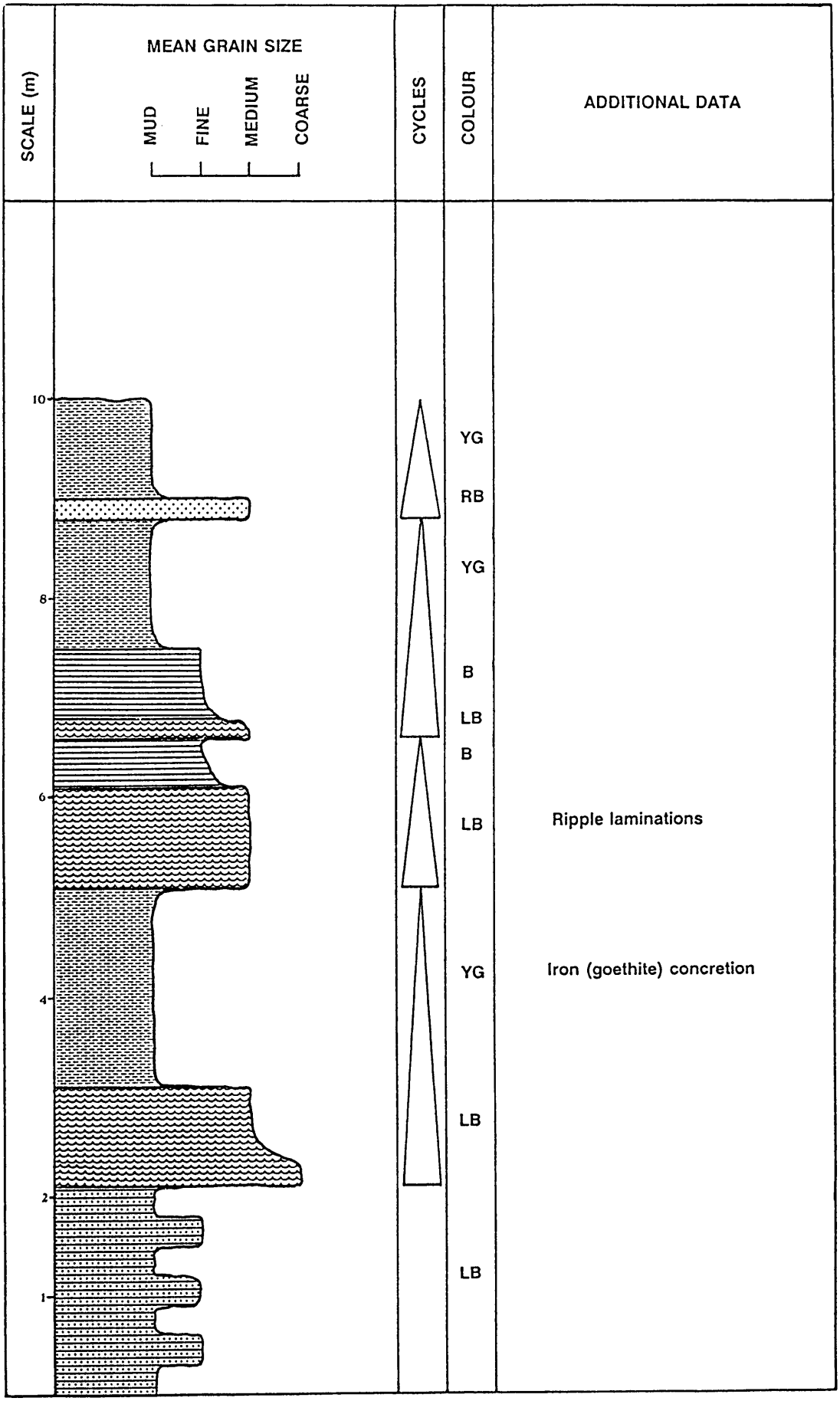

FIGURE 13. A lithostratigraphic profile of the Harrismith member.

4.1.2 PETROGRAPHY OF THE SEDIMENTARY ROCKS

4.1.2.1 Microscopical characteristics of the sandstones

Thin-sections of sandstone samples from the *Dicynodon - Theriognathus* Assemblage Zone (Schoondraai Member) and the *Lystrosaurus - Procolophon* Assemblage Zone (Harrismith Member) were studied. Sample JS(SL)94-2 was collected from the *Lystrosaurus - Procolophon* Assemblage Zone on the farm Venus 1320, Verkykerskop district (Fig. 3a). Samples JS(SD)94-6, JS(SD)94-9 and JS(SD)94-10 were collected from the *Dicynodon - Theriognathus* Assemblage Zone, also on the farm Venus 1320. Samples JS(SL)94-12, JS(SL)94-13 and JS(SL)94-14 were collected from the *Lystrosaurus - Procolophon* Assemblage Zone on the farm Langlaagte 389, Senekal district (Fig. 3b).
A general description of all the thin-sections is given here and Table 7 gives a detailed description of each thin-section separately.

Grain size

The grain size of the sandstones ranges from 0.129mm to 0.581mm. According to the Udden-Wentworth size classification (Pettijohn *et al.*, 1972), the sandstones range from fine- to coarse-grained, with an average of 0.283mm.

Sorting

The sorting of the sandstones is moderate to good.

Compaction

The compaction of the sandstones is good. No unfilled pore spaces are visible and the sheet silicates are deformed due to compaction of the original voids between the sand grains (Fig. 14).

TABLE 7. Petrographic description of the sedimentary sandstone thin-sections.

SAMPLE	BIOZONE	GRAIN SIZE	PHI (ø) SCALE	SORTING	GRAIN COMPOSITION	GRAIN SHAPE	CLASSIFICATION (Dott, 1964)
JS(SL)94-2	Lystrosaurus (Venus 1320)	0.129mm - 0.371mm mean = 0.194mm	+3 to +1	Moderate	Quartz: 61% Feldspar: 22% Mica: 10% Clay: 7% Iron oxide: -	low sphericity sub-rounded to sub-angular	Feldspathic arenite
JS(SD)94-6	Dicynodon (Venus 1320)	0.242mm - 0.581mm mean = 0.387mm	+2 to +1	Good	Quartz: 59.5% Feldspar: 27% Mica: 11% Clay: 1.5% Iron oxide: 1.0%	low sphericity sub-rounded to sub-angular	Feldspathic arenite
JS(SD)94-9	Dicynodon (Venus 1320)	0.145mm - 0.306mm mean = 0.232mm	+3 to +1	Moderate	Quartz: 62.5% Feldspar: 19% Mica: 7% Clay: 11% Iron oxide: 0.5%	low sphericity sub-rounded to sub-angular	Feldspathic arenite
JS(SD)94-10	Dicynodon (Venus 1320)	0.129mm - 0.339mm mean = 0.214mm	+3 to +1	Moderate	Quartz: 59% Feldspar: 21.5% Mica: 4.5% Clay: 8% Iron oxide: 7%	low sphericity sub-rounded to sub-angular	Feldspathic arenite
JS(SL)94-12	Lystrosaurus (Langlaagte 389)	0.226mm - 0.435mm mean = 0.321mm	+3 to +1	Moderate	Quartz: 60% Feldspar: 20% Mica: 9% Clay: 10.5% Iron oxide: 0.5%	low sphericity sub-rounded to sub-angular	Feldspathic arenite
JS(SL)94-13	Lystrosaurus (Langlaagte 389)	0.242mm - 0.419mm mean = 0.313mm	+3 to +1	Moderate	Quartz: 57.5% Feldspar: 24.5% Mica: 5.5% Clay: 12% Iron oxide: 0.5%	low sphericity sub-rounded to sub-angular	Feldspathic arenite
JS(SL)94-14	Lystrosaurus (Langlaagte 389)	0.258mm - 0.403mm mean = 0.323mm	+2 to +1	Good	Quartz: 59% Feldspar: 23% Mica: 8.5% Clay: 9% Iron oxide: 0.5	low sphericity sub-rounded to sub-angular	Feldspathic arenite

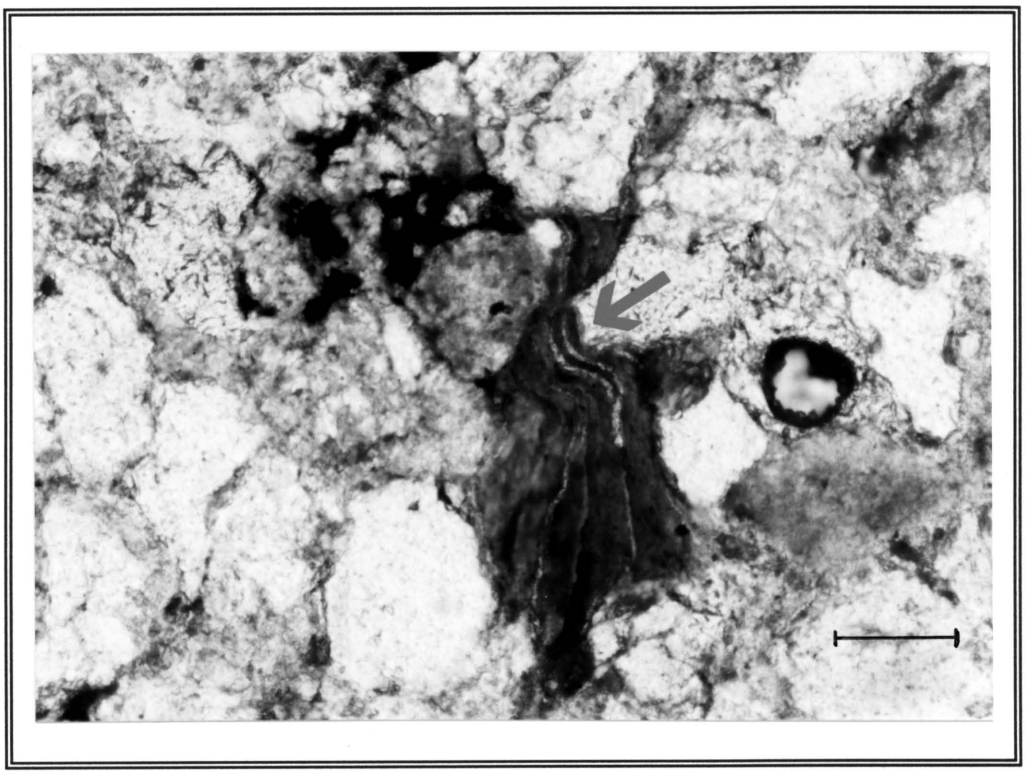

FIGURE 14. Deformation of sheet silicates due to the good compaction of the sandstone (Sample JS(SL)94-12). Scale bar = 100µm

Grain composition

The mineralogical composition determined by point-counting of the sandstones is as follows:

Quartz:	57.5% - 62.5%
Feldspar:	19% - 27%
Mica:	4.5% - 11%
Clay matrix	1.5% - 12%
Iron oxide	0.5% - 7%

The feldspars consist of orthoclase and polysynthetically-twinned plagioclase (Fig. 15). Microcline feldspar grains also occur. The micas consists mainly of biotite, with minor muscovite. The clay minerals that are present in the thin-sections occur as matrix. The

biotite most probably alters to iron-rich clay. Thin hematite flakes are interspersed with the clays, but also occur as a coating on detrital grains (Fig. 16). Platy, euhedral crystals, possibly hematite, are also present (Fig. 17).

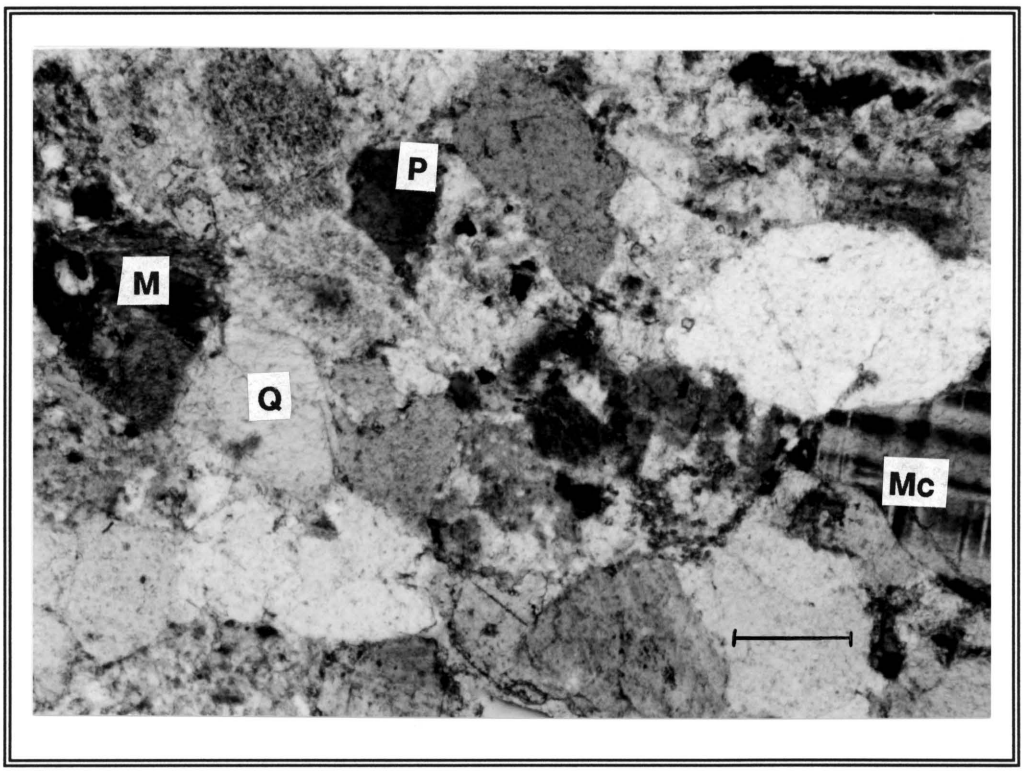

FIGURE 15. Microcline (Mc), twinned plagioclase (P), quartz (Q) and mica (M) grains from a sandstone of the *Dicynodon - Theriognathus* Assemblage Zone (Sample JS(SD)94-6). Crossed nicols. Scale bar = 100µm

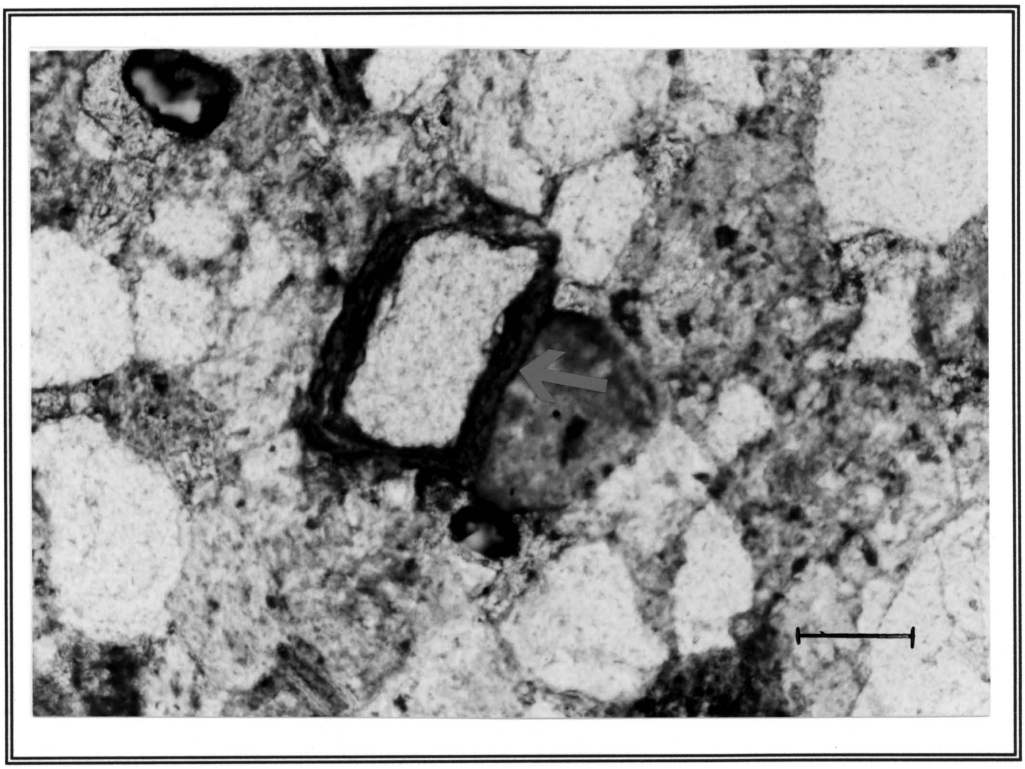

FIGURE 16. Hematite coating on a detrital grain from a sandstone of the *Lystrosaurus* - *Procolophon* Assemblage Zone (Sample JS(SL)94-13). Scale bar = 100µm.

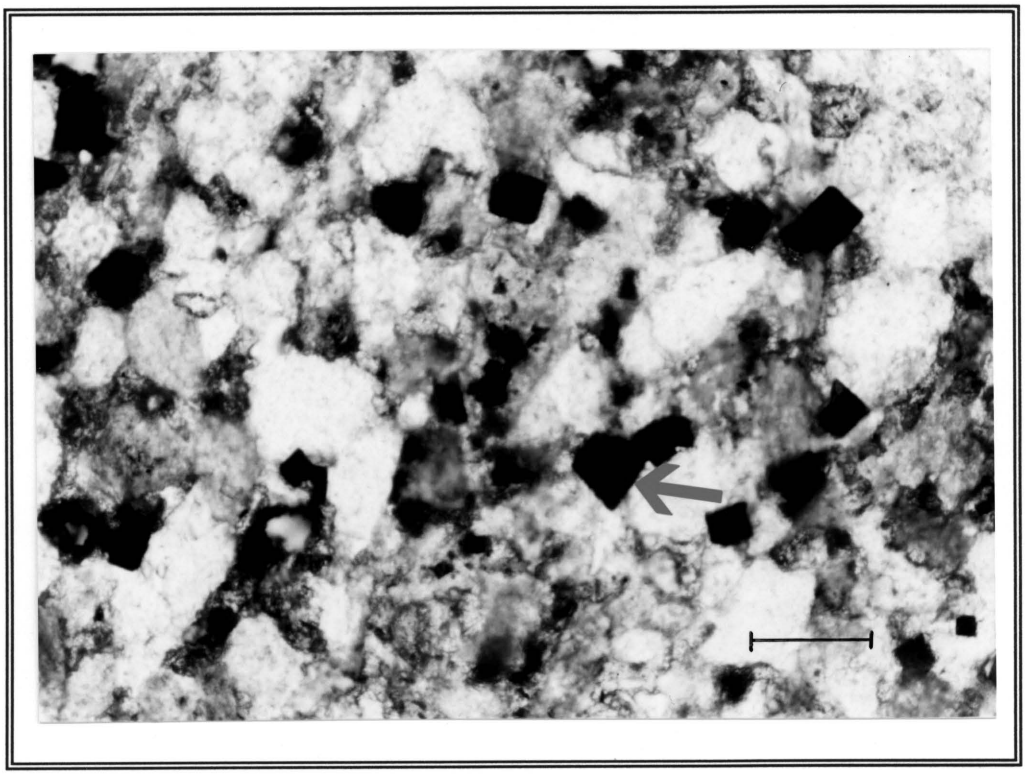

FIGURE 17. Platy, euhedral hematite crystals in the sandstone (Sample JS(SL)94-13). Scale bar = 100µm.

Grain shape

Grain shapes range from sub-angular to sub-rounded. The sphericity of the grains is low.

Diagenesis

From the thin-sections of the sandstones, the presence of hematite (red pigment) can be detected. The relevant diagenetic process includes the ageing and dehydration of brown, amorphous ferric oxide to goethite and the subsequent dehydration of goethite to hematite. Warm climates promote the alteration of brown (limonite) to red (hematite) pigments that cover sand grains (Van Houten, 1968; Pettijohn *et al.*, 1973). According to Van Houten (1968) and Walker (1967), most of the diagenetic hematite in sandstones owes its origin to *in situ* alteration of iron-rich minerals in hot, dry regions. In one of the sandstone samples, JS(SD)-10, brownish-red nodules can be observed. Nodules in sandstone are textural evidences of diagenesis (Pettijohn *et al.*, 1973). The mineralogy of the grains inside the nodules is the same as outside the nodules. The cement in the nodules is hematite and hematite overgrowths are present on the grains. Clay deformation and the formation of clays from micas are also part of the observed diagenesis.

Classification

The sandstones are classified as feldspathic arenites according to the classification system of Dott (1964). Arkoses are usually derived from a highly feldspathic igneous or metamorphic terrain, and form in close proximity to their sources and have a very limited distribution (Pettijohn *et al.*, 1973). The sandstones of the study area were therefore probably derived from a granitoid source area.

4.1.2.2 Clay mineralogy and diagenesis

Seven samples of mudrock were collected from the farm Venus 1320 in the Verkykerskop district (Fig. 3a). Samples JSL1-94, JSL3-94 and JSL4-94 were collected from the *Lystrosaurus - Procolophon* Assemblage Zone (Harrismith Member) and samples JSD5-94, JSD7-94, JSD8-94 and JSD11-94 from the *Dicynodon - Theriognathus* Assemblage Zone (Schoondraai Member).
The x-ray diffraction results are given in Table 8.

TABLE 8. X-ray diffraction results of the mudrock samples (%).

SAMPLE	BIOZONE	SMECTITE	ILLITE	CHLORITE	QUARTZ	PLAGIOCLASE
JSL1-94	*Lystrosaurus* (top)	13	20	4	51	11
JSL3-94	*Lystrosaurus*	8	16	15	47	14
JSL4-94	*Lystrosaurus*	13	13	11	48	15
JSD5-94	*Dicynodon*	7	12	11	43	27
JSD7-94	*Dicynodon*	8	10	12	52	18
JSD8-94	*Dicynodon*	11	21	3	53	11
JSD11-94	*Dicynodon* (base)	6	17	1	65	11

The clay minerals present in the seven samples are smectite (6% - 13%), illite (10% - 21%) and chlorite (1% - 15%), which are associated with quartz (43% - 65%) and plagioclase, the latter probably albite (11% - 27%). No potassium feldspar appears to be present. The illite has a shoulder towards larger Å-values. This indicates the presence of illite-smectite interstratifications with a composition close to illite. These interstratifications constitute some proportions of the clay, but it is difficult to quantify them. These interstratifications, with a composition close to illite, are probably due to the breakdown of illite (Dr. D. Bühmann, pers. comm., 1995).

In the samples, the illite/smectite ratio varies from 1:1 to 2:1. Illite is normally a ubiquitous detrital phase in mudrocks (Rampino, 1983) and is commonly derived mainly from weathered micas, essentially muscovite. Illite also forms directly from solution at low and high temperatures, and by the conversion of smectite to illite/smectite during burial (Weaver, 1989).

Fine-grained, vitreous, volcanic debris is generally accepted as the source of smectite clay (Weaver, 1959; Grim, 1968). The presence of this clay mineral in all the samples could indicate the presence of a volcanogenic component. According to Rampino (1982) and Rampino and Reynolds (1983), discrete illite and mixed-layered smectite/illite represent altered volcanogenic material that has been partially illitized during mild burial diagenesis.
The illite present in the analysed mudrock samples was most probably derived from weathered micas.

It is difficult to visualise a source area lacking potassium feldspar. Potassium feldspar is stable in an acidic diagenetic environment, whereas plagioclase is stable in an alkaline diagenetic environment (Velde, 1985). The absence of potassium feldspar and presence of plagioclase in the present samples may, therefore, indicate that the diagenetic environment was alkaline. Another peculiar phenomenon is the occurrence of plagioclase and smectite. Smectite is diagenetically stable up to 100°C (Burst, 1959; Weaver, 1959; Dunoyer de Segonzac, 1969; Muffler and White, 1969; Browne and Ellis, 1970; Iijima, 1970; Perry and Hower, 1970; Van Moort, 1971 and Weaver and Beck, 1971). Plagioclase forms at a diagenetic temperature above 100°C (Dunoyer de Segonzac, 1970; Velde, 1985). At this temperature, smectite will alter to chlorite or mica (Porrenga, 1967; Rex, 1967; Velde, 1985). The smectite in the Beaufort samples examined here may have formed after diagenesis, due to weathering in a temperate climate where the drainage was moderately good (Jackson, 1959).

There appears to be a tendency for the percentage illite and quartz to decrease from the base of the sampled succession towards the approximate Permian-Triassic boundary. The percentages then increase again towards the top of the Normandien Formation succession studied here. The percentages of chlorite and plagioclase

increase from the base towards the Permian-Triassic boundary, and then decrease towards the top of the succession studied here (Fig. 18). The reason for these tendencies is not clear.

The fact that neither cristobalite nor laumontite is present in the samples, strongly suggests that the mudrocks are not bentonite. Cristobalite forms by *in situ* weathering of volcanic ash (McLachlan and Jonker, 1990) and laumontite is a product of the diagenetic alteration of fine-grained or glassy volcanic debris (Fuller, 1971; Elliot and Watts, 1974).

The X-ray diffraction results from the *Dicynodon - Theriognathus* Assemblage Zone and the *Lystrosaurus - Procolophon* Assemblage Zone show that the mudrocks are not bentonitic or tuffaceous. Diagenesis of the sediments most probably took place in a terrestrial, alkaline environment. As the temperature increased during diagenesis, the initial mixed layered structure of the clay minerals decreased its expandability. Quartz also formed during this stage. Further reduction in the expandability resulted in the production of chlorite. This condition persisted until no expandable material was present, only illite + chlorite + quartz remained (Velde and Bystrom-Bruzewitz, 1972). Chlorite could also have been formed from the iron in hematite. If the hematite was reduced during burial diagenesis, it would have reacted with silicates to form chlorite (Velde, 1985).

As the clay mineral smectite probably formed post-diagenetically, a volcanogenic component was most likely absent in the mudrocks. The illite-smectite interstratifications, which were probably formed due to the breakdown of illite, also indicate that the mudrocks began to alter due to weathering.

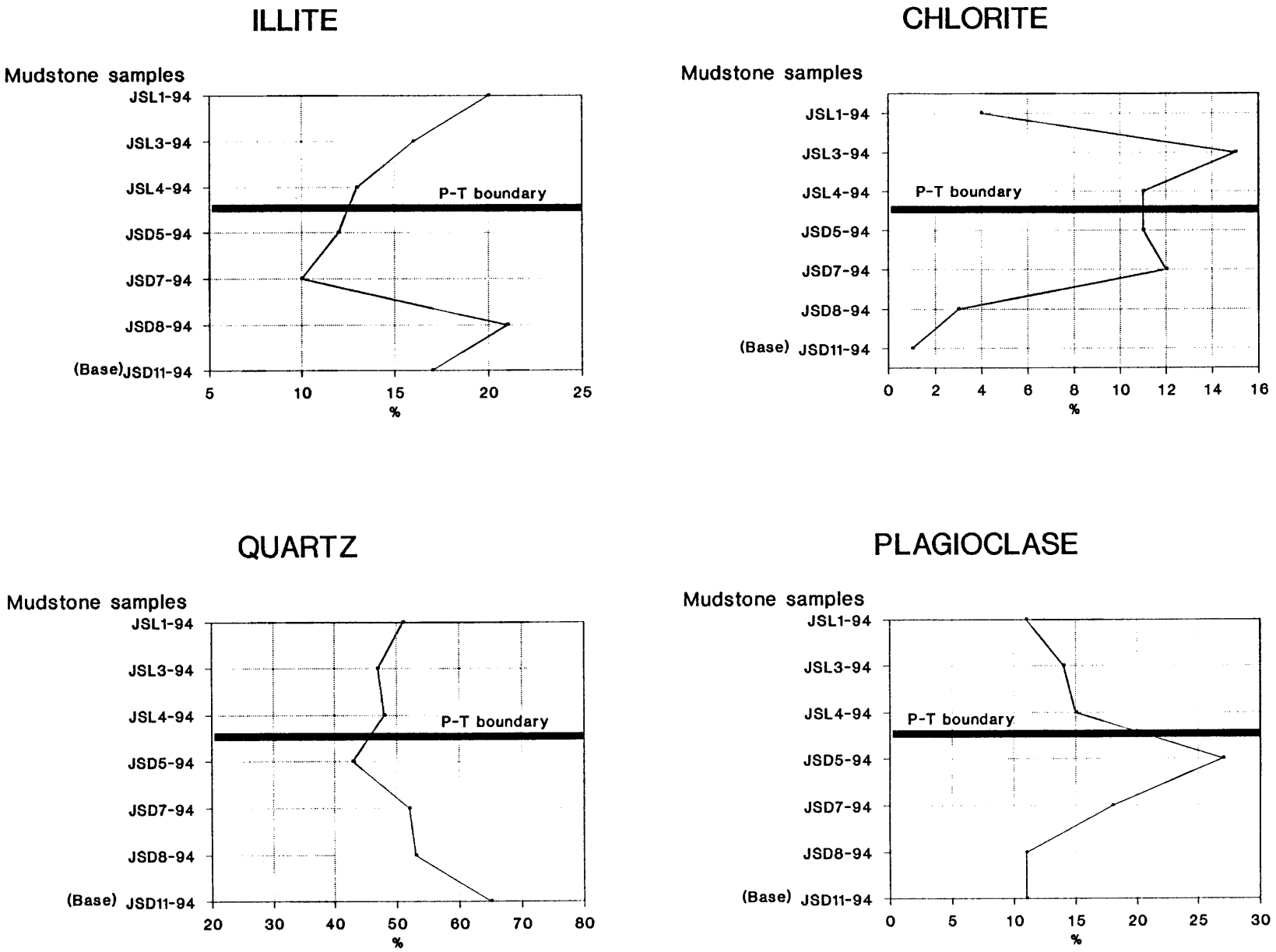

FIGURE 18. Variations of the mineral concentrations (%) in the mudrocks across the Permian-Triassic boundary in the Normandien Formation succesion sampled in this study.

4.1.3 GEOCHEMISTRY OF THE SEDIMENTARY ROCKS

4.1.3.1 Major elements

The samples of mudrock for major element analyses were collected from the farm Venus 1320 in the Verkykerskop district (Fig. 3a). Samples JSL1-94, JSL3-94 and JSL4-94 were collected from the *Lystrosaurus - Procolophon* Assemblage Zone (Harrismith Member) and samples JSD5-94, JSD7-94, JSD8-94 and JSD11-94 from the *Dicynodon - Theriognathus* Assemblage Zone (Schoondraai Member).
The major elements (expressed as concentration of oxides in wt%) were analysed on fusion discs and Fe_2O_3 (t) represents total Fe reported as Fe_2O_3. The results are given in Table 9.
The major element distribution across the Permian-Triassic boundary is shown in Figs. 18 and 19.

The mudrocks are relatively consistent in composition (Table 9). As seen from the appropriate figures, SiO_2 and Al_2O_3 fluctuate throughout the succession of mudrocks sampled. The variation of other major oxides (Fe_2O_3, TiO_2, MgO, CaO, K_2O and Na_2O) is also erratic showing no significant trends towards either depletion or enrichment from the base to the top of the succession. The Permian-Triassic boundary, which is situated approximately at the *Dicynodon - Theriognathus* Assemblage Zone and the *Lystrosaurus - Procolophon* Assemblage Zone transition, is placed between sample JSD-5 and sample JSL-4 (Figs. 18 and 19). No major variations can be detected from the major element distribution through the succession and the variation is generally small enough so that no extraordinary event is suspected.

TABLE 9. Major elements (conc. in wt%).

SAMPLE	JSL-1	JSL-3	JSL-4	JSD-5	JSD-7	JSD-8	JSD-11
SiO_2	61.68	62.15	60.49	64.96	66.82	61.17	64.95
TiO_2	0.82	0.70	0.69	0.73	0.62	0.74	0.75
Al_2O_3	17.98	16.27	14.99	16.46	15.10	16.53	15.53
Fe_2O_3(t)	6.45	6.17	4.96	4.96	4.65	7.78	5.52
MnO	0.07	0.06	0.08	0.08	0.06	0.28	0.05
MgO	1.37	1.68	1.65	1.58	1.55	2.13	1.60
CaO	0.53	1.12	1.28	1.50	1.55	1.41	1.18
Na_2O	0.71	1.03	1.05	1.35	1.62	1.05	1.47
K_2O	3.61	3.15	2.42	2.86	2.47	3.25	3.03
P_2O_5	0.08	0.16	0.14	0.14	0.11	0.32	0.16
H_2O-	2.51	2.34	3.30	1.72	1.35	1.12	1.82
H_2O+	3.64	3.44	3.08	3.00	2.74	3.95	3.22
CO_2	0.45	1.08	5.43	0.44	0.22	0.30	0.30
S	0.005	1.010	0.011	0.006	0.006	0.005	0.001
TOTAL	99.92	99.34	99.58	99.79	98.87	100.03	99.58
Org. C	0.044	-	0.805	0.051	-	-	0.017
CIA	78.76	75.43	75.94	74.44	72.81	74.33	73.22

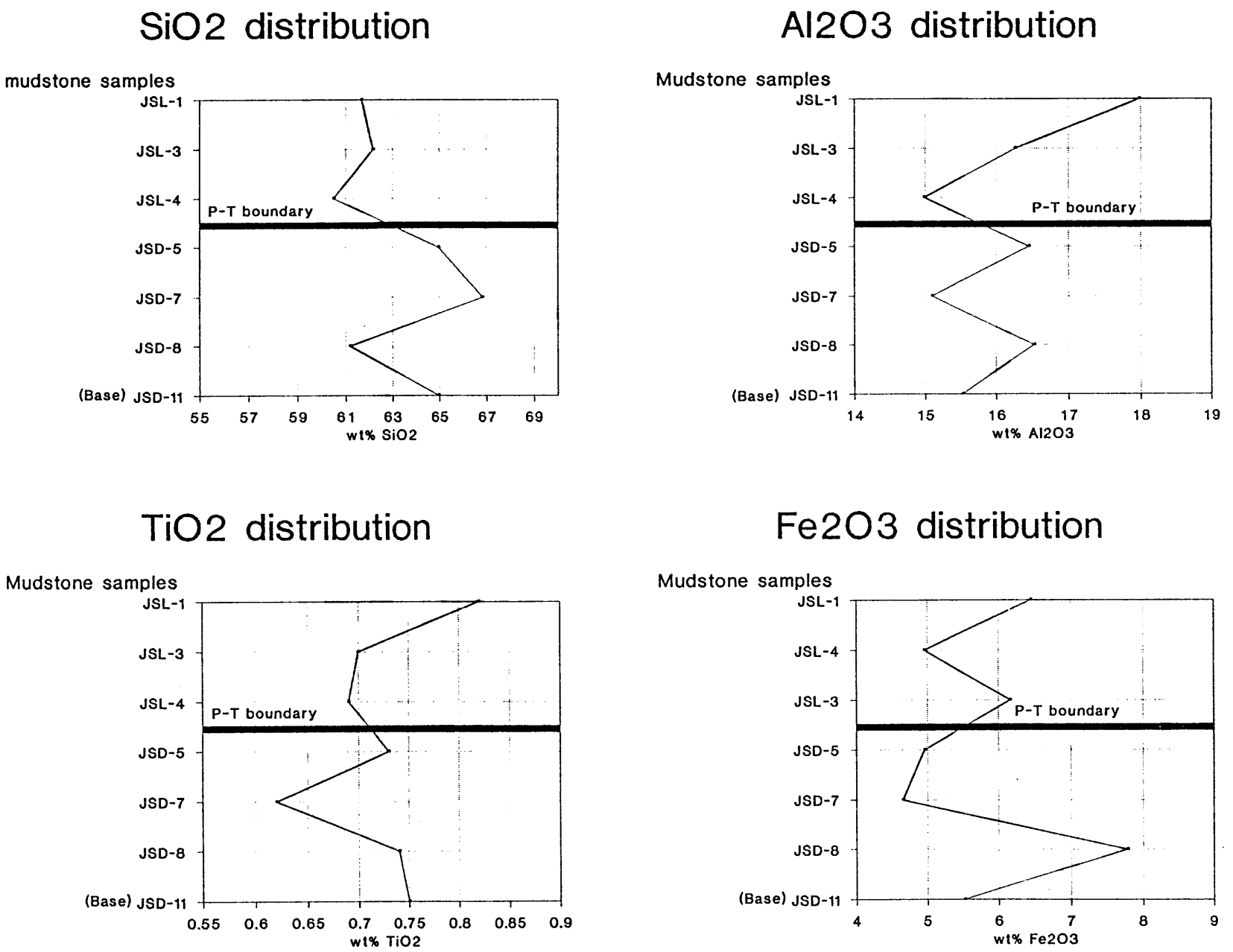

FIGURE 19. Major element distribution across the *Dicynodon - Theriognathus* and *Lystrosaurus - Procolophon* Assemblage Zones.

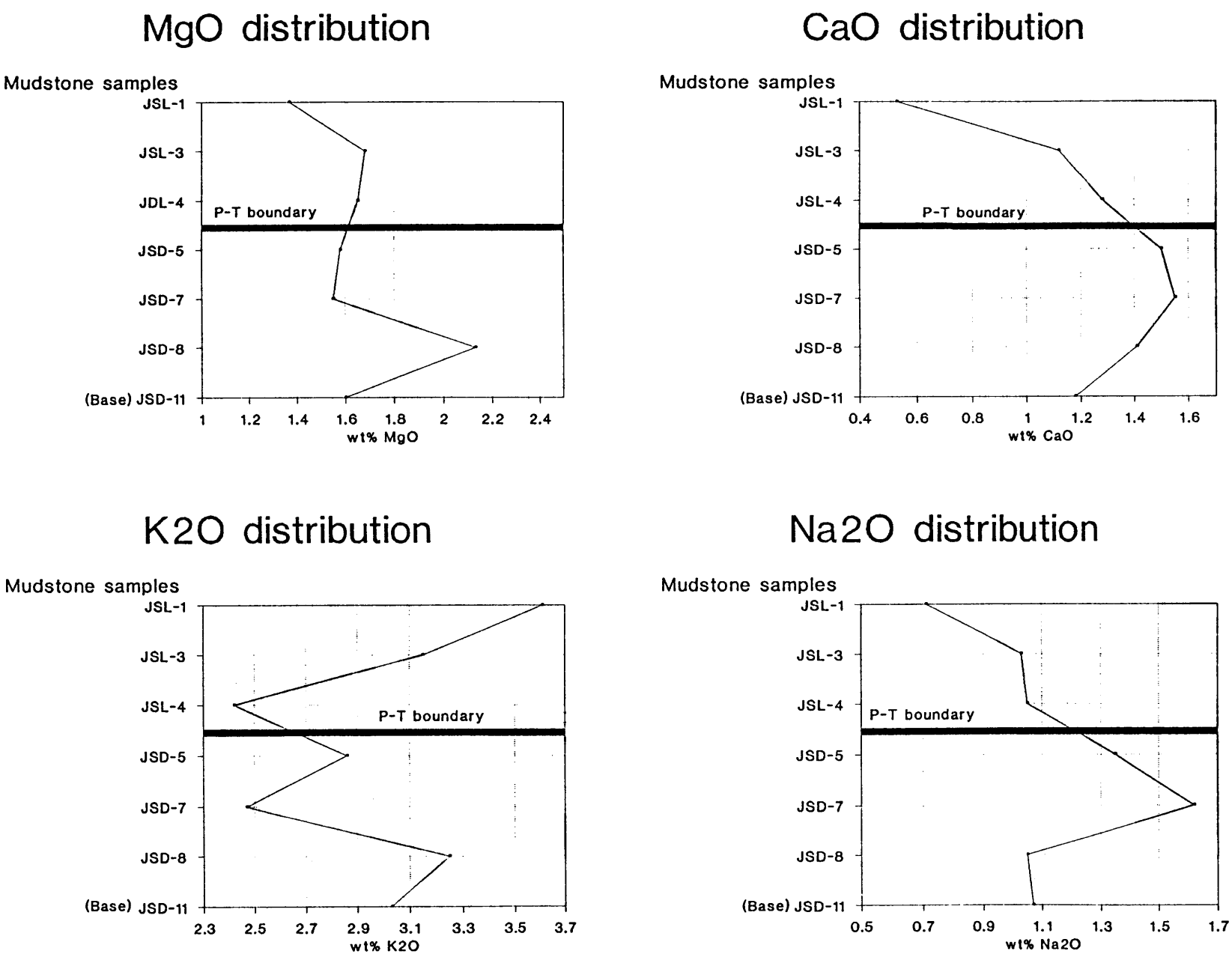

FIGURE 19. Major element distribution (continued).

The source area and synsedimentary weathering conditions of the mudrocks are reflected in the "Chemical Index of Alteration" (CIA)(Nesbitt and Young, 1982). The index is defined as follows:

$$CIA = [Al_2O_3/(Al_2O_3 + CaO + Na_2O + K_2O)] \times 100 .$$

The CIA index for the mudrocks sampled here is also shown in Table 9, along with standard values determined by Nesbitt and Young (1982) (Fig. 20).
There is a trend from low values in fresh rocks to progressively higher values in more intensely altered materials. The changes in CIA reflect changes in the proportion of feldspar and the various clay minerals in the profiles.

Fig. 20 shows the variation of the CIA values of the mudrocks from base to the top of the sampled Normandien Formation succession (basal sample is JSD-11 and top sample is JSL-1).
It is evident from Fig. 20 that the CIA for the mudrock samples varies from 72.81 to 78.76. These CIA-values are consistent with those of the "average shales" of Nesbitt and Young (1982). The highest value (thus highest degree of syndepositional detritus weathering) occurs near the top of the succession (sample JSL-1) and values decline slightly towards the base, although it seems that sample JSD-8 is slightly more weathered than samples JSD-7 and JSD-11.

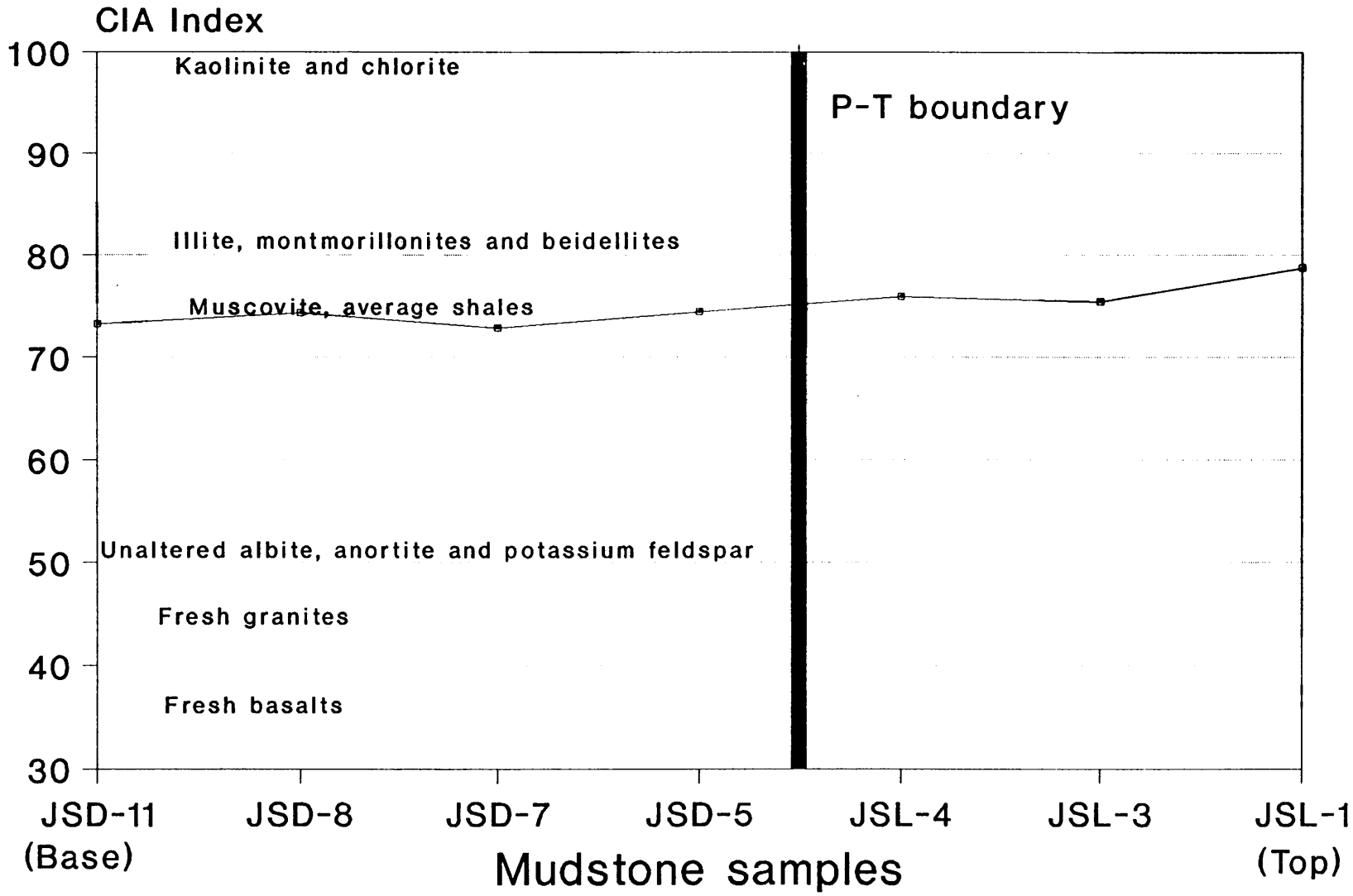

FIGURE 20. CIA-values for the mudrocks of the *Dicynodon - Theriognathus* and *Lystrosaurus - Procolophon* Assemblage Zones. Standard values of CIA-index for minerals and rocks from Nesbitt and Young (1982).

Acid volcanic material has a low TiO_2/Al_2O_3 ratio (<0.02)(Clark *et al.*, 1986). The TiO_2/Al_2O_3 ratio in typical shales may range from 0.035 to 0.05 (Spears and Kanaris-Sotiriou, 1979; Clark *et al.*, 1986). The TiO_2/Al_2O_3 ratio of the present samples is shown in Table 10.

TABLE 10. The TiO_2/Al_2O_3 ratio of the mudrock samples.

SAMPLE	BIOZONE	TiO_2/Al_2O_3 RATIO	INFERRED ROCK TYPE: VOLCANIC 0R SHALE
JSL-1	*Lystrosaurus* (top)	0.046	Shale
JSL-3	*Lystrosaurus*	0.043	Shale
JSL-4	*Lystrosaurus*	0.046	Shale
JSD-5	*Dicynodon*	0.044	Shale
JSD-7	*Dicynodon*	0.041	Shale
JSD-8	*Dicynodon*	0.045	Shale
JSD-11	*Dicynodon* (base)	0.048	Shale

As seen from Table 10, the samples tend to reflect shale rather than volcanic material.

The TiO_2/Al_2O_3 binary diagram after McLennan *et al.* (1979) can also be used to determine the probable source rocks of the mudrocks. The results of these data are given in Fig. 21 and indicate that the source area of the mudrocks was probably basaltic-granitic.

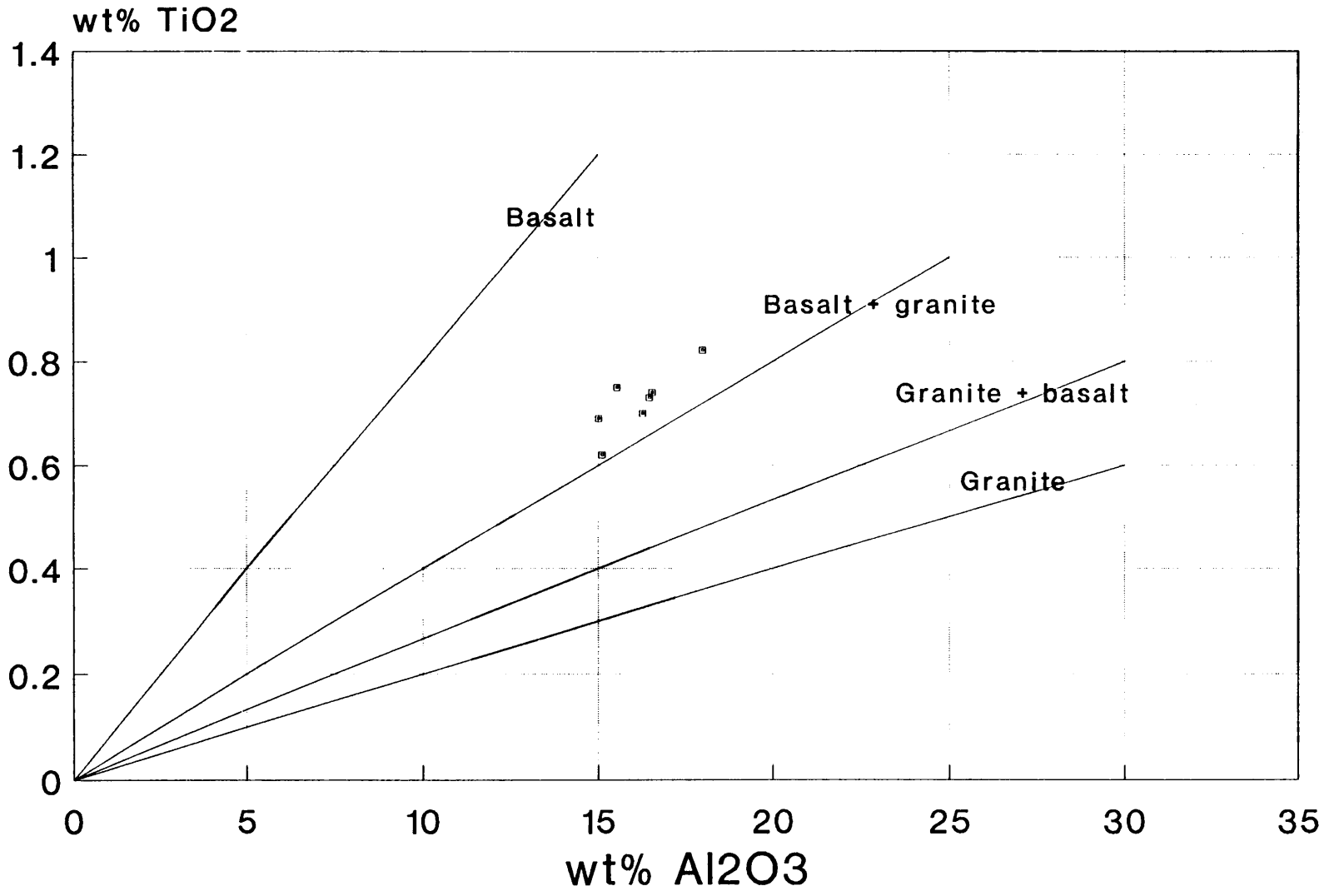

FIGURE 21. TiO_2/Al_2O_3-ratios of the mudrock samples and inferred source rock composition. (After McLennan *et al.*, 1979).

4.1.3.2 Trace elements

All the samples (JSL1-94, JSL3-94, JSL4-94, JSD5-94, JSD7-94, JSD8-94 and JSD11-94) submitted for major element XRF analyses, were also analyzed for common trace elements. The trace elements (concentrations in ppm) were analyzed on pressed pellets. The results are given in Table 11.

TABLE 11. Trace elements from pressed pellets

SAMPLE	JSL-1	JSL-3	JSL-4	JSD-5	JSD-7	JSD-8	JSD-11
Ba	1073	1270	558	1356	1095	1135	599
Cr	48	36	38	34	28	49	54
Cu	30	22	26	17	9	23	29
Ga	27	23	21	23	21	27	22
Hf	7	8	7	8	8	7	5
Mo	<2	<2	<2	<2	<2	<2	<2
Nb	23	21	20	20	19	20	20
Ni	27	23	23	19	20	40	30
Pb	33	31	27	26	24	28	22
Rb	200	177	124	155	139	172	155
Sc	16	13	13	14	10	13	9
Sr	153	195	243	316	481	180	148
Ta	<5	<5	<5	<5	<5	7	<5
Th	23	19	17	18	16	18	14
U	8	5	8	5	4	5	<2
V	102	84	84	88	72	99	108
W	6	<5	<5	7	<5	<5	<5
Y	56	32	42	37	31	39	29
Zn	116	87	99	92	76	103	98
Zr	235	266	248	269	242	189	148

The probable source rocks can also be inferred from the Cr/Zr ratios. Low Cr/Zr ratios point to predominantly granitic sources whereas higher Cr/Zr ratios point to contributions from ultramafic (komatiitic) rocks (Wronkiewicz and Condie, 1987). Oberthur (1986) considered Cr/Zr ratios > 1.20 as relatively high. The Cr/Zr ratios of the mudrocks are shown in Table 12.

TABLE 12. Cr/Zr ratios for the mudrock samples.

BIOZONES	SAMPLE	Cr/Zr RATIO	INFERRED SOURCE ROCKS
Dicynodon (base)	JSD-11	0.36	Granitic
Dicynodon	JSD-8	0.26	Granitic
Dicynodon	JSD-7	0.12	Granitic
Dicynodon	JSD-5	0.13	Granitic
Lystrosaurus	JSL-4	0.15	Granitic
Lystrosaurus	JSL-3	0.14	Granitic
Lystrosaurus (top)	JSL-1	0.20	Granitic

The data from the Cr/Zr ratio table show that the source area was probably granitic with little or no contribution from ultramafic rocks.

The trace elements rubidium (Rb), boron (B), vanadium (V) and copper (Cu) have been used as palaeosalinity indicators for the Beaufort Group mudrocks (Zawada, 1987). Many workers, including Cody (1971) have observed some useful results from palaeosalinity studies, but equally many researchers have had no success. No single trace element can be considered as an ideal palaeosalinity indicator. The availability of more data would have enabled a more complete discussion regarding the

palaeosalinity of the Beaufort Group. The purpose of the present determinations is therefore to see if there is any indication of strong relative changes across the Permian-Triassic boundary.

Rubidium is concentrated in marine shales (Degens *et al.*, 1957). Wedepohl (1978) stated that the Rb concentration of seawater is higher than that of fresh water, but that the concentration in sediments is low. According to Horstman (1957), adsorption plays an important role in the concentration of Rb.

Goldschmidt and Peters (1932) stated that marine clays have a higher concentration of boron (B) than fresh water clays. According to Wedepohl (1978), the initial concentration of B in a sediment can be modified by the content of detrital minerals present, rate of deposition and diagenesis. Cody (1971) therefore suggests that B can only serve to detect major differences in palaeosalinity.

The Rb/K ratio can also be used as an index of palaeosalinity. According to Campbell and Williams (1965), who worked on shales of the Lower Cretaceous in Canada, Rb/K ratios of approximately 250 are considered to be indicative of fresh water to brackish conditions. Values of <165 are indicative of marine conditions. These values are calculated as follows:

$$\frac{1}{(Rb/K \times 10^{-5})}$$

The data concerning the Rb/K ratios for the present study are given in Table 13.

TABLE 13. Rb/K ratios for the mudrock samples.

SAMPLE	BIOZONE	Rb (ppm)	WT% K_2O	%K	Rb/K x 10^{-5}	1/(Rb/K x 10^{-5})
JSL-1	*Lystrosaurus* (top)	200	3.61	3.01	0.0066	152
JSL-3	*Lystrosaurus*	177	3.15	2.63	0.0067	149
JSL-4	*Lystrosaurus*	124	2.42	2.02	0.0061	163
JSD-5	*Dicynodon*	155	2.86	2.38	0.0065	153
JSD-7	*Dicynodon*	139	2.47	2.06	0.0067	149
JSD-8	*Dicynodon*	172	3.25	2.71	0.0063	159
JSD-11	*Dicynodon* (base)	155	3.03	2.53	0.0061	163

The results from the Normandien Formation mudrock samples (Table 13) indicate a mean Rb/K value of 155. According to Campbell and Williams (1965) these values could indicate marine conditions.

Degens *et al.* (1957) also gave mean concentrations of Rb in sedimentary rocks (shales), as approximately 139 ppm for fresh water, 187 ppm for brackish water and 281 ppm for marine water deposits. The Rb concentrations of the mudrock samples range from 124 ppm to 200 ppm with a mean concentration of 160 ppm. From these data the inferred conditions were brackish to fresh water rather than marine. Such results as these support the generally accepted unreliability of palaeosalinity indicator elements. However, there is no evidence of major relative changes across the Permian-Triassic boundary.

4.1.3.3 Platinum group elements (PGE)

Platinum group elements are depleted in the earth's crust relative to their cosmic abundance. High concentrations of iridium (Alvarez *et al.*, 1980) and other noble metals (Ganapathy, 1980; Kyte *et al.*, 1980; Smit and Hertogen, 1980) correlate with well-defined extinctions of marine organisms at the Cretaceous-Tertiary boundary. To several workers, these results indicate a major impact event which caused the mass extinction at this boundary (Asaro *et al.*, 1982; Sun *et al.*, 1984 and Xu *et al.*, 1985). The attention then shifted to the Permian-Triassic boundary, as this boundary records the greatest mass extinction in the Phanerozoic (Zhou and Kyte, 1988). Several research groups have analysed Permian-Triassic boundary sedimentary rocks for iridium, with conflicting results. Negative results were obtained by Asaro *et al.* (1982), Alekseev *et al.* (1983), Clark *et al.* (1986), Zhou and Kyte, (1988), whereas positive results were reported by Sun *et al.* (1984) and Xu *et al.* (1985). Asaro *et al.* and Alekseev *et al.* also argued that the negative results did not disprove an impact, and that sediments at the boundary could have been formed from the impact of a comet or a non-chondritic asteroid.

Evidence of an impact origin for the sedimentary rocks at the Permian-Triassic boundary includes the abundance of shattered mineral grains, shock lamellae in quartz, small shatter cones on clasts and a PGE anomaly (Keays *et al.*, 1981). According to Asaro *et al.* (1982), an iridium anomaly is present when the iridium concentration is higher than 0.055 ppb. The typical iridium concentration for continental crust is approximately 50 pg/g (or 0.05ppb) as determined in Mississippi Delta sediments by Fenner and Presley (1984). Rampino (1982) stated that no data are available for iridium behaviour during weathering, transportation, etc. Deep sea sediments can have an iridium concentration ranging from 0.83 ppb to as high as 7.6 ppb. Several workers have found iridium concentrations in deep-sea deposits that can be considered anomalous in terms of crustal abundances (Hariss *et al.*, 1968; Crocket *et al.*, 1973; Crocket and Kuo, 1979; and Kyte *et al.*, 1980). Manganese nodules and crusts in deep sea sediments have Ir concentrations up to 23.1ppb, average = 9ppb (Hariss *et al.*, 1968).

According to Bowles (1986), Mountain and Wood (1988) and Plimer and Williams (1988), PGE might be more mobile in some sedimentary environments than previously thought. There is evidence that volcanic aerosols might add to a PGE enrichment of the crust (Zoller, 1983; Koeberl, 1989). Tredoux *et al.* (1989) also stated that PGE anomalies in the sedimentary record cannot be used as unambiguous indicators of extraterrestrial influx, due to a lack of knowledge and data concerning the behaviour of the PGE in the sedimentary cycle.

Seven mudrock samples were analysed for the platinum group elements in the present study and especially for iridium. Results are shown in Table 14. The detection limit of NiS-NAA for each element (McDonald, 1993) is also shown.
Only the standards had values above the background values of the reagents. This implies that no PGE's are present in the samples, or that the concentrations are below the detection limit.

Blanks contained no concentrations of Pt, Pd or Au, but were contaminated for Ir, Ru and Os. The contamination was most probably brought about by the PGE traces in the nickel carbonate reagent. Tredoux (1990) and McDonald (1993) also expierenced contamination of the $NiCO_3$ reagent with PGE's.
The chondrite-normalized values of Ir, Ru and Os are always less than the values of Pt and Pd (Tredoux *et al.* 1989; Tredoux, 1990; Dr. R.J. Hart, pers. comm., 1995). The blank values of Ir, Ru and Os in this study are more than the blank values of Pt and Pd. This also implies that the blanks were contaminated.

TABLE 14. PGE and Au concentrations (ppb) of the mudrocks using NiS-NAA and the detection limits for each element. **ND** indicates that the element was not detected.

SAMPLE	Os	Ir	Ru	Rh	Pt	Pd	Au
JSD-11	ND	ND	ND	ND	ND	ND	ND
JSD-8	ND	ND	ND	ND	ND	ND	ND
JSD-7	ND	ND	ND	ND	ND	ND	ND
JSD-5	ND	ND	ND	ND	ND	ND	N66D
JSL-4	ND	ND	ND	ND	ND	ND	ND
JSL-3	ND	ND	ND	ND	ND	ND	ND
JSL-1	ND	ND	ND	ND	ND	ND	ND
Blank1 (B1)	ND	ND	ND	ND	ND	ND	ND
Blank2 (B2)	ND	ND	ND	ND	ND	ND	ND
Blank3 (B3)	ND	ND	ND	ND	ND	ND	ND
SARM-7 1:10	6.3	7.4	43	24	374	153	31
SARM-7 1:20	3.15	3.7	21.5	12	187	76.5	15.5
WITS-1	1.44	1.55	5.51	1.26	13.9	8.3	4.9
DETECTION LIMITS	0.2	0.005	1.0	0.35	2.5	0.8	0.001

4.1.4 The interpretation of the sedimentary lithofacies (Schoondraai and Harrismith Members)

A general interpretation of the different sedimentary rocks present in both the Schoondraai Member and the Harrismith Member will be given to avoid repetition. The facies described earlier in detail exhibited relatively small differences between the two members, and, for the sake of clarity and brevity, many facies are considered together below.

The **mudrocks** indicate suspension settling of very fine material in a low energy setting. The presence of horizontal laminae also suggests suspension settling (Harms *el al.*, 1975). The massive nature of some of the mudrocks may be due to the rapid deposition of sediment (Blatt *et al.*, 1972) or to organic activity (Reineck and Singh, 1973), although the former is the most likely. A lens of medium-grained sandstone is also present in lithofacies 2 of the Schoondraai Member. This lens probably indicates a small channel of moderate energy, eroding into the mudrock.
The X-ray diffraction analyses which were done on the mudrock samples, showed that the mudrocks were not bentonites (altered volcanic ash) or volcanic tuffs. Although the presence of the clay mineral smectite usually indicates a volcanic source for sediments (Weaver, 1959; Grim, 1968), the smectite in these samples most probably formed post-diagenetically due to weathering in a temperate climate where the drainage was moderately good. No cristobalite or laumontite is present to substantiate the presence of altered volcanic ash. The TiO_2/Al_2O_3 ratios of the mudrocks fall within the range for typical shales (0.035 - 0.05) and not in the range for acid volcanic material (< 0.02) (Spears and Kanaris-Sotiriou, 1979; Clark, *et al.*, 1986).

The **fine-grained sandstones** are most likely products of a low energy setting (lower flow regime) (Harms and Fahnestock, 1965). This is supported by the presence of ripple marks (Harms and Fahnstock, 1965; Simons, *et al.*, 1965). However, the massive character of some of the sandstones may suggest rapid deposition (Blatt *et al.*, 1972), and the planar stratification may reflect a high energy system (upper flow regime)(Harms *el al.*, 1975). Interbedded sandstone and mudrock lithofacies point to a fluctuation in energy levels - periods of suspension settling followed by periodic

higher energy traction sedimentation (Harms and Fahnstock, 1965; Hobday, 1973). The Harrismith Member, in places, has fine-grained sandstones with a reddish-brown colour. This colour may be due to oxidation during or after deposition. The upward-fining that occurs in almost all of the fine-grained lithofacies suggests a decrease in energy.

The **medium-grained sandstones** formed in a moderate to high energy setting, probably mostly in the upper parts of the lower flow regime and lower parts of the upper flow regime. The presence of horizontal laminae points to upper flow regime conditions, and the planar cross-bedding and cross-laminae present in the sandstone are evidence of the migration of small-scale, straight-crested bedforms under lower flow regime conditions (Allen, 1963; Simons *et al.*, 1965). Some medium-grained sandstones in the Schoondraai Member have a reddish colour, again probably indicating oxidation during or after deposition.

The **coarse-grained sandstones** also indicate a moderate to high energy setting (Simons *et al.*, 1965). Planar cross-bedding supports the migration of small-scale, straight-crested bedforms under lower flow regime conditions (Allen, 1963; Simons *et al.*, 1965). Some of the sandstones are well-sorted, which indicates an effective transport system (Brush, 1965). Massive sandstones can form in the upper flow regime, thus possibly implying higher energy conditions (Simons *et al.*, 1965; Conaghan and Jones, 1975), or very rapid deposition (Blatt *et al.*, 1972).

In the Schoondraai Member, calcareous concretions (dolomite) are present in the mudrocks of lithofacies 2. According to Dickson and Barber (1976), the formation of carbonate concretions can be linked to the distribution of organic matter, either as sporadic large carcasses, or small carcasses and microscopic organic detritus concentrated in particular horizons. Weeks (1957), Berner (1968), Sass and Kolodny (1972) and others have suggested that the decay of organic matter is the controlling factor, and Zangerl *et al.* (1969) demonstrated a close association between buried carcasses and concretions. Berner (1968a, b) proved experimentally that the Ca^{2+} from seawater will precipitate as a calcium salt, or as a soap of fatty acids, and is later converted to calcite. This conversion involves a density increase which causes

shrinkage of the concretion.

Studies of carbon and oxygen isotopic ratios support the organic influence in the precipitation of some concretions (Hodgson, 1966; Galimov *et al.*, 1968; Hoefs, 1970; Sass and Kolodny, 1972; Tan and Hudson, 1974). Tan and Hudson (1974) found that early diagenetic concretions, where the carbon is derived from decomposing organic matter, have negative values for $\delta^{13}C$. Late-diagenetic concretions, where decomposition of organic matter plays no part, have positive $\delta^{13}C$ values.

4.1.5 Palaeoenvironmental interpretation.

Schoondraai Member.

Lithofacies 1 and 2 represent the deposition of fine material, probably on a floodplain as a result of vertical accretion from overbank floods carrying suspended fine material. The massive nature of lithofacies 2 is probably the result of bioturbation, or rapid sediment deposition caused by a sudden decrease in energy. These conditions are compatible with a floodplain environment. The sandstone lens (lithofacies 2), with its erosive lower contact, probably indicates a small-scale channel cutting into the softer floodplain sediments (mud). The calcareous concretions which are present in lithofacies 2 could be due to abundant organic material, such as carcasses. This inferred floodplain palaeoenvironment would have been favourable for terrestrial life. After deposition, the conditions would have been wet and anaerobic, in order to preserve the carcasses of vertebrate fauna.

Lithofacies 3 consists of interbedded sandstone and mudrock, which are also compatible with floodplain deposition. These alternating beds of sandstone and mudrock probably developed in periods of intermittent flooding (sandstone) followed by suspension settling (muds), possibly due to seasonal control. Abundant signs of organic life such as fossil leaf imprints, fossil wood and vertebrate fossils, indicate a favourable environment for terrestrial life forms.

Lithofacies 4 is supportive of fluvial channel deposits, which tend to be upward-fining. This could be the result of channel migration under declining energy conditions. Cross-

bedded sandstones are attributed to deposition by migrating sand bars. The upward-fining cycles and the horizontal laminae of these sandstones (lithofacies 4) support deposition of the sandy sediment in an aqueous setting rather than an aeolian setting. Lithofacies 5 is also possibly compatible with fluvial channel deposits. Its massive sandy character can be due to rapid deposition or diagenesis.

The sandstones are classified as feldspathic arenites (Dott, 1964), with evidence for a granitoid source area. Such immature sandstones are consistent with fluvial sedimentation and seasonal flood deposits. Results from the clay mineralogy and the TiO_2/Al_2O_3 ratios show that the mudrocks are not bentonites. The synsedimentary weathering conditions of the mudrocks are reflected by the "Chemical Index of Alteration" (CIA). This index for the present samples is consistent with "average shales" (Nesbitt and Young, 1982). Information from the trace elements (Cr/Zr ratios) also suggests a probable granitic source for the Schoondraai Member mudrocks.

Harrismith Member.

This inferred palaeoenvironment differs relatively little from that proposed for the underlying Schoondraai Member.

Lithofacies 1, with its massive mudrock, is compatible with floodplain deposition. The yellow-green colour, as well as the iron oxide concretions (probably goethite) point to oxidation, and therefore aerobic conditions in a wet environment.

Lithofacies 2 consists of interbedded sandstone and mudrock, which possibly also indicate floodplain conditions, where flooding results in the formation of sandstone, and suspension settling in the formation of mudrock.

Lithofacies 3, 4 and 5 suggest fluvial channel deposition, because of the presence of upward-fining cycles, cross-bedding and ripple cross-lamination (lithofacies 4). The presence of plane bedding (lithofacies 3) and the massive character of lithofacies 5 suggest higher energy conditions such as in the upper flow regime. The reddish-brown colour of lithofacies 5 indicates oxidising conditions, probably when the environment became more arid. These arid conditions are also evident from the many casts of desiccation cracks associated with fossil finds (Groenewald, 1984; Rubidge *et al.*, 1991).

Regardless of small differences from the Schoondraai Member, the same inferred palaeoenvironmental conditions can be interpreted for the Harrismith Member from petrography, clay mineralogy, major and trace elements and absence of PGE concentrations in the rocks. Although some of the clay mineralogy trends seem to be different across the Permian-Triassic boundary, this is not confirmed by the geochemistry. The Harrismith sandstones can be classified as feldspathic arenites with a probable granitic source area. The clay mineralogy, TiO_2/Al_2O_3 ratios and CIA indicate that the mudrocks were not derived from altered volcanic ash or tuffs, but are "average shales", with a probable granitic source. Theron (1973) and Hobday *et al.* (1978) noted the presence of a major granitic source area to the southeast of the present subcontinent. PGE concentrations are very low or absent.

The proposed palaeoenvironment for the Schoondraai and Harrismith members agrees with the work of Groenewald (1984) on the sedimentology of the Beaufort Group in the northeastern Orange Free State. Turner (1977) proposed similar conditions in this study of the inferred fluvial palaeoenvironment (Model A) of the Lower Beaufort in the northeastern Orange Free State. Work by Theron (1973), Stavrakis (1980) and Hiller and Stavrakis (1984), mainly on sedimentary facies in the southeastern Karoo basin, is compatible with the model proposed here for the correlated facies in the nortern part of the Karoo basin. The inferred Normandien Formation palaeoenvironment is also consistent with the findings of Smith (1990), who studied alluvial paleosols and pedofacies sequences in the lower Beaufort in the southwestern part of the Karoo basin.

The palaeocurrent transport direction, indicated by cross-bedding, cross-laminae and ripple marks, tends to be from the northeast and southeast, towards the west for both members. These observations agree with the findings of Groenewald (1984), which suggest a northeastern, eastern and southeastern source area. Theron (1973) and Hiller and Stavrakis (1984) also noted general westward-directed palaeocurrent trends.

4.2 PALAEONTOLOGY: PETRIFIED WOOD

Previous research.

Warren (1912) described coniferous petrified wood from Upper Ecca (Permian) to Cretaceous strata. These woods belong to the class Gymnospermae, genus *Dadoxylon*. Walton (1925) described various specimens from the Karoo Supergroup of the Cape Province, identified as *Dadoxylon arberi*, class Gymnospermae.
Müller-Stoll and Mädel (1962) studied upper Cretaceous angiosperm woods from Pondoland, Cape Province, and Kräusel (1920), wood of the class Gymnospermae from the Karoo Supergroup in Namibia. Erasmus (1976a and b) studied fossil wood of Cretaceous and pre-Cretaceous age. Dr. M.K. Bamford (1993), from the Bernard Price Institute for Palaeontology at the University of the Witwatersrand, is at present working on fossil wood of Tertiary age (class Angiospermae), as well as Permian-Triassic wood (class Gymnospermae) of the Karoo Supergroup (pers. comm., 1995).

Terminology.

Much confusion exists around the usage of the genera *Dadoxylon* Endlicher and *Araucarioxylon* Kraus for fossil araucaroid wood (Erasmus, 1976a). The non-committal name *Dadoxylon* Endlicher has been used for secondary araucaroid wood types for a very long time. Many species of Palaeozoic and Mesozoic woods, Cordaitales and Coniferales woods, have been ascribed to this genus. Attempts were made to split the taxon, without any success. *Dadoxylon* has thus become a "collecting box" (Erasmus, 1976b). Both names were used by some authors, with *Dadoxylon* being applied to Palaeozoic woods and *Araucarioxylon* to Mesozoic and younger woods. According to Erasmus (1976a), the name *Dadoxylon* applies to both araucaroid Coniferales and Cordaitales woods. However, Lepekhina and Yatsenko-Khmelevsky (1966) stated that gymnosperm fossil wood from any deposit (including Palaeozoic wood) is found as fossil stems, with preserved pith and adjacent primary xylem and also in the form of secondary wood only. The genus *Araucarioxylon* is common among those fossils with **only secondary wood**. *Dadoxylon*, together with many other genera, is determined by the presence of **primary xylem structure and pith**. Greguss (1967) suggested that specimens with multiseriate xylem rays should be included in the genus *Dadoxylon*, whereas specimens with uniseriate xylem rays be ascribed to the genus

Araucarioxylon. However, this does not account for woods with uniseriate rays with biseriate portions.

Identification of fossil wood.

The specimens of petrified wood in the present study will, therefore, be studied according to characteristic features such as the presence/absence of pith, tracheid pitting and ray type.

Some of the present petrified wood specimens are well preserved, making identification possible from thin-sections. The aim of this study is to infer any palaeoenvironmental changes across the Permian-Triassic boundary from changes in the anatomy of the petrified wood. It is therefore beyond the scope of this study to identify the petrified wood to species-level. The cross-field pits are also seldom preserved, and they are important in species identification.

The wood was identified according to the arrangement of the tracheid pits. Three types of arrangements can be distinguished. The araucaroid-type of arrangement has alternating tracheid pits. The genera *Araucarioxylon* and *Dadoxylon* have this alternating arrangement (Fig. 22a.). The family Podocarpaceae and others have opposite-arranged tracheid pits in horizontal pairs, as well as uniseriate pitting. This is called abietoid-type arrangement (Fig. 22b.). The typical araucaroid pattern is totally absent. Genera that have this abietoid pit arrangement include *Mesembrioxylon, Podocarpoxylon* and *Phyllocladoxylon* and the rest of the Coniferales. The third or transition type has a mixed pit arrangement. The pits thus have both the araucaroid and abietoid arrangement in varying proportions (Fig. 22c.). According to Kräusel (1919), these transitional wood types are placed into the family Protopinaceae with genera such as *Australoxylon, Protophyllocladoxylon* and *Protopodocarpoxylon*, to name just a few.

It has been proposed that the araucaroid-type was the original type and that the abietoid- type has been derived from it. The mixed-type was thus an intermediate or transitional stage between the araucaroid and abietoid types. The araucaroid-type is considered to be older than the abietoid-type (Walton, 1925; Greguss, 1955), but still occurs in present-day living trees.

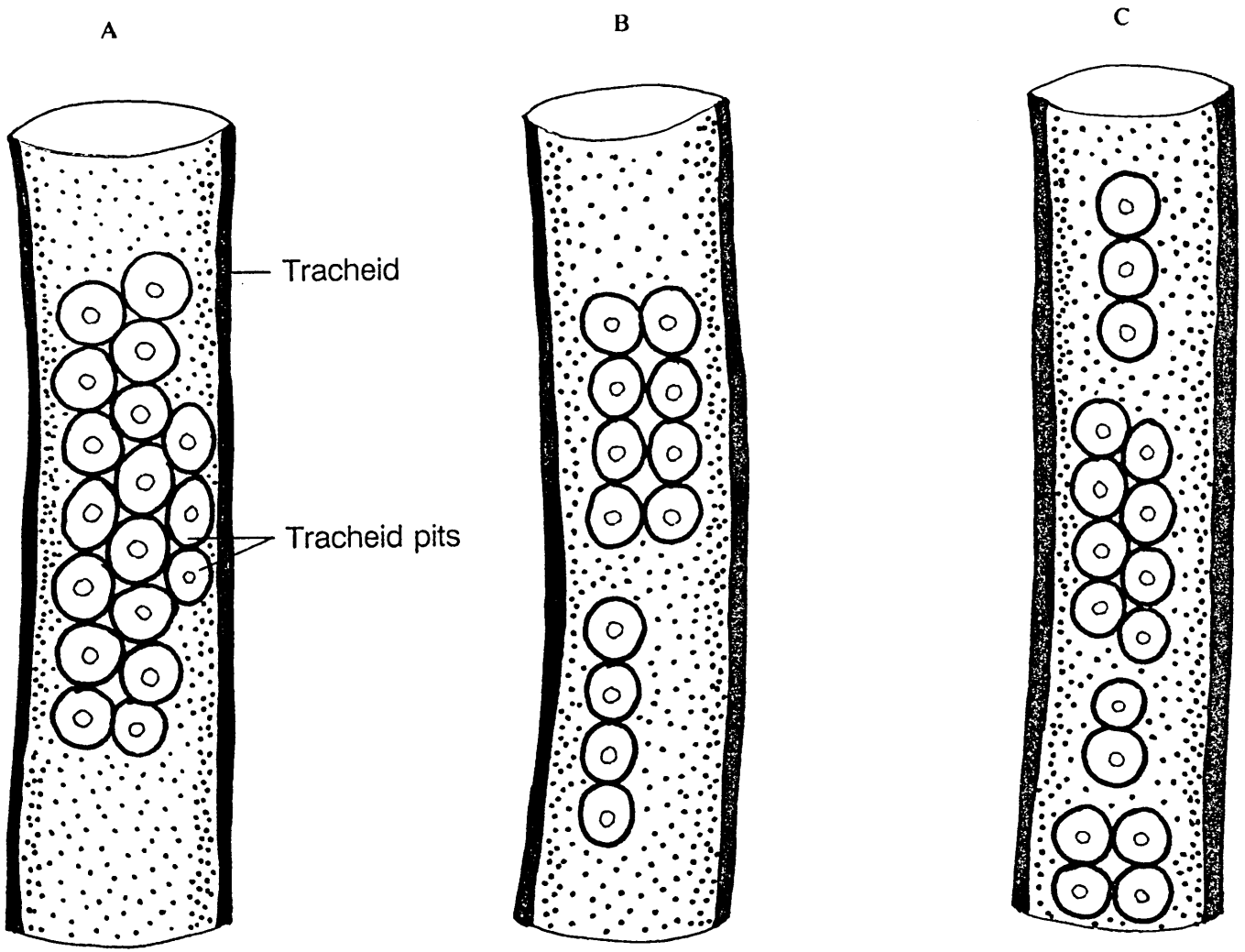

FIGURE 22. Tracheid pits with (A) araucaroid, (B) abietoid and (C) mixed arrangements, seen in tangential section.

Fossil wood was collected from the two assemblage zones, the *Dicynodon - Theriognathus* Assemblage Zone (Harrismith area) and the *Lystrosaurus Procolophon* Assemblage Zone (Senekal area). Specimens and slides are housed at the Palaeontological Section of the Council for Geoscience, Pretoria, South Africa.
Three thin sections were made from each specimen and are described in detail. The growth rings were also measured and used for palaeoclimatic interpretations (see section 4.2.3).

4.2.1 The *Dicynodon - Theriognathus* Assemblage Zone

Specimens JS1-93 to JS8-93 (total of 8 specimens) were collected from the farm Waterfall 1157 (28°17' S, 29°23'15" E) in the Van Reenen district (Fig. 3a). The petrified wood was found in sandstone. The size of the petrified wood ranges from pieces approximately 20cm in diameter to trunks 2m in length and 0.5m to 1m in diameter. Specimen JS9-93 was collected from the farm Venus 1320 (27°54' S, 29°26' E) in the Verkykerskop district (Fig. 3a). This wood was found in interbedded sandstone and mudrock. Specimens JS1-94 and JS2-94 were collected from the farm Schuinshoogte 506 (27°42' S, 29°03' E) in the Warden/Vrede district (Fig. 3a). These trunks were found *in situ* in weathered soil and have a length of approximately 10m and a diameter of 1m. All the specimens belong to the class Gymnospermae.

Specimen JS1-93
Locality: Farm Waterfall 1157, Van Reenen.
Size of specimen: axial(a) dimension = 11cm, radial(r) dimension = 12cm, tangential(t) dimension = 5cm (See Fig. 4 for explanation of dimensions).
Cross-section: Growth rings irregular, ring boundaries distinct and marked by thicker walled tracheids. Broad and irregular false rings are also present. The growth rings have a wavy appearance, probably due to the lithification process. A brownish-black substance, probably representing resin bodies, is also present within the lumina of some of the tracheid cells. The tracheid cells are square-shaped. The diameter of the tracheids is 32-48µm, with an average of 43µm. The thickness of tracheid walls is 3-

12µm, being 8µm on average.

Radial and tangential sections are poorly preserved. No information can be obtained.

Specimen JS2-93

Locality: Farm Waterfall 1157, Van Reenen.

Size of specimen: a = 17cm, r = 10cm and t = 5cm.

Cross-section: Consists of small sections of fossil wood due to the brittle nature of the specimen. The wood structure is well defined in some sections and poorly in other sections. The ring boundaries are marked by thicker walls. The well preserved tracheids have a rounded to almost square outline, with an average diameter of 43µm (range 32-64µm). The tracheid wall thickness varies from 3-9µm, with an average of 7µm. A black substance (probably iron oxide) occurs throughout the thin-section. Analyses of the thin-section by scanning electron microscope (SEM) show the presence of iron. Following the idea of Warren (1912), iron in solution probably infiltrated the early wood and was then precipitated as oxide. The brownish-black substance in some of the cells is thought to be resin bodies. There is a small branch coming off the main trunk.

Radial and tangential sections were too poorly preserved to show any cellular detail.

Specimen JS3-93

Locality: Farm Waterfall 1157, Van Reenen.

Size of specimen: a = 13cm, r = 10cm and t = 6cm.

Cross-section: The growth rings are well preserved and regular, although false growth rings are also present. The false rings are disturbed and deformed over a width of approximately 4mm. The width of a growth ring is approximately 0.5mm, and ring boundaries are marked by changing density and thicker walled tracheids. The tracheids have a almost square outline and vary in size from 24-48µm (average 38µm). The average tracheid wall thickness is 5µm (range 3-9µm). Fossil resin is also present and the colour ranges from golden yellow to brown.

Radial section: Pits on the radial walls of the tracheids are bordered. Multiseriate pits are rounded, with an alternate arrangement (Fig. 23), and are contiguous. Pit pores

are rounded, with a width of 4µm. Pits are 9-12µm in diameter. No cross field pits were observed.

Tangential section: The rays appear uniseriate. The number of cells ranges from 2-14 cells (7 cells on average) and they are 97-467µm in height. The shape of the ray cells is rounded, with a diameter of 40-48µm. Tangential walls of the tracheids are unpitted.

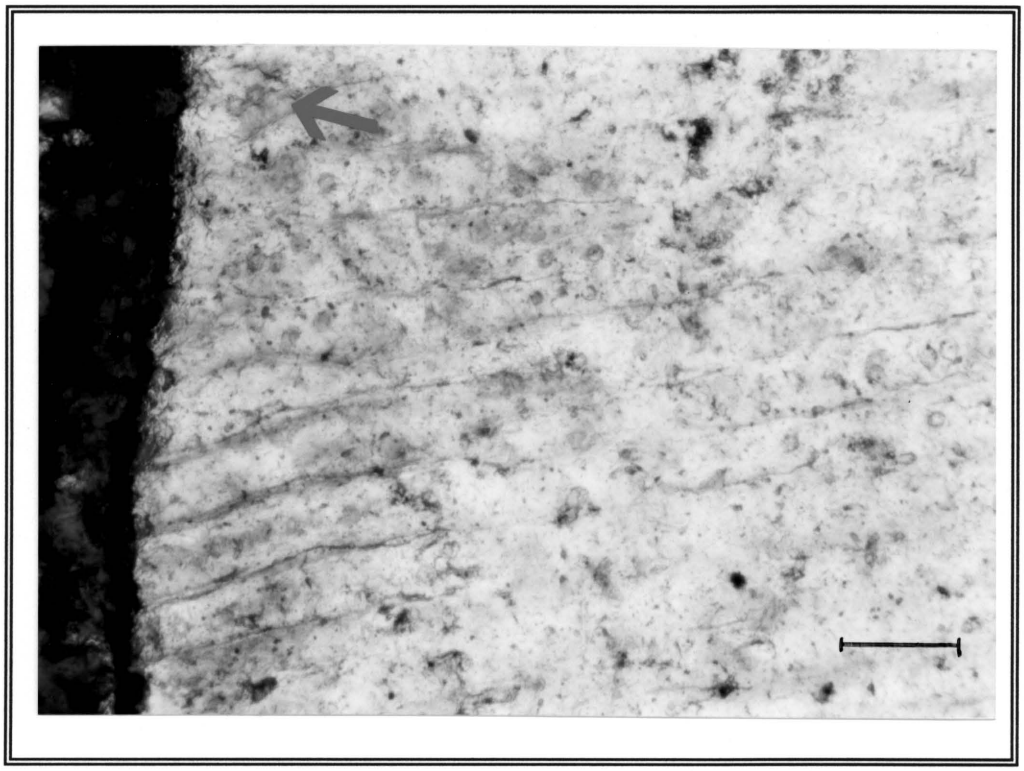

FIGURE 23. Longitudinal radial section. Bordered radial tracheid pits with an araucaroid arrangement (Specimen JS3-93). Scale bar = 100µm.

Specimen JS4-93

Locality: Farm Waterfall 1157, Van Reenen.

Size of specimen: a = 16cm, r = 14cm and t = 8cm.

Cross-section: Specimen poorly preserved. The growth rings are irregular and distorted, and ring boundaries are marked by thicker tracheid walls . Tracheid diameter ranges from 32-56µm (average 41µm). The average tracheid wall thickness is 5µm (range 3-9µm). The tracheids have a rounded to almost square outline. Brownish-black

resin is also present and colours the cells golden-brown.

Radial section: Bordered pits are present on the radial walls. Pits are uni- to multiseriate, rounded and separate. Pit pores are rounded with a width of 2-4µm. The pits measure 6-12µm in diameter. The multiseriate pits are arranged in stellate groups of one to two cells, and also have an araucaroid arrangement. The arrangement of pits for this specimen can thus be described as mixed. The auracaroid type predominates.

Tangential section: The rays are uniseriate ranging from 4-14 cells high (average of 9), and are about 177-484µm in height. Ray cells are square-shaped with a diameter of 32-48µm. Tangential walls are unpitted.

Specimen JS5-93

Locality: Farm Waterfall 1157, Van Reenen.

Size of specimen: a = 15cm, r = 15cm and t = 8cm.

Cross-section: Well preserved, with irregular growth rings. False rings are also present, which may be an indication of a sudden change in climate, probably due to cold or frost (Fritts, 1976). The shape of the tracheid cells is rounded to almost square. The ring boundaries are defined and marked by thicker walled tracheids. The average tracheid diameter is 38µm (range 16-48µm). The tracheid wall thickness varies from 3-9µm (average 5µm). The width of the late wood is much larger than that of the early wood. The early wood was subjected to drier or colder periods (less favourable conditions) during growth.

Radial section: Pits are bordered, uni- to multiseriate, rounded and separate. Pit pores are rounded with a width of 2-4µm. The pits measure 6-12µm in diameter. Multiseriate pits have an araucaroid arrangement (Fig. 24). The wood can be placed in the genus *Araucarioxylon*.

Tangential section: The rays are uniseriate and the height ranges from 2-17 cells (11 cells on average), 97-937µm in height. The ray cells are oval with a horizontal diameter of 16µm and a vertical diameter of 32-48µm. The tracheid walls are unpitted.

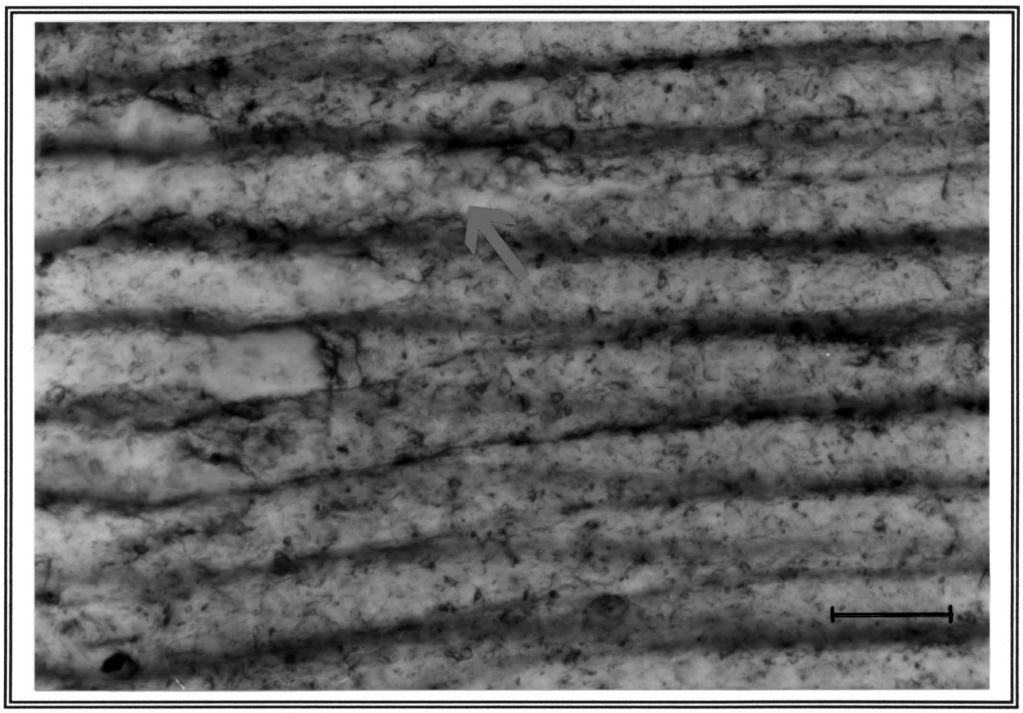

FIGURE 24. Longitudinal radial section. Bordered radial tracheid pits with an araucaroid arrangement (Specimen JS5-93). Scale bar = 100µm.

Specimen JS6-93

Locality: Farm Waterfall 1157, Van Reenen.

Size of specimen: a = 12cm, r = 14cm and t = 9cm.

Cross-section: Well preserved with irregular growth rings. Ring boundaries well defined (Fig. 25) and marked by thicker walled tracheids. The tracheids are almost square in outline and vary in diameter from 24-72µm (mean diameter 45µm). Tracheid wall thickness ranges from 1-3µm, being 2µm on average. Black "holes" are present. The origin of these holes is not clear, but they could have formed prior to petrification.

Radial section: The tracheids show bordered pits (Fig. 26), which are uni- to biseriate, rounded and separate. Pit pores are rounded, with a diameter of 2-4µm. The pits measure 9-12µm in diameter. The multiseriate pits are alternate, and the specimen can thus be placed in the genus *Araucarioxylon*.

Tangential section: The rays are uni- to partly biseriate (the latter are seldom present) (Fig. 27), with 2-14 cells (10 cells on average), 129-516µm in height. The ray cells are oval with horizontal diameter of 24-32µm and a vertical diameter of 48-64µm. Tracheid walls are unpitted.

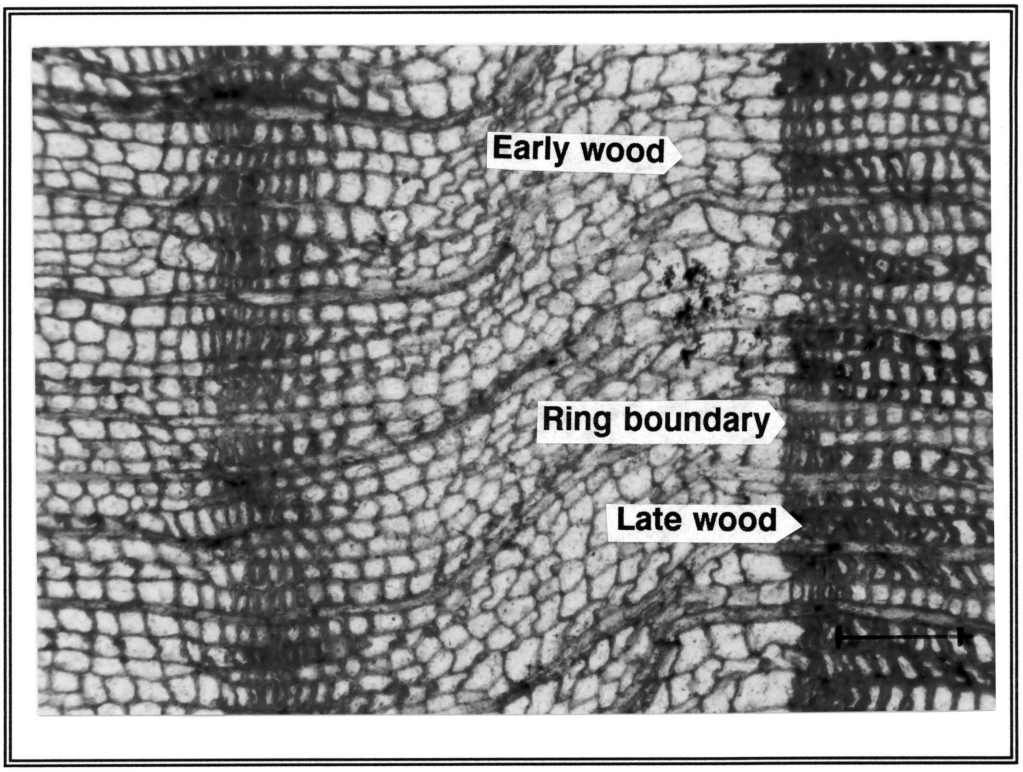

FIGURE 25. Cross-section. Clearly visible ring boundaries showing the difference between early and late wood cells in terms of colour change, wall thickness and radial diameter of the tracheids. (Specimen JS6-93). Scale bar = 100µm.

FIGURE 26. Longitudinal radial section. Bordered radial tracheid pits with an araucaroid arrangement (Specimen JS6-93). Scale bar = 50µm.

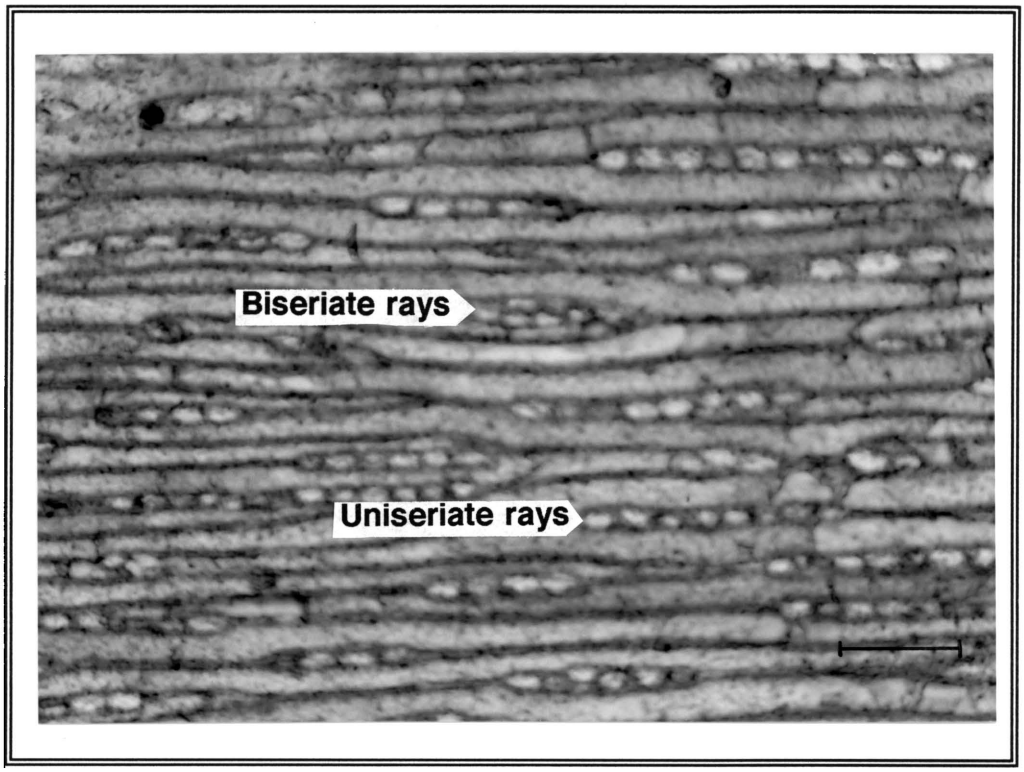

FIGURE 27. Longitudinal tangential section. Uniseriate and biseriate rays (Specimen JS6-93). Scale bar = 100µm.

Specimen JS7-93

Locality: Farm Waterfall 1157, Van Reenen.

Size of specimen: a = 12cm, r = 11cm and t = 8cm.

Cross-section: the growth rings are regular and boundaries are shown by the darkening of tracheids. The tracheids have a rounded to almost square outline with a mean diameter of 49µm (range 24-64µm). The tracheid wall thickness ranges from 3-6µm (average 5µm). False rings are also present.

Radial section: Pits are bordered, multiseriate, rounded to hexagonal and contiguous. From the alternate arrangement of the pits, the wood can be placed in the genus *Araucarioxylon*. Pit pores are rounded and 4-8µm in width. The pits are 12-16µm in diameter.

Tangential section: Rays are uniseriate with 4-18 cells (9 cells on average), and are 194-677µm in height. The ray cells are rounded with a diameter of 32-48µm. Tracheid walls are unpitted.

Specimen JS8-93

Locality: Farm Waterfall 1157, Van Reenen.

Size of specimen: a = 7cm, r = 14cm and t = 5cm.

Cross-section: Growth rings regular and well defined. Ring boundaries are marked by changing densities of the tracheids. False rings are also present. The tracheids have a squarish outline and vary from 16-64µm (average 48µm) in diameter. The tracheid walls have a mean thickness of 2µm (range 1-3µm).

Radial section: No information obtained due to poor preservation.

Tangential section: The rays are uniseriate, ranging from 3-17 cells (10 cells on average), 145-677µm in height. Ray cells are oval with a horizontal diameter of 24-32µm and a vertical diameter of 40-48µm. The tracheid walls are unpitted.

Specimen JS9-93

Locality: Farm Venus 1320, Verkykerskop.

Size of specimen: a = 17cm, r = 12cm and t = 6cm.

The specimen has a dark brown colour, probably due to iron components.

Cross-section: Due to the dark colour, only the regular "outlines" of the growth rings can be recognised. The cells seem to be deformed. This deformation can be due to compaction during lithification (Warren, 1912).

Radial and tangential sections are poorly preserved and too dark to give any information about the cellular structure.

Specimen JS1-94

Locality: Farm Schuinshoogte 506, Warden.

Size of specimen: a = 25cm, r = 14cm and t = 5cm.

Cross-section: The specimen is not well preserved and the growth rings seem to be regular, but deformed. The tracheids have an almost square outline, but most of them are deformed. Diameter of the tracheids ranges from 32-64µm with an average of 44µm. Tracheid wall thickness measures 2µm on average (range 1-3µm).

Radial section shows a cellular structure that is poorly preserved.

Tangential section: Due to poor preservation, very little detail is visible, but the rays

seem to be uniseriate and range in height from 4-20 cells, with 10 cells on average. Ray cells are rounded. Tangential walls of the tracheids are unpitted.

Specimen JS2-94

Locality: Farm Schuinshoogte 506, Warden.

Size of specimen: a = 14cm, r = 13cm and t = 5cm

Cross-section: The specimen is poorly preserved. The growth rings seem to be regular.

Radial section: shows no pitting between ray parenchyma cells and axial tracheids. Radial tracheid pits are not preserved.

Tangential section: Uni- to partly biseriate rays are visible. The rays range from 3-25 cells (12 cells on average), 145-1016µm in height. The ray cells are oval with a horizontal diameter of 24-32µm and a vertical diameter of 32-48µm. The tracheid walls are unpitted.

4.2.2 The *Lystrosaurus Procolophon* Assemblage Zone

Specimens JS3-94 to JS13-94 (total of 11 specimens) were collected from the Senekal district (Fig. 3b). The zone where the wood was collected is approximately 12km in width and stretches 30km from east to west. According to Botha and Visser (1970), a petrified tree trunk of about 3m in length and 4.25m circumference was found *in situ* on the farm Langlaagte 389. The maximum diameter of the trunk was 1.14m. Six roots were visible and approximately 50 growth rings were present.

Although the wood examined here comes from the Katberg Formation (equivalent to the Verkykerskop Formation in the Harrismith area)(Groenewald, 1984),it is still from the *Lystrosaurus Procolophon* Assemblage Zone (Hiller and Stavrakis, 1984)(See table 4). No wood was found in the Harrismith Member (Normandien Formation) or the Verkykerskop Formation. These two units represent the *Lystrosaurus Procolophon* Assemblage Zone in the Harrismith area.

The petrified wood was collected from the farm Langlaagte 389 (28°20'28" S, 27°24'44" E) in the Senekal district (Fig. 3b). The wood was found in *in situ* weathered soil, together with sandstone. The size of the wood ranges from approximately 10cm in diameter and 10cm in length to as big as 50cm in diameter and 1m in length. The collected petrified wood was all from the class Gymnospermae.

Specimen JS3-94

Locality: Farm Langlaagte 389, Senekal.

Size of specimen: a = 16cm, r = 10cm and t = 9cm.

Cross-section: The specimen is only partially preserved. The growth rings seem to be irregular and exhibit a "chevron-type" deformation (Fig. 28). This deformation is caused by the collapse under pressure of the large, thin-walled early wood tracheids, whereas thick-walled late wood tracheids are more resistant. The pressure is produced during lithification compaction. Ring boundaries are marked by a change in the colour of the tracheids. Undeformed tracheid cells have a rounded to oval outline. Tracheid diameter is 34µm on average (range 32-40µm). The tracheid wall thickness varies from 3-6µm, with an average of 5µm. A euhedral mineral, with a dark reddish-brown colour, is also present throughout the thin-section. The mineral is probably hematite.

Radial section: Pits are simple, uni- to multiseriate, rounded and separate. The multiseriate arrangement of the pits is of araucaroid-type, characteristic of the genus *Araucarioxylon*. The pits are 9-12µm in diameter. The early wood appears light brown whereas the late wood appears dark brown. The dark reddish-brown minerals are also visible.

Tangential section: The rays are uniseriate and range from 3-14 cells (8 cells on average), 81-452µm in height. Ray cells are rounded and 24-32µm in diameter. The tracheid walls are unpitted.

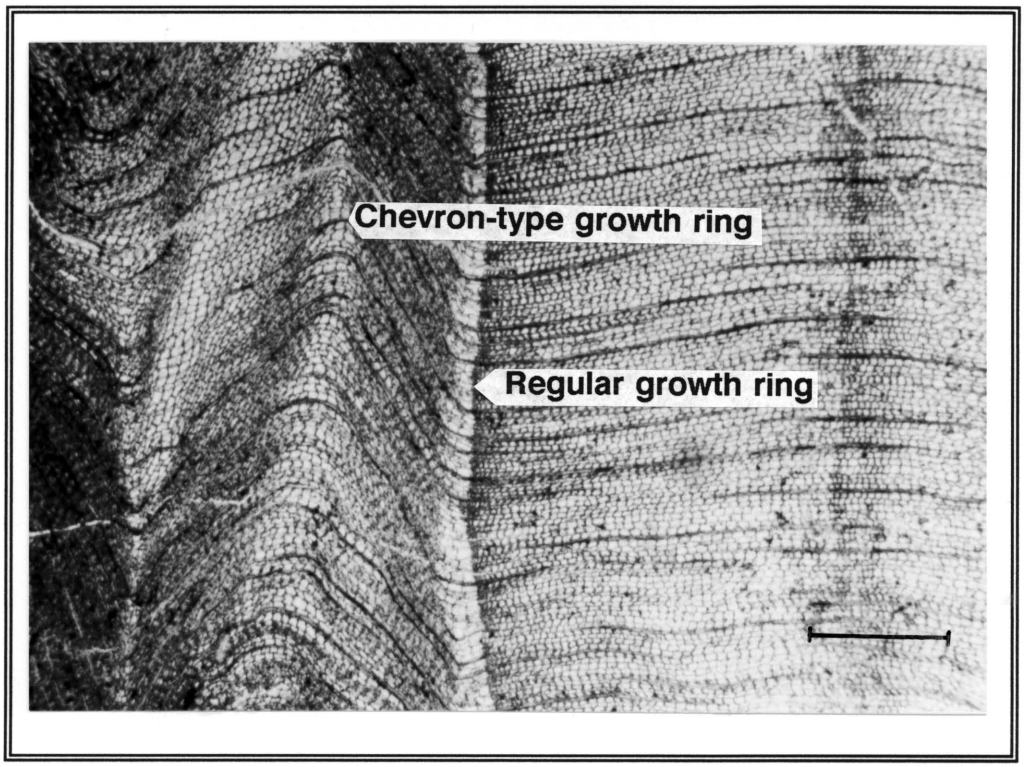

FIGURE 28. Cross-section. A regular growth ring together with a "chevron-type" deformed ring (Specimen JS3-94). Scale bar = 500µm.

Specimen JS4-94

Locality: Farm Langlaagte 389, Senekal.

Size of specimen: a = 14cm, r = 10cm and t = 9cm.

Cross-section: Regular growth rings, but deformation and distortion of the squarish tracheids occurs. Ring boundaries are marked by a change in tracheid colour. "Chevron-type" deformation is also visible from the darker coloured late wood (Fig. 29). The diameter of the tracheids ranges from 16-48µm, with a mean diameter of 37µm. The average width of the tracheid walls is 4µm (range 3-6µm). Dark reddish-brown mineral deposits, probably hematite, are present.

Radial and tangential sections show no cellular detail. Dark reddish-brown disc-like bodies (Fig. 30) occur together with euhedral minerals of the same colour (Fig. 31). With the aid of the scanning electron microscope (SEM) the discs were identified as iron oxide (probably hematite).

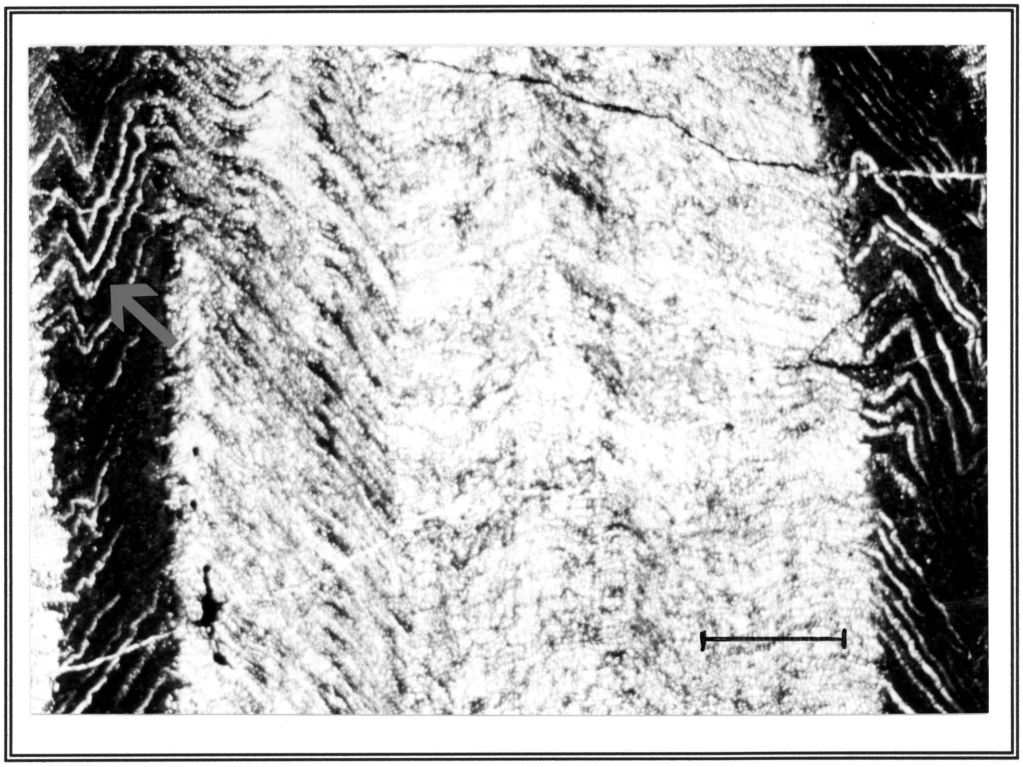

FIGURE 29. Cross-section. "Chevron-type" deformation of the growth rings clearly visible in the darker coloured late wood (Specimen JS4-94).
Scale bar = 500µm.

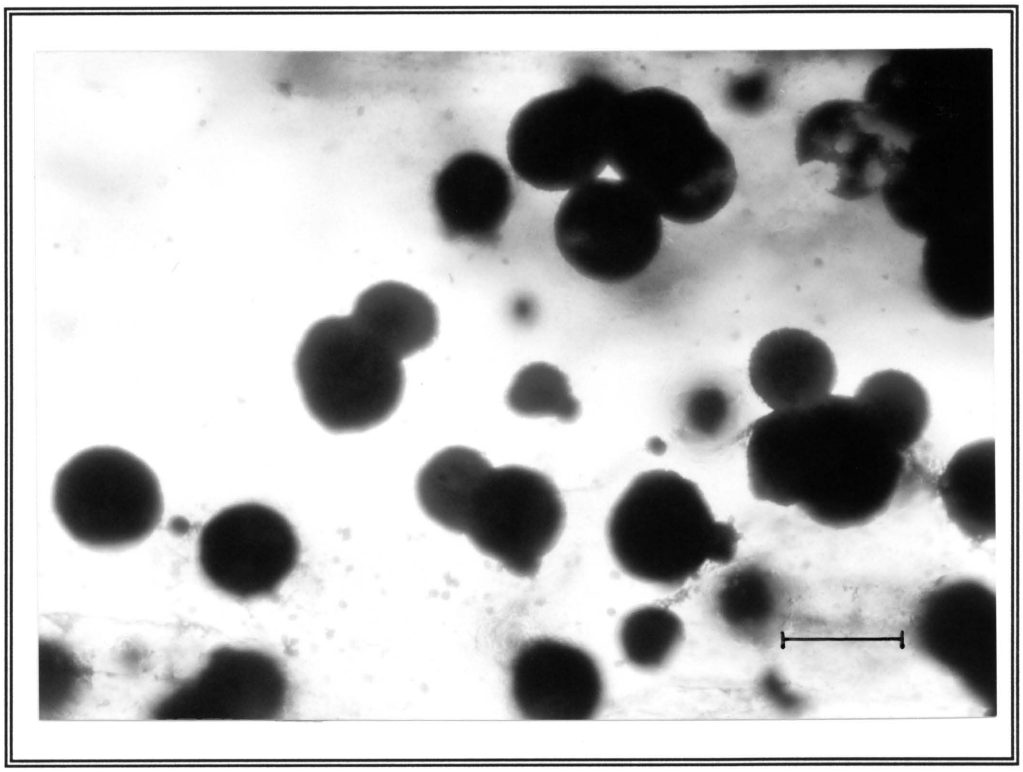

FIGURE 30. Longitudinal tangential section. Disc-like bodies with the same colour as the reddish euhedral minerals (Specimen JS4-94). Scale bar = 50µm.

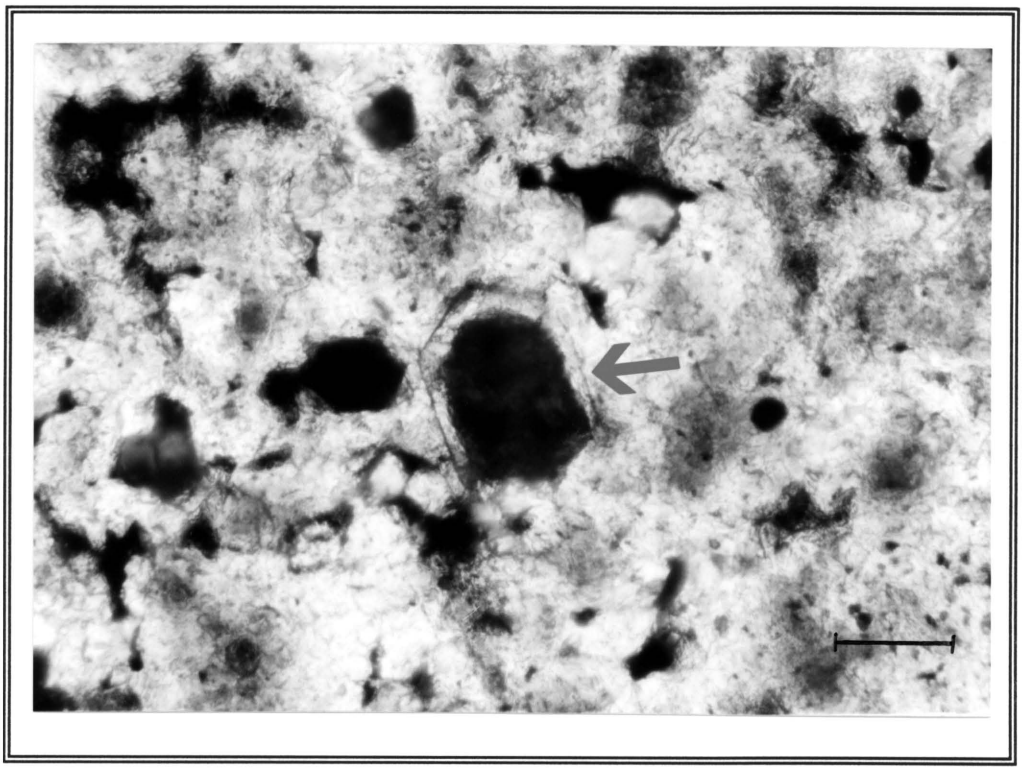

FIGURE 31. Longitudinal tangential section. Unidentified euhedral crystal replaced by iron oxide (Specimen JS4-94). Scale bar = 50µm.

Specimen JS5-94

Locality: Farm Langlaagte 389, Senekal.

Size of specimen: a = 15cm, r = 9cm and t = 7cm.

Cross-section: Growth rings seem to be regular, but the individual tracheid cells are deformed and poorly preserved. "Chevron-type" deformation is present together with dark reddish-brown hematite (Fig. 32).

Radial and tangential sections: The specimen is poorly preserved. Hematite and quartz can be recognised from the thin-sections.

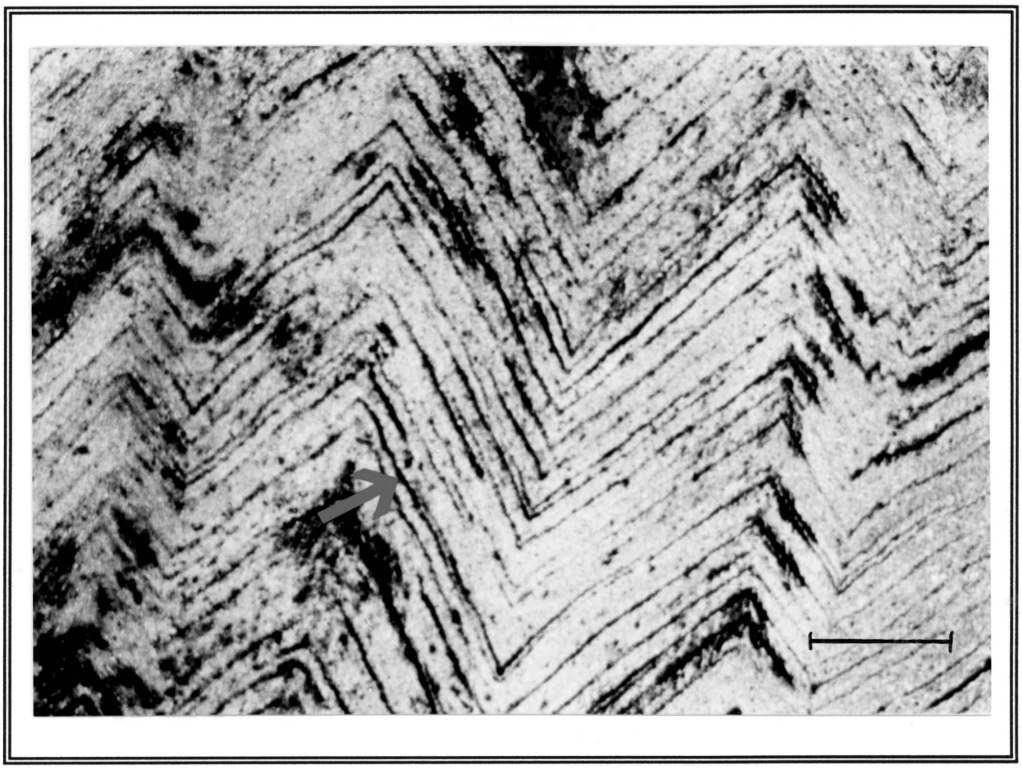

FIGURE 32. Cross-section. "Chevron-type" deformation of the growth rings together with hematite (Specimen JS5-94). Scale bar = 500µm.

Specimen JS6-94

Locality: Farm Langlaagte 389, Senekal.

Size of specimen: a = 11cm, r = 12cm and t = 9cm.

Cross-section: The specimen is well preserved and shows regular growth rings. Ring boundaries are defined and marked by thicker walled tracheids. False growth rings are also present. The false growth rings are very broad (approximately 30 cells in width) in comparison to the ring boundaries (about 3 cells in width). The tracheids have a rounded outline, but many cells are bent and deformed, probably due to compaction (Warren, 1912). The diameter of the tracheids is 49µm on average (range 24-80µm), whereas the thickness of the walls varies from 3-6µm, averaging 4µm.

Radial section: Pits are simple, multiseriate, hexagonal and contiguous. The pits measure 12-19µm in diameter. Greenish-brown spots occur throughout the thin-section. These spots are most likely residual debris from an insect (beetle or borer) that bored through the wood. This debris is called "frass" (Cichan and Taylor, 1982; Mason, 1992; Dr. M.K. Bamford, pers. comm., 1995). No evidence of resin production

by the plant, as a defence against the attack, was observed. The trunk was most probably already dead when it was bored. Broken-down cell walls can be observed in close proximity to the greenish-brown spots (Figs. 33 and 34).

Tangential section: Rays are uni- and partly biseriate and vary from 3-19 cells (9 cells on average), 97-548µm in height. The ray cells are rounded, with a diameter of 24-32µm. The tracheid walls are unpitted.

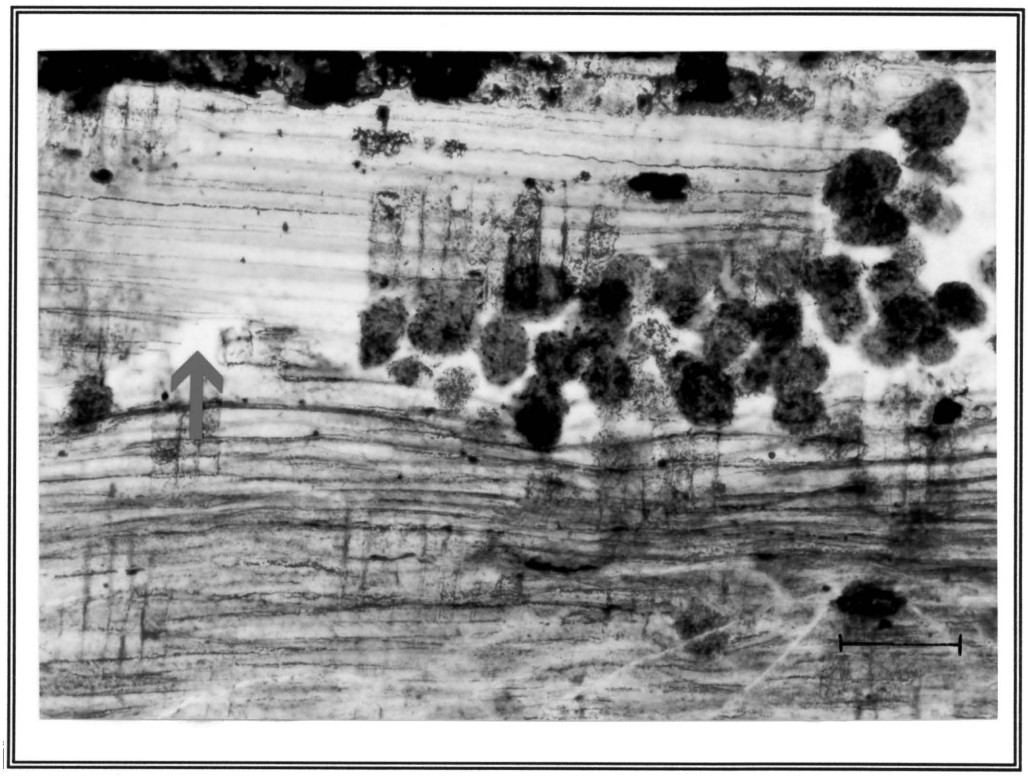

FIGURE 33. Longitudinal radial section. Greenish-brown spots present in the wood. The destruction of the wood is obvious. (Specimen JS6-94).
Scale bar = 100µm.

FIGURE 34. Longitudinal radial section. Broken-down cell walls in close proximity to the greenish-brown spots (Specimen JS6-94). Scale bar = 50µm.

Specimen JS7-94

Locality: Farm Langlaagte 389, Senekal.

Size of specimen: a = 9cm, r = 13cm and t = 10cm.

Cross-section: The growth rings are regular and ring boundaries are marked by thicker walled tracheids. False growth rings also occur. The rounded to oval tracheids are deformed in the false growth ring zone, where "chevron-type" deformation occurs. A reddish-brown to black opaque mineral (hematite) is also present (Fig. 35), as well as a greyish-black mineral with a metallic lustre in oblique incident light (probably pyrite)(Fig. 36). Measured tracheid diameter has an average value of 38µm (range 16-64µm). The tracheid wall thickness varies from 3-6µm, averaging 4µm.

Radial section: Pits on the radial walls of the tracheids are simple, multiseriate, hexagonal and contiguous. The diameter of the pits is 12-15µm. Pits are arranged in an araucaroid way, probably indicating the genus *Araucarioxylon*. The wood is very light coloured, but the early wood and late wood can be distinguished from each other by the darker colour of the latter.

Tangential section: Specimen is not well preserved. Rays are uniseriate and range from 3-22 cells (7 cells on average), 113-677µm in height. The ray cells are oval with

a horizontal diameter of 16-24µm and a vertical diameter of 24-32µm. Tracheid walls are unpitted.

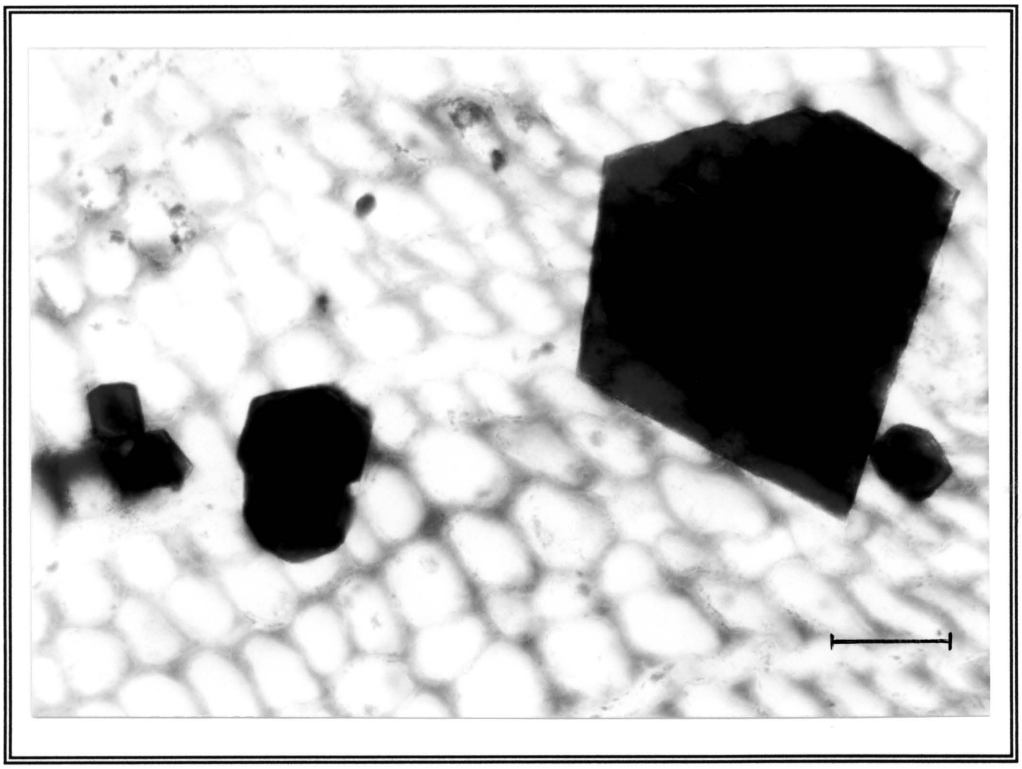

FIGURE 35. Cross-section. Reddish-black euhedral minerals (probably hematite) present in the petrified wood (Specimen JS7-94). Scale bar = 50µm.

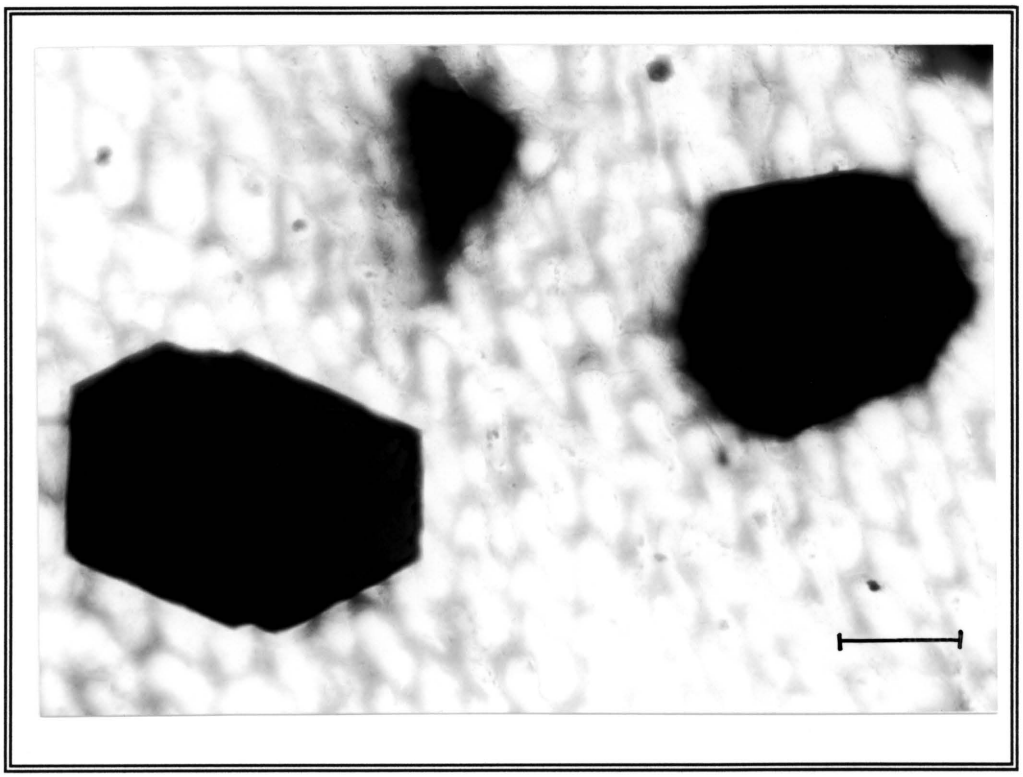

FIGURE 36. Cross-section. Greyish-black euhedral mineral with a metallic lustre (probably pyrite)(Specimen JS7-94). Scale bar = 50µm.

Specimen JS8-94

Locality: Farm Langlaagte 389, Senekal.

Size of specimen: a = 17cm, r = 17cm and t = 12cm.

Cross-section: Only a small, but well preserved piece of wood was studied. Growth rings are regular, with thicker tracheid walls to mark the ring boundaries. Tracheids have a rounded to almost square outline, average diameter of 44µm (range 16-64µm) and a wall thickness that varies from 3-6µm, averaging 4µm. The wood in the thin-section has a yellow-red colour, which appears black under the microscope. The colour is most probably due to goethite.

Radial section: Pits are bordered, uni- to multiseriate, round to hexagonal and contiguous. The pit pores are round with a diameter of 4-8µm. The pits measure 9-12µm in diameter. Cross-field pits are bordered with 2-3 pits, 4-8µm in diameter, in each cross-field. These oval pits are arranged in two vertical rows (Fig. 37). The bordered, radial tracheid pits are of araucaroid-arrangement, characteristic of the genus *Araucarioxylon* (Fig. 38).

Tangential section: Rays are uniseriate, ranging from 2-20 cells (10 cells on average), 81-710µm in height. The ray cells are rounded with a diameter of 24-32µm. The tracheid walls are unpitted.

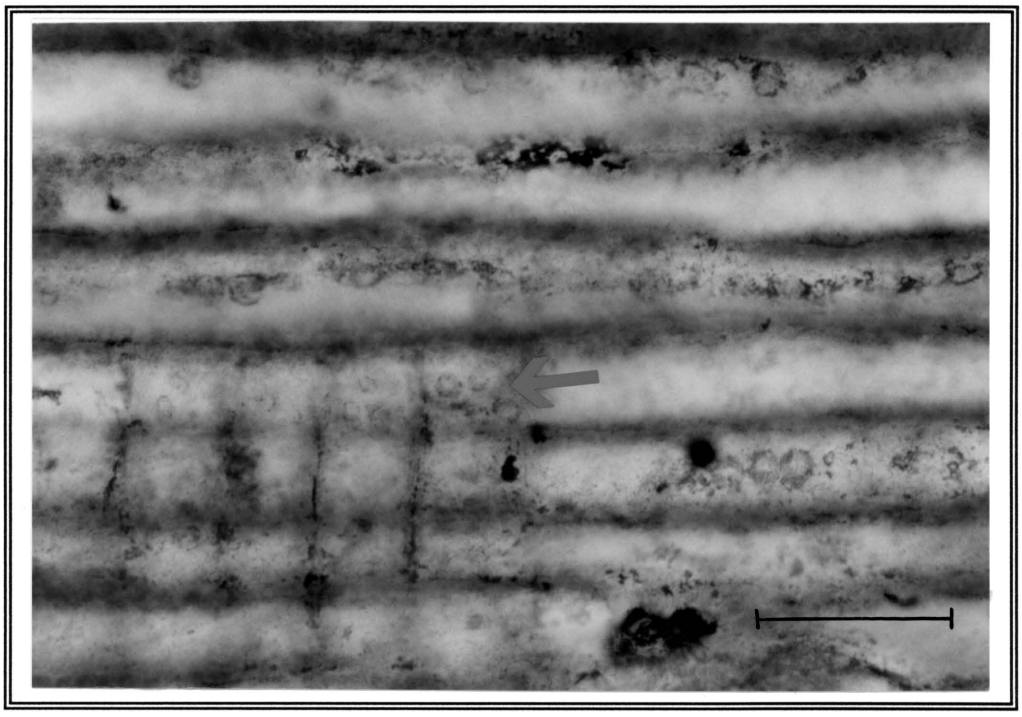

FIGURE 37. Longitudinal radial section. Bordered, cross-field pits arranged in two vertical rows (horizontal in the photograph) (Specimen JS8-94). Scale bar = 50µm.

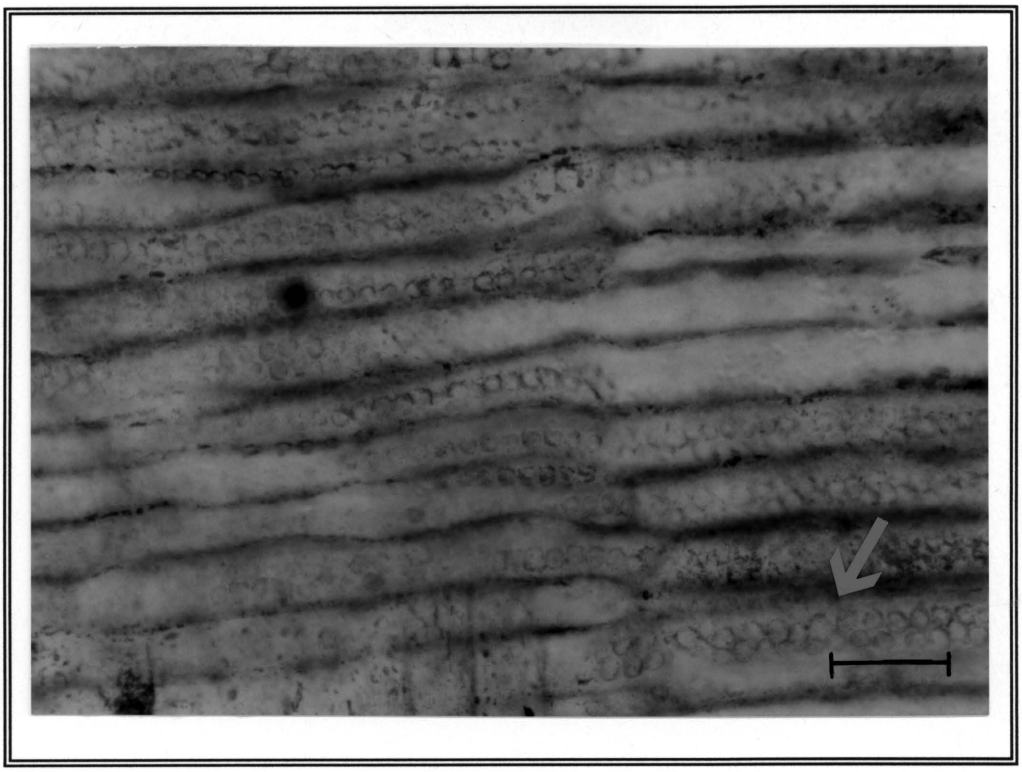

FIGURE 38. Longitudinal radial section. The tracheid pits are arranged alternately (Specimen JS8-94). Scale bar = 50µm.

Specimen JS9-94

Locality: Farm Langlaagte 389, Senekal.

Size of specimen: a = 16cm, r = 20cm and t = 10cm.

Cross-section: The growth rings are regular and fairly well preserved. The late wood zone is broad. Ring boundaries are marked by a colour change of the tracheids. Tracheids are almost square in shape, but many are deformed and distorted. Wall thickness of the tracheids ranges from 3-6µm (average 4µm), whereas the average diameter is 36µm (range 16-48µm). "Chevron-type" deformation is also visible. Peculiar rhombus-shaped cavities, sometimes partly filled with a black substance, are also present (Fig. 39). These cavities may be due to the crystallisation of a euhedral carbonate mineral. This crystallisation occured **after** the wood was buried but before petrification, as areas characterised by these cavities, are distorted. The minerals were probably weathered or broken down after petrification, thereby preserving only the negative crystal cavity and not the minerals.

Radial section: Specimen has a yellowish-brown colour. Pits are bordered, uni- to biseriate, rounded and separate. Pit pores are round with a width of 2-4µm. The pits

measure 6-9µm in diameter and they seem to be alternately arranged. Cross-field pits are bordered and vary from 4-8µm in diameter. Each cross field has 3-4 alternately arranged, oval pits (Fig. 40). The observed rhombic pattern is also present.

Tangential section: The rays are uniseriate, ranging from 3-15 cells (7 on average), 113-548µm in height. The ray cells are round, with a diameter of 32-48µm. The tracheid pits seem to have an araucaroid arrangement. The tracheid walls on the tangential walls are unpitted.

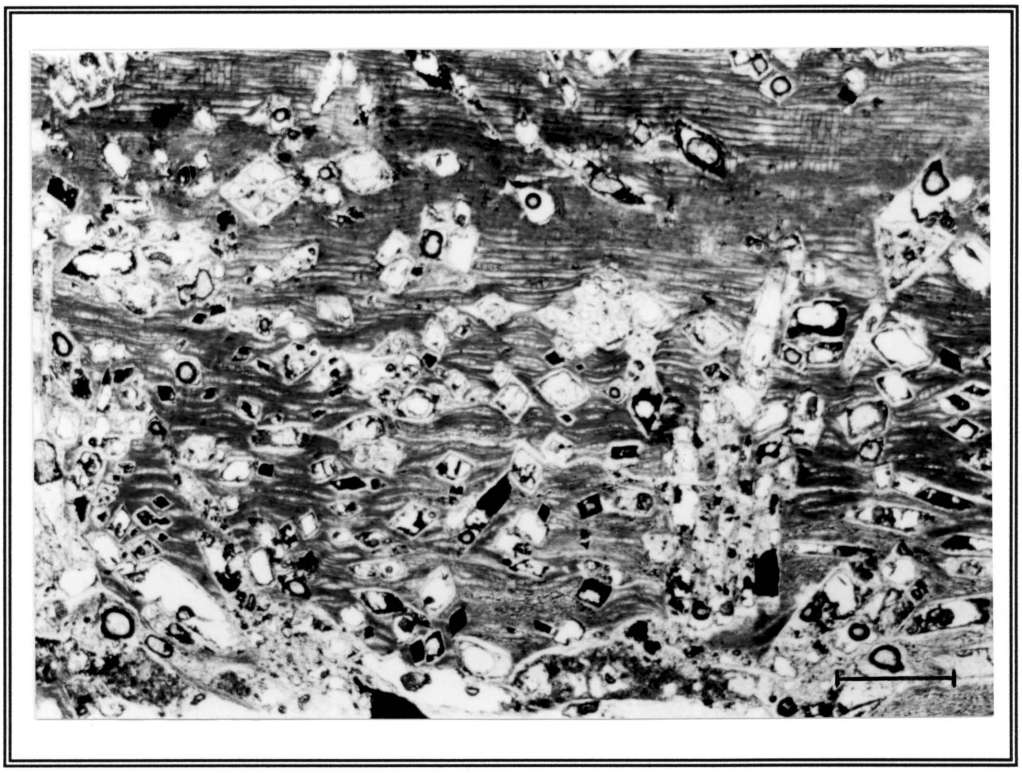

FIGURE 39. Cross-section. Rhombus-shaped pattern partly filled with a black mineral, probably iron oxide (Specimen JS9-94). Scale bar = 500µm.

FIGURE 40. Longitudinal radial section. Cross-fields with 3 to 4 alternately arranged, bordered pits in each field (Specimen JS9-94). Scale bar = 50µm.

Specimen JS10-94

Locality: Farm Langlaagte 389, Senekal.

Size of specimen: a = 13cm, r = 15cm and t = 11cm.

Cross-section: The growth rings are regular and boundaries are shown by a change in tracheid density. False growth rings also occur. Irregular and deformed tracheids are present, but most of them are approximately square in outline. These irregular cell sizes can indicate limiting climatic factors which influenced the growth rate of the tree. The big cells point to favourable growth conditions, and the small ones to limiting growth conditions. Tracheid cell diameter varies from 16-80µm, averaging 48µm. The tracheid walls have an average thickness of 3µm (range 3-4µm). Reddish-black minerals (hematite) also occur.

Radial section: Pits on the radial walls are bordered, uni- to multiseriate, round and separate. They seem to be alternately arranged. Pit pores are round, with a width of 2-4µm. The diameter of the pits ranges from 6-12µm.

Tangential section: The rays are fairly well preserved and are uniseriate to rarely biseriate, ranging from 2-20 cells (9 on average), 81-597µm in height. Ray cells are square in shape and 24-32µm in diameter. Tracheid walls are unpitted.

Specimen JS11-94

Locality: Farm Langlaagte 389, Senekal.

Size of specimen: a = 11cm, r = 18cm and t = 11cm.

Cross-section: The specimen is moderately well preserved, with regular growth rings. The tracheids are deformed and ring boundaries can be observed due to thicker late wood cells. Tracheid diameter is 34µm on average (range 16-48µm), and the thickness of the tracheid walls varies from 3-6µm, averaging 4µm. A reddish-black mineral (hematite) is present (Fig. 41), as well as a greyish-black cubic mineral (pyrite) (Fig. 42). The latter has a metallic lustre when the thin-section is studied macroscopically. (See section 4.2.4., on the mineralogy of the petrified wood).

Radial section: Pits are bordered, uniseriate, round and separate. The pit pores are round with a width of 2-4µm. The pits measure 6-12µm in diameter.

Tangential section: shows poor preservation of the cellular structure.

Specimen JS12-94

Locality: Farm Langlaagte 389, Senekal.

Size of specimen: a = 13cm, r = 16cm and t = 10cm.

Cross-section: The growth rings are regular, and boundaries are shown by thicker walled tracheids. False growth rings also occur. Tracheids have an almost square outline, measure 16-48µm in diameter (average 29µm), and have an average cell wall thickness of 4µm (range 3-6µm).

Radial section: Pits on the radial walls are bordered, uni- to triseriate, round and separate. Pit pores are round, with a diameter of 2-4µm. The radial pits are 9-12µm in diameter and are arranged in an araucaroid way, probably indicating the genus *Araucarioxylon*. The cross-field pits are bordered. Each cross field has 1-4 round pits, 6-8µm in diameter, arranged in two horizontal rows (Fig. 43). A reddish-black mineral (hematite) is also present.

Tangential section: The rays are uniseriate with the height varying from 2-24 cells (12 on average), 97-855µm in height. Ray cells are approximately square and measure 32-48µm in diameter. The tracheid walls are unpitted.

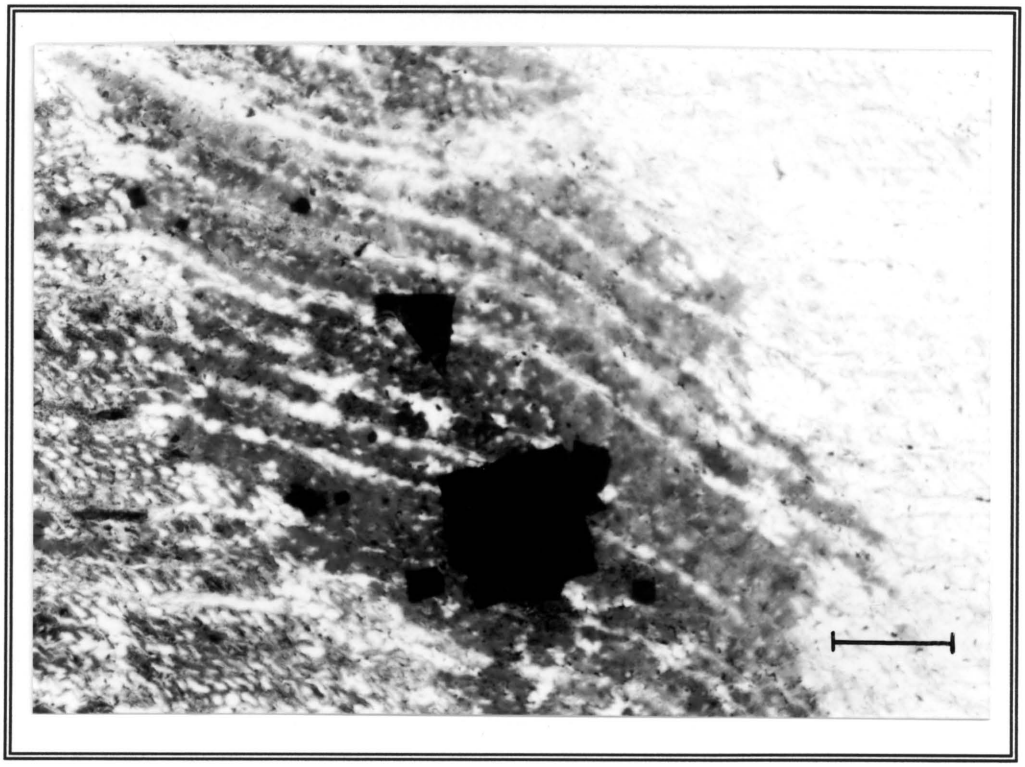

FIGURE 41. Cross-section. Reddish-black mineral, probably hematite (Specimen JS11-94). Scale bar = 100µm.

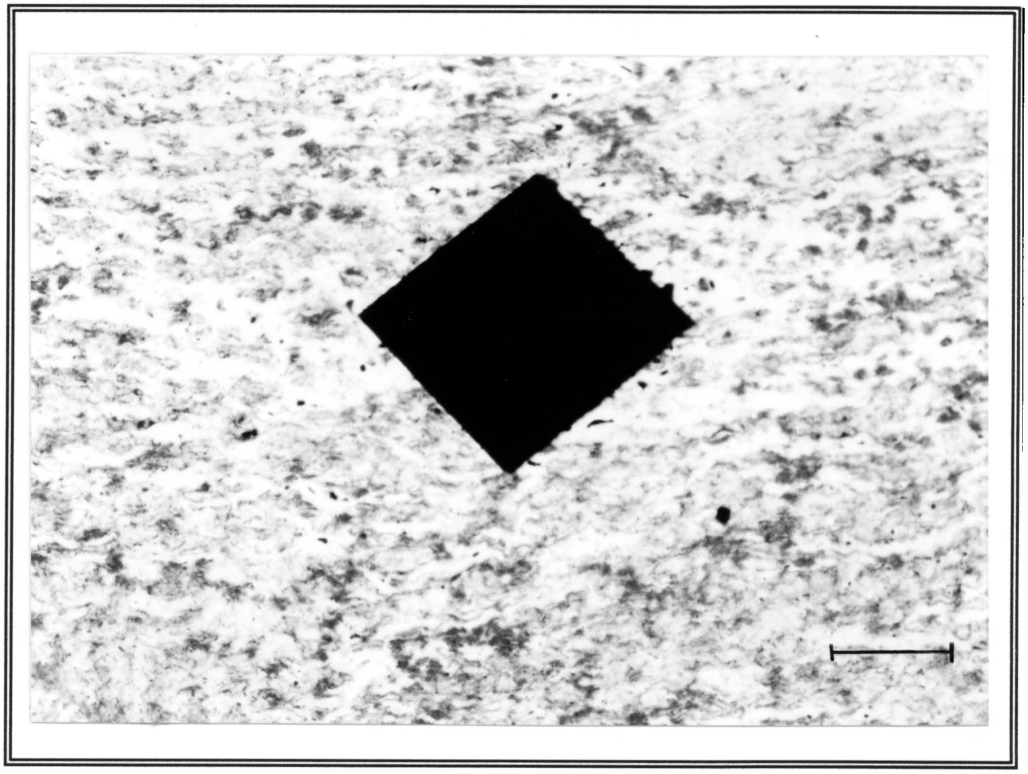

FIGURE 42. Cross-section. Greyish-black mineral with a metallic lustre and silvery colour in reflected light, probably pyrite. (Specimen JS11-94). Scale bar = 100µm.

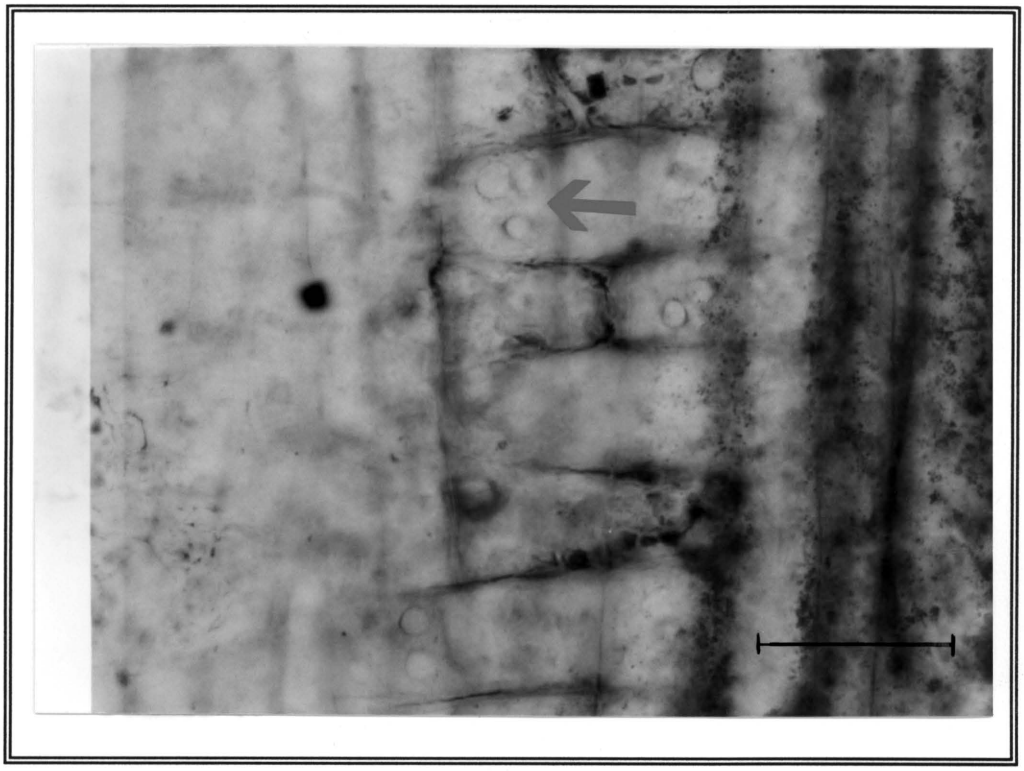

FIGURE 43. Longitudinal radial section. Cross-fields with 1 to 4 round pits in each field, arranged in two horizontal rows (Specimen JS12-94). Scale bar = 50µm.

Specimen JS13-94

Locality: Farm Langlaagte 389, Senekal.

Size of specimen: a = 14cm, r = 16cm and t = 10cm.

Cross-section: The specimen is lightly coloured. Growth rings are regular. Ring boundaries are marked by a change in tracheid densities. False growth rings are also present. The tracheids are square, 32-64µm in diameter (average 45µm) and have an average wall thickness of 3µm (range 3-4µm). A reddish-black mineral (hematite) is also present.

Radial section: Pits are bordered, uniseriate, round and separate. Pit pores are round, with a width of 4-6µm. The radial pits have a diameter of 9-12µm.

Tangential section: Most of the rays are uniseriate, but a few are biseriate. The rays range from 2-24 cells (7 cells on average), 81-855µm in height. Ray cells have a rounded outline and measure 32-48µm in diameter. Tangential walls of the tracheids are unpitted.

4.2.3 Growth ring analysis

Four Parameters are used in growth ring analysis (Creber and Chaloner, 1984):

1. The width of the ring, which depends on the length of the "growth season";
2. The width of the early wood and its proportion to the whole ring, which reflects the environmental temperature;
3. The variation in the cell size across the ring, the ratio of large early wood cells to small late wood cells, which may reflect rainfall patterns; and
4. The variability of the ring widths, from one year to the next, which may reflect climatic variations from year to year.

The growth rings were measured on petrographic thin-sections as well as in transverse section viewed under a dissecting microscope. The ring measurements were taken along a radial line to obtain a long series of rings. Some of the measurements had to be off-set relative to adjacent radii, because of poor cellular preservation. Each growth ring measurement started at the beginning of each growth season.

The variability in width of the rings from year to year is calculated as the difference in width between a pair of consecutive rings divided by their average width (Creber, 1977). This gives the degree of variability between years and these values are known as the annual sensitivity (AS).

The average of the annual sensitivity for each tree is known as the mean sensitivity (MS) (Fritts, 1976). The mean sensitivity gives an indication of the response of the tree to the variations in climate that may have influenced its growth. The mean sensitivity is calculated by the following formula:

$$MS = \frac{1}{n-1} \sum_{t=1}^{t=n-1} \left| \frac{2(x_{t+1} - x_t)}{x_{t+1} + x_t} \right|$$

x = ring width

n = number of rings

t = year number of each ring

Mean sensitivity values range from 0 (no variation from year to year) to a theoretical maximum of 2 (greatest variation). An arbitrary value of 0.3 is taken to separate "sensitive" trees from "complacent" trees (Fritts, 1976).

"Sensitive" trees (MS > 0.3) are inferred to have grown under limiting factors of climate. "Complacent" trees (MS < 0.3), on the other hand, would have grown under a favourable, uniform climate (Fritts, 1976).

Tables 15 and 16 show the results of the growth ring analysis for both the *Dicynodon - Theriognathus* Assemblage Zone and the *Lystrosaurus Procolophon* Assemblage Zone from this study.

TABLE 15. Results of the growth ring analyses from the *Dicynodon - Theriognathus* Assemblage Zone.

ASSEMBLAGE ZONE	SPECIMEN NR.	NUMBER OF RINGS	MEAN RING WIDTH (mm)	MAXIMUM RING WIDTH (mm)	MINIMUM RING WIDTH (mm)	MEAN SENSITIVITY
Dicynodon	JS1-93	4	13.5	18	10	0.28
Dicynodon	JS2-93	8	4.5	9	0.9	0.52
Dicynodon	JS3-93	4	8.4	11	6	0.34
Dicynodon	JS4-93	19	2.9	6	0.5	0.53
Dicynodon	JS5-93	8	3.7	8	1.9	0.36
Dicynodon	JS6-93	17	4.4	10.5	1	0.53
Dicynodon	JS7-93	10	4.3	7.5	0.8	0.72
Dicynodon	JS8-93	13	4.8	8.5	1.3	0.39
Dicynodon	JS9-93	3	9.3	14	9	0.76
Dicynodon	JS1-94	16	4	6.9	1	0.31
Dicynodon	JS2-94	26	5.6	9	2	0.37

TABLE 16. Results of the growth ring analyses from the *Lystrosaurus - Procolophon* Assemblage Zone.

ASSEMBLAGE ZONE	SPECIMEN NR.	NUMBER OF RINGS	MEAN RING WIDTH (mm)	MAXIMUM RING WIDTH (mm)	MINIMUM RING WIDTH (mm)	MEAN SENSITIVITY
Lystrosaurus	JS3-94	15	2.2	5	1	0.24
Lystrosaurus	JS4-94	19	2.3	3.9	1	0.28
Lystrosaurus	JS5-94	19	2.9	4.2	1.5	0.42
Lystrosaurus	JS6-94	28	3.8	8	1	0.43
Lystrosaurus	JS7-94	47	2.6	7	0.4	0.34
Lystrosaurus	JS8-94	57	2.8	8.2	0.7	0.44
Lystrosaurus	JS9-94	24	3.4	8	1	0.47
Lystrosaurus	JS10-94	37	1.9	4.5	0.2	0.47
Lystrosaurus	JS11-94	38	3.0	7.5	1	0.48
Lystrosaurus	JS12-94	13	4.8	8.5	1.9	0.42
Lystrosaurus	JS13-94	25	4.7	10.1	0.9	0.42

From both the *Dicynodon - Theriognathus* Assemblage Zone and the *Lystrosaurus - Procolophon* Assemblage Zone, a total of 22 ring series were measured, which ranged from 3 rings to 57 rings. The rings were characterised by a wide zone of large early wood cells, and a zone of smaller late wood cells which varied from broad, eg. 18mm, to narrow, eg. 0.2mm. The growth rings (early wood and late wood) of some of the samples are very wide when compared to the overall data from the growth ring analyses. The rings were mostly very prominent, although sections occurred where the preservation of the growth rings was poor. The average ring width for the *Dicynodon - Theriognathus* Assemblage Zone was 5.94 mm (n=128) and for the *Lystrosaurus - Procolophon* Assemblage Zone, 3.13 mm (n=272).

The mean sensitivity (MS) for all but three of the specimens in both assemblage zones exceeds 0.3. The trees are therefore "sensitive" and grew under limiting climatic factors.

The average ring width for the *Dicynodon - Theriognathus* Assemblage Zone (5.94 mm) is roughly twice the average ring width of the *Lystrosaurus - Procolophon* Assemblage Zone (3.13 mm).

The variations in growth ring width from one season to the next is shown in Figure 44 for the wood of the *Dicynodon - Theriognathus* Assemblage Zone, and in Figure 45 for the wood of the *Lystrosaurus - Procolophon* Assemblage Zone. There is a tendency of increased ring sizes with time in the woods of the *Dicynodon - Theriognathus* Assemblage Zone, indicating a probable improvement in the climatic setting favouring tree growth. Woods of the *Lystrosaurus - Procolophon* Assemblage Zone exhibit a decrease in ring sizes with time. This tendency may point to a decrease in favourable tree growth conditions due to climatic deterioration.

The data of growth ring widths for each specimen are given in Tables 17 and 18.

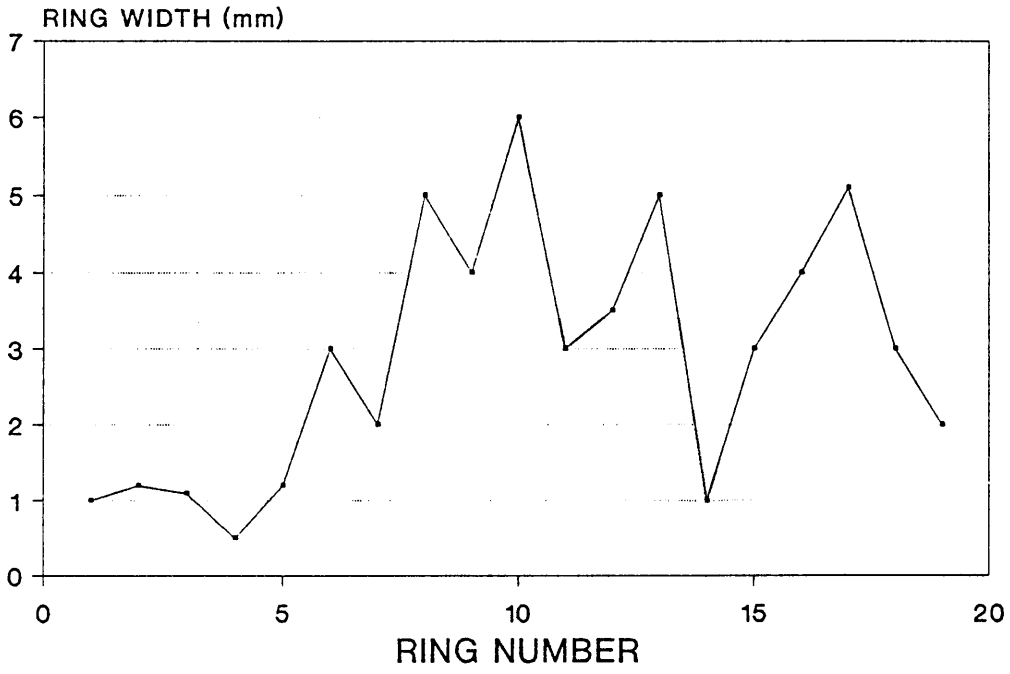

Specimen JS4-93

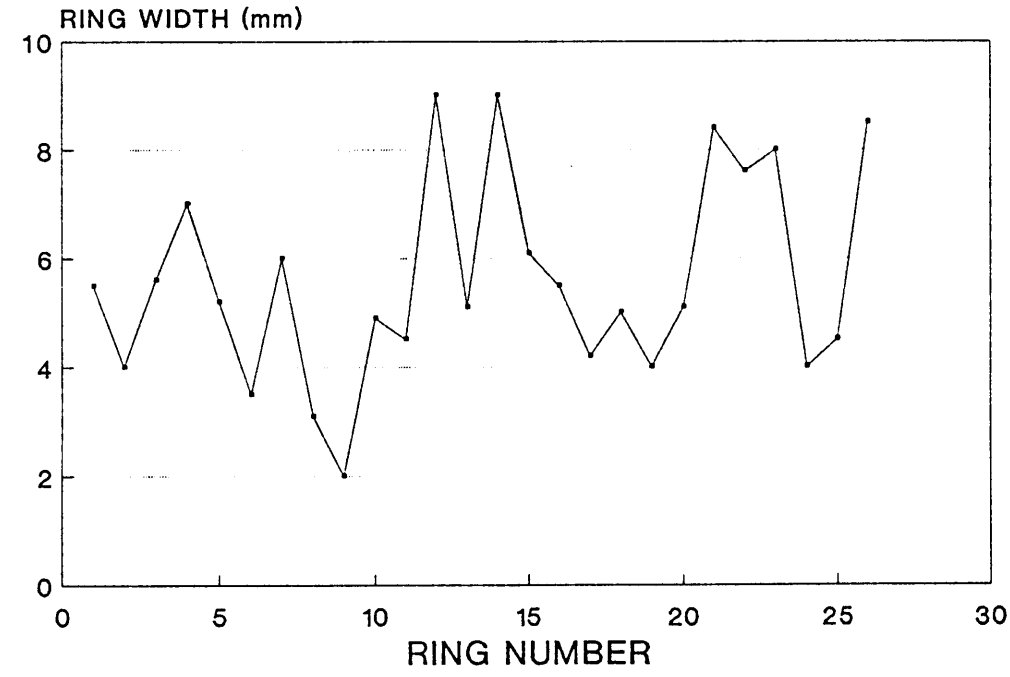

Sample JS2-94

FIGURE 44. Growth ring variations of wood from the *Dicynodon - Theriognathus* Assemblage Zone.

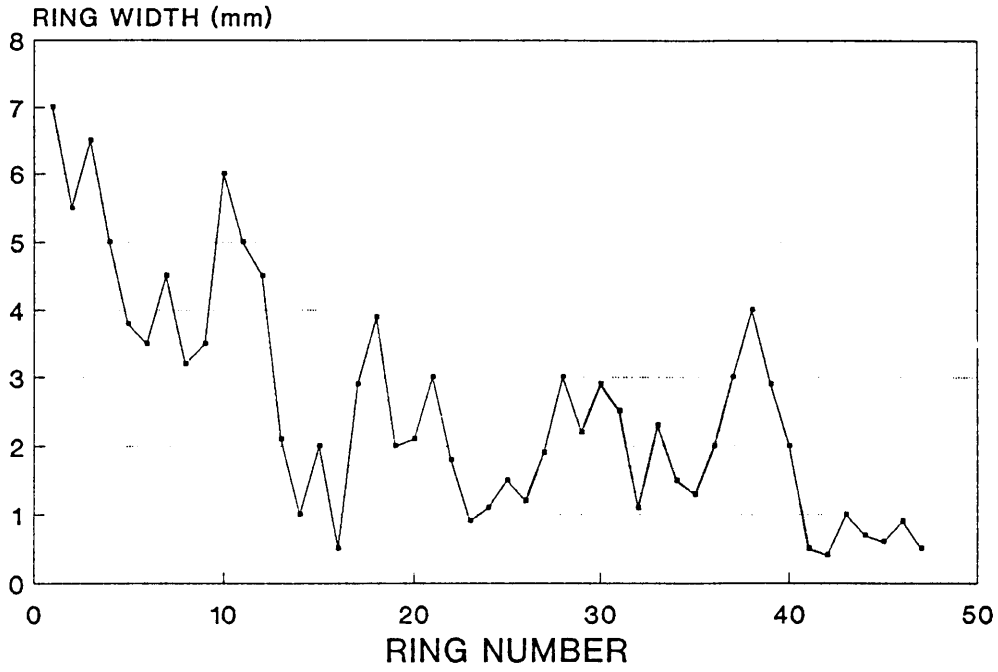

Sample JS7-94

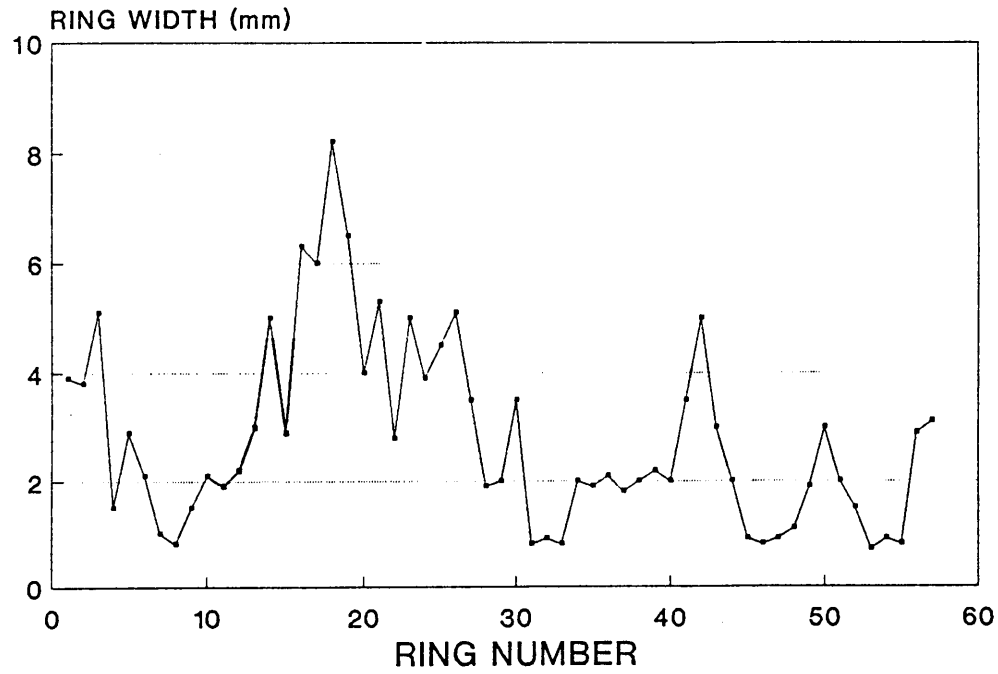

Sample JS8-94

FIGURE 45. Growth ring variations of wood from the *Lystrosaurus - Procolophon* Assemblage Zone

TABLE 17. Growth ring width (mm) of the wood specimens from the *Dicynodon - Theriognathus* Assemblage Zone.

Dicynodon	GROWTH RING WIDTH (mm)
JS1-93	14; 18; 12; 10.
JS2-93	9; 8; 5; 6; 3; 0.9; 1; 3.
JS3-93	6; 9.5; 11; 7.
JS4-93	1; 1.2; 1.1; 0.5; 1.2; 3; 2; 5; 4; 6; 3; 3.5; 5; 1; 3; 4; 5.1; 3; 2.
JS5-93	2.5; 3.4; 3.9; 3; 2.9; 1.9; 4; 8.
JS6-93	2; 1.9; 2.1; 2; 5; 10; 6.9; 9; 5.5; 2.8; 2; 2; 4.8; 5; 1.8; 1; 10.5.
JS7-93	7; 4; 6; 7.5; 2.3; 0.8; 3; 5.2; 6; 1.
JS8-93	5.5; 3; 3.1; 3.2; 1.3; 3.5; 3.2; 4.9; 6.1; 9; 7; 4; 8.5.
JS9-93	14; 5; 9.
JS1-94	6.9; 5; 5.6; 6.2; 5.1; 4; 3; 2; 1; 1.9; 2.1; 2.8; 6.1; 3.8; 4.1; 4.2.
JS2-94	5.5; 4; 5.6; 7; 5.2; 3.5; 6; 3.1; 2; 4.9; 4.5; 9; 5.1; 9; 6.1; 5.5; 4.2; 5; 4; 5.1; 8.4; 7.6; 8; 4; 4.5; 8.5.

TABLE 18. Growth ring width (mm) of the wood specimens from the *Lystrosaurus* - *Procolophon* Assemblage Zone.

Lystrosaurus	GROWTH RING WIDTH (mm)
JS3-94	3; 2.7; 5; 3; 2.1; 1.9; 2.2; 2; 1.8; 2; 1; 1.1; 1.2; 1.7; 1.9.
JS4-94	2.9; 3.9; 2.5; 1.8; 3.6; 2.5; 2.1; 2.2; 1.8; 2.5; 2.1; 2.6; 2; 2; 2.1; 2; 1.8; 1; 2.2.
JS5-94	2.5; 2.1; 2.7; 2; 3.1; 1.5; 4; 2.7; 3; 4.2; 3; 3.9; 2; 1.5; 4; 2.9; 3.8; 3; 2.9.
JS6-94	7; 4; 5; 3.2; 8; 3.6; 2; 5; 4; 2.9; 5; 3; 3.8; 2.5; 4; 2.9; 4; 1; 1.5; 1.5; 4.2; 5.8; 2.6; 2.9; 4; 3.9; 4; 4.
JS7-94	7; 5.5; 6.5; 5; 3.8; 3.5; 4.5; 3.2; 3.5; 6; 5; 4.5; 2.1; 1; 2; 0.5; 2.9; 3; 2; 2.1; 3; 1.8; 0.9; 1.1; 1.5; 1.2; 1.9; 3; 2.2; 2.9; 2.5; 1.1; 2.3; 1.5; 1.3; 2; 3; 4; 2.9; 2; 0.5; 0.4; 0.7; 0.6; 0.9; 0.5.
2JS8-94	3.9; 3.8; 5.1; 1.5; 2.9; 2.1; 1; 0.8; 1.5; 2.1; 1.9; 2.2; 3; 5; 2.9; 6.3; 6; 8.2; 6.5; 4; 5.3; 2.8; 5; 3.9; 4.5; 5.1; 3.5; 1.9; 2; 3.5; 0.8; 0.9; 0.8; 2; 1.9; 2.1; 1.8; 2; 2.2; 2; 3.5; 5; 2; 0.9; 0.8; 0.9; 1.1; 1.9; 3; 2; 1.5; 0.7; 0.9; 0.8; 2.9; 3.1.
JS9-94	2.9; 4.5; 8; 3.9; 6.2; 6.7; 1.1; 2; 3; 1.8; 3; 1.5; 1.9; 1.5; 1; 3; 2.9; 2.6; 6; 3.9; 3; 2.9; 3.5; 3.8.
JS10-94	3; 2.1; 1.1; 2.9; 2.2; 2; 3; 2.8; 0.9; 0.5; 3.1; 3; 1.9; 1; 0.8; 3; 3.1; 4.5; 3.4; 1.5; 1.3; 1.4; 2; 1.8; 2; 3.1; 1.9; 1.8; 0.5; 0.3; 0.4; 0.5; 0.6; 0.5; 0.2; 0.5; 3.
JS11-94	7.5; 2; 1; 4; 2.2; 5; 2; 3; 4; 4.1; 5; 6.5; 1.5; 1.7; 2.9; 3.5; 4.8; 4; 2.9; 3; 1.5; 1.4; 2.9; 1.8; 3; 2.1; 3.8; 2; 1; 2; 3.1; 2.
JS12-94	4; 3.1; 5.2; 3.2; 4; 5.8; 5.9; 6.1; 8.5; 6; 1.9; 4.9; 4.1.
JS13-94	1.9; 10.1; 6.9; 6.8; 5; 6.9; 8; 3.1; 5.8; 6; 5.5; 7; 2.8; 1.5; 4.1; 6.8; 4.5; 56.1; 4.9; 6; 3.5; 1.1; 0.9; 1; 1.3.

4.2.4 Mineralogy of the petrified wood

The petrifying mineral of the wood in the Karoo Supergroup is normally silica, although fluorapatite has also been found in the Dwyka Group (Snyman, 1992). This is consistent with the findings of Bühmann *et al.* (1989), who studied phosphorite bands near the Dwyka-Ecca boundary; apatite was one of the minerals present.
Warren (1912) also found that the majority of specimens from various parts of Natal and Zululand kept in the Natal Museum, were silicified. Specimens from a phosphate bed near Weenen, Natal consist of phosphate of lime. A specimen consisting of calcium carbonate was collected by the Natal Museum, but is Cretaceous in age.
The museum also possesses black, fossilized wood from a lignite seam, with a probable late Tertiary to Recent age. The wood is dicotyledonous. All the wood from the Natal Museum except for the latter specimen, is coniferous. The Bernard Price Institute for Palaeontological Research, University of the Witwatersrand, also houses dicotyle wood from Zululand and Pondoland.

The petrifying mineral detected by petrographic microscope in the thin-sections of both the *Dicynodon - Theriognathus* Assemblage Zone (Schoondraai Member) and the *Lystrosaurus Procolophon* Assemblage Zone (Harrismith Member and Katberg Formation), is quartz. The mineral generally shows a wavy extinction. It is also possible that the silica in the cells is amorphous, whereas it is crystalline in cavities outside the cells (Warren, 1912).

From analyses carried out by EDAX on the thin-sections of the *Dicynodon - Theriognathus* Assemblage Zone (Schoondraai Member), the presence of the elements silica, zinc and iron (most probably zinc oxide and iron oxide) was determined.
The *Lystrosaurus Procolophon* Assemblage Zone (Harrismith Member) also shows the presence of the elements silica, zinc and iron (most probably zinc oxide and iron oxide).

The relative abundance (X) of the elements present is tabulated in Table 19. A high abundance of a certain element is shown as XXX, a low abundance as X.

TABLE 19. The relative abundance of silica, iron and zinc present in petrified wood.

BIOZONE	SAMPLE	Si	Fe	Zn
Lystrosaurus - Procolophon Assemblage Zone	JS3-94	XXX	-	XX
	JS4-94	XXX	XX	XXX
	JS5-94	XXX	XX	X
	JS6-94	XXX	X	XX
	JS7-94	XX	XX	XXX
	JS8-94	XX	X	XXX
	JS9-94	XX	XXX	XXX
	JS10-94	XX	XX	XXX
	JS11-94	XX	X	XXX
	JS12-94	XX	XX	XXX
	JS13-94	XX	XX	XXX
Dicynodon - Theriognathus Assemblage Zone	JS1-93	XXX	X	XXX
	JS2-93	XXX	X	XX
	JS3-93	XXX	X	XX
	JS4-93	XXX	X	XX
	JS5-93	XXX	X	XXX
	JS6-93	XXX	X	XXX
	JS7-93	XXX	X	XXX
	JS8-93	XXX	X	XXX
	JS9-93	XXX	X	XX
	JS1-94	XXX	X	XXX
	JS2-94	XXX	X	XXX

The petrified wood showed two types of quartz in thin-section, namely radiating microcrystalline quartz (**chalcedony**) (Fig. 46) and coarse crystalline **quartz** with easily visible individual crystals (Fig. 47). Both forms commonly occur together (Fig. 48), bands of fibrous, radiating chalcedony giving way to bands of irregularly shaped quartz grains. According to Stein (1982), quartz appears to grow as either masses of chalcedonic fibres or as euhedral crystals. It is also believed that chalcedony is probably formed by the crystallisation of colloidal silica (opaline silica), whereas quartz is formed by direct crystallisation from solution (Scurfield and Segnit, 1984).
Another possibility is the transformation of opal to chalcedony to quartz, due to the diagenesis of the sandstones (Dapples, 1967).

The X-ray diffraction traces (d-values in Å units) from the wood specimens (Fig. 49) only show the presence of crystalline quartz. The quartz crystallinity index (Q.C.I.) shows variations of the quartz quintuplet in the wood specimens (Table 20). The values are low, showing that the quartz in the petrified wood specimens is poorly crystallised, when compared to the powder standard (Pietersburg quartz) used (Fig. 50).

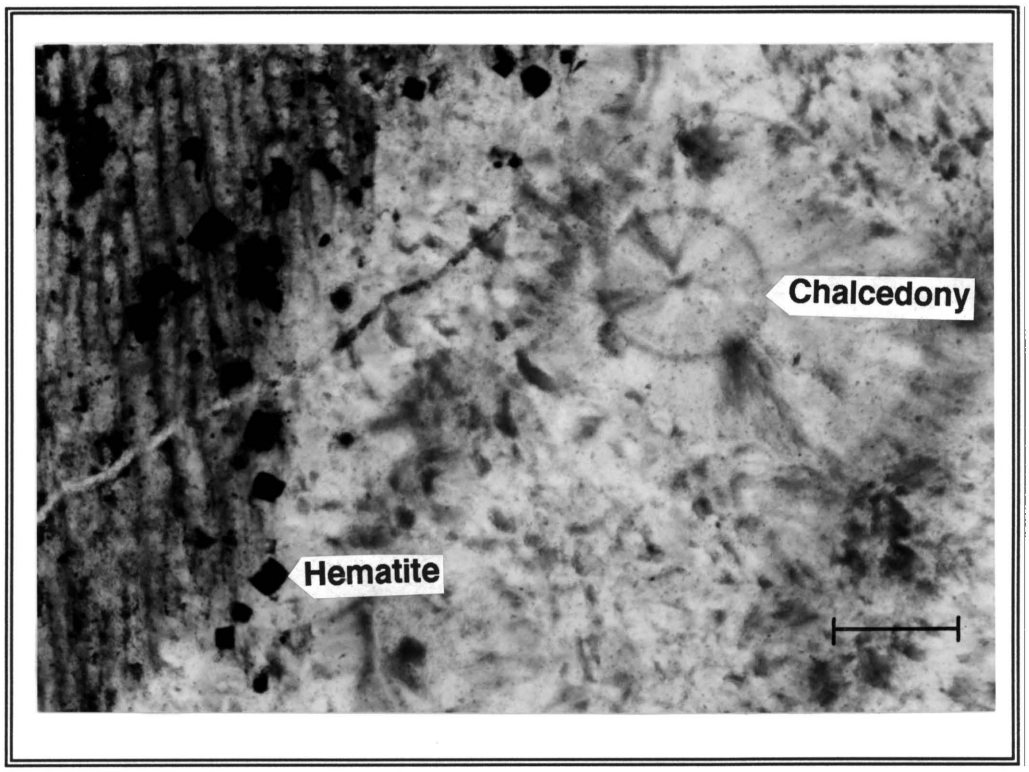

FIGURE 46. Radiating microcrystalline chalcedony and hematite. Crossed nicols, quartz wedge, first order interference colours.
(Specimen JS5-94). Scale bar = 100µm.

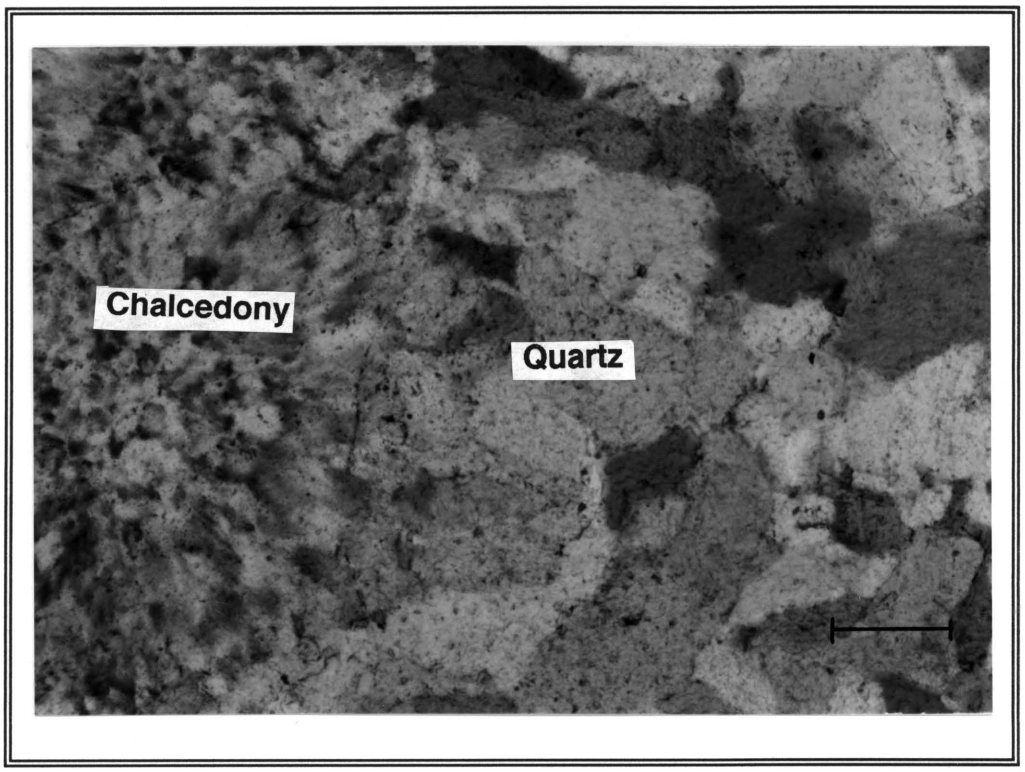

FIGURE 47. Coarse crystalline quartz and chalcedony, crossed nicols. Quartz wedge, first order interference colours (Specimen JS5-94). Scale bar = 100µm.

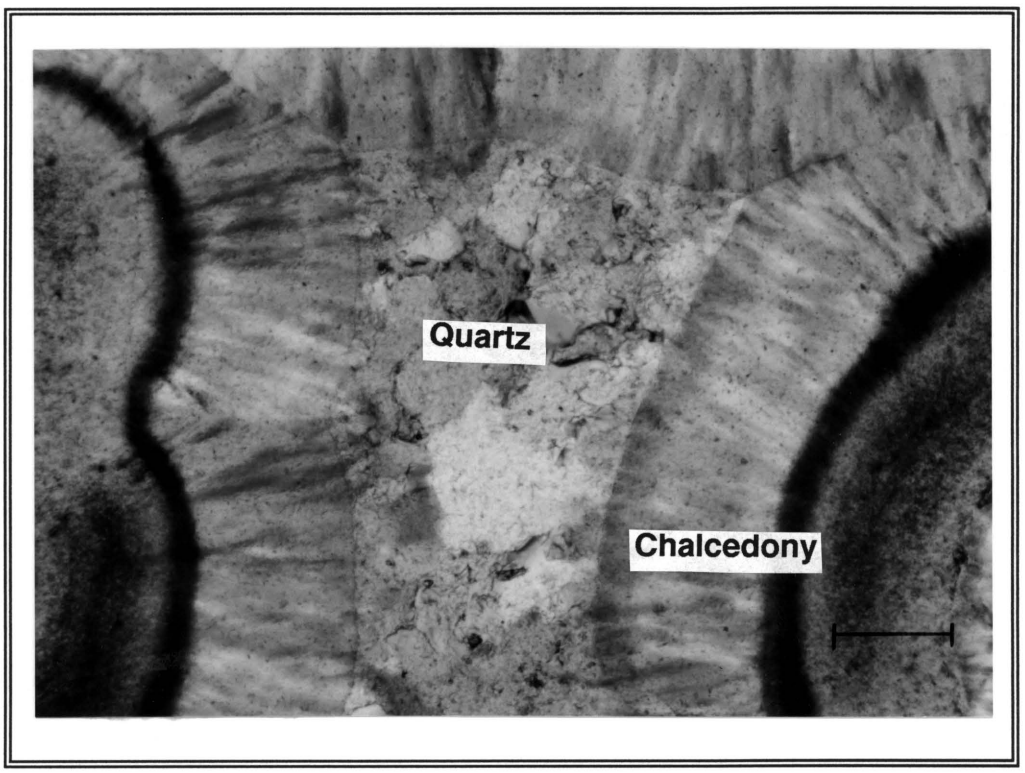

FIGURE 48. Radiating microcrystalline chalcedony as well as coarse, crystalline quartz. Crossed nicols, quartz wedge, first order interference colours. (Specimen JS5-94). Scale bar = 100µm.

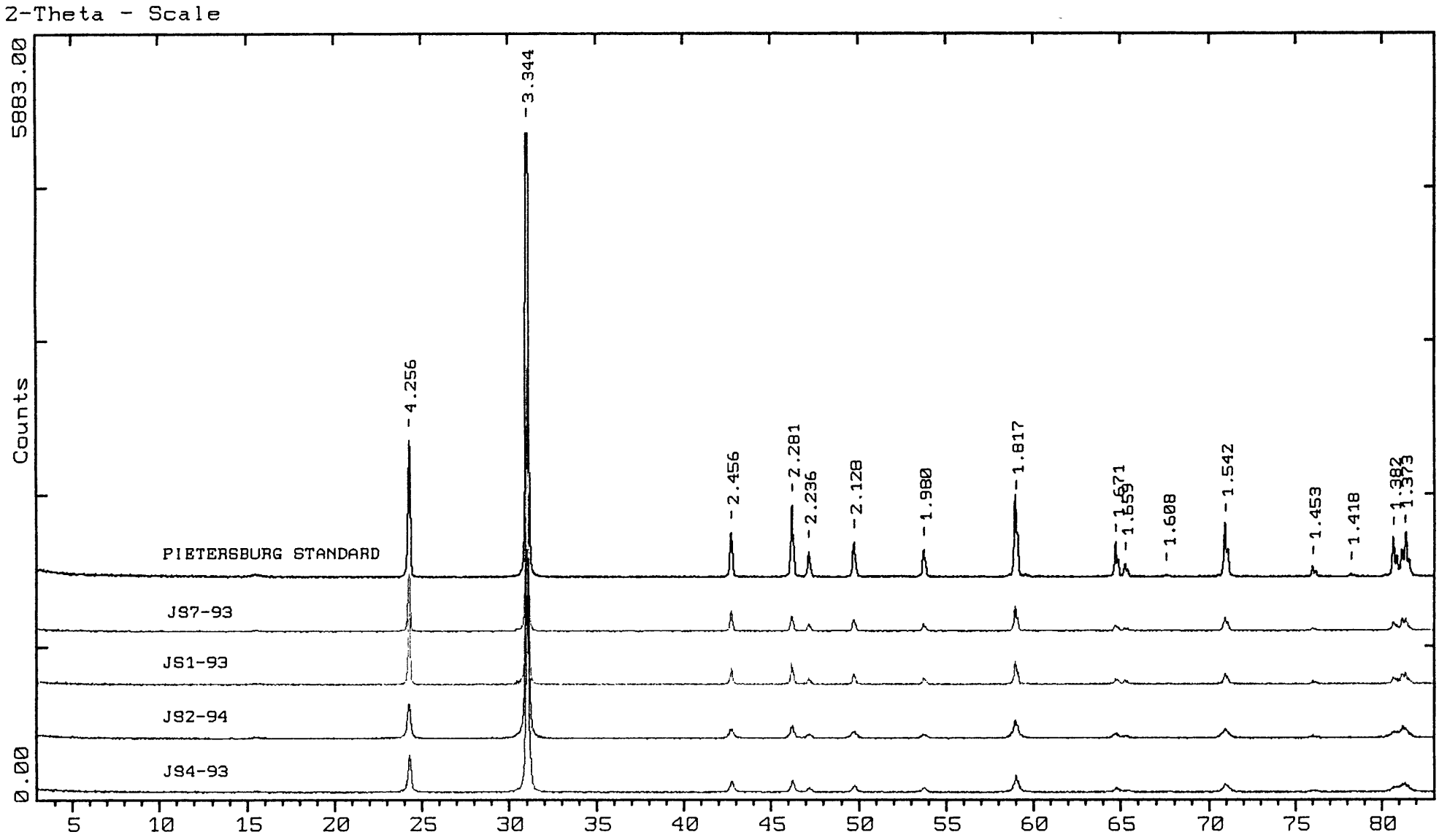

FIGURE 49. X-ray diffraction traces of selected petrified wood specimens, compared to a pure quartz standard from Pietersburg.

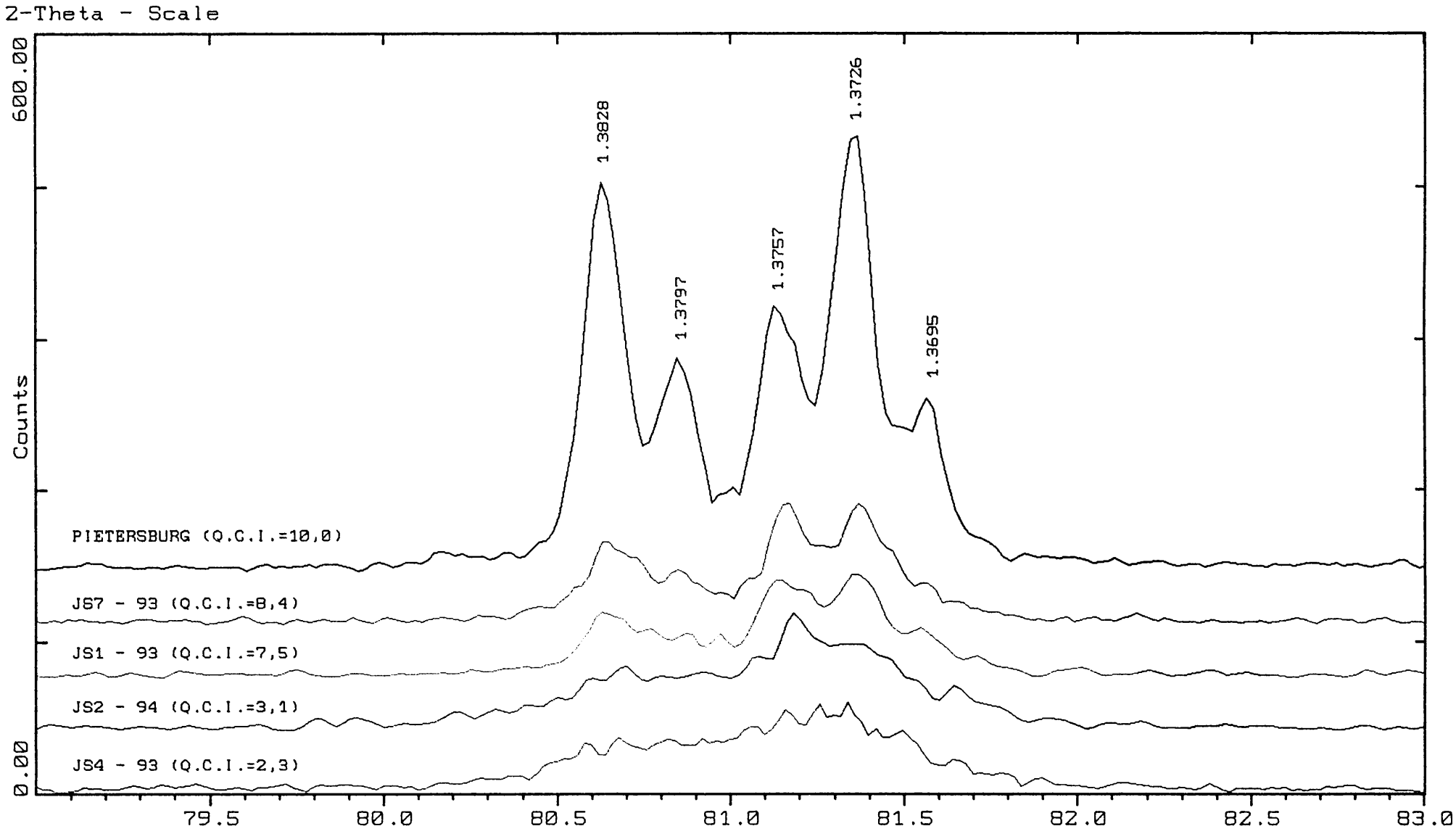

FIGURE 50. Quartz crystallinity index variations shown by the 80° - 82°2θ Co K_α quartz quintuplet of selected petrified wood specimens compared to a quartz standard from Pieterburg with an index of 10.

TABLE 20. Quartz crystallinity index of the petrified wood samples. Normalised value based on an arbitrary crystallinity of 10 for the standard (clear quartz).

H = Height; **V** = Valley

BIOZONE	SPECIMEN	H	V	H - V	H-V/H	NORMALISED
Lystrosaurus - Procolophon	JS13-94	98	43	55	0.56	6.7
	JS12-94	79	43	36	0.46	5.5
	JS11-94	89	44	45	0.51	6.1
	JS10-94	75	51	24	0.32	3.8
	JS9-94	95	53	42	0.44	5.3
	JS8-94	99	56	43	0.43	5.2
	JS7-94	98	57	41	0.42	5.0
	JS6-94	84	54	30	0.36	4.3
	JS5-94	73	40	33	0.45	5.4
	JS4-94	73	44	34	0.44	5.2
	JS3-94	79	46	33	0.42	5.0
Dicynodon - Theriognathus	JS2-94	50	37	13	0.26	3.1
	JS1-94	49	22	27	0.55	6.6
	JS9-93	42	29	13	0.31	3.7
	JS8-93	30	15	15	0.50	6.0
	JS7-93	63	19	44	0.70	8.4
	JS6-93	38	23	15	0.39	4.7
	JS5-93	35	26	9	0.26	3.1
	JS4-93	42	34	8	0.19	2.3
	JS3-93	42	27	15	0.36	4.3
	JS2-93	41	25	16	0.39	4.7
	JS1-93	51	19	32	0.63	7.5

Two euhedral minerals are also present in the petrified wood. The first is reddish-black with a hexagonal crystal habit. The mineral was identified as hematite (Fe_2O_3), based on its habit. The SEM showed only the presence of iron and a small amount of silica.
The second mineral has a greyish-black colour and a cubic crystal habit. A macroscopic study of the relevant thin-section indicated a metallic lustre for the mineral. The mineral was identified as pyrite by SEM. Although the presence of zinc was determined in the petrified wood by means of EDAX, no minerals containing zinc (sphalerite) were detected. The zinc is most probably present as zinc oxide, originally adsorbed as zinc ions on colloidal iron oxide.

According to Berner (1983) and Berner and Raiswell (1983), pyrite forms during shallow burial, when reaction of detrital iron minerals with H_2S occurs. H_2S is produced by the reduction of dissolved sulphate by bacteria using sedimentary organic matter as reducing agent, thus forming in anoxic conditions. Major controlling factors for pyrite formation in **marine sediments** are:
(1) The amount of organic matter in a sediment.
(2) The amount of reactive iron minerals in a sediment.
(3) The availability of dissolved sulphate.

Dissolved sulphate concentrations in **fresh water** are much less than in sea water. Therefore, sulphate is rapidly and totally consumed by sulphate reduction at depths of only a few centimeters (Berner, 1983). Little pyrite and much organic matter is left behind. In contrast to marine sediments, sulphate is the principal factor controllling pyrite formation in fresh water sediments. Pyrite thus most likely formed under reducing conditions when the wood was buried by sediments after deposition of the logs. When the anoxic conditions changed to oxidising conditions, the pyrite was oxidised to goethite. *In situ* dehydration of goethite at the surface in a dry, hot environment gives rise to hematite (Van Houten, 1968; Walker, 1967):

$$\text{Reactive minerals} + H_2S \xrightarrow{\text{reduction}} \text{pyrite } (FeS_2)$$

$$FeS_2 \xrightarrow{\text{oxidation}} \text{goethite } (FeO(OH))$$

$$FeO(OH) \xrightarrow{\text{dehydration}} \text{hematite } (Fe_2O_3)$$

4.3 DISCUSSION

The Permian-Triassic boundary in South Africa occurs within the stratigraphic succession of the Beaufort Group, Karoo Supergroup. The exact locality of the boundary has not been determined, but it is traditionally placed at the contact between the basal *Dicynodon - Theriognathus* Assemblage Zone and the overlying *Lystrosaurus - Procolophon* Assemblage Zone. The Permian-Triassic boundary in the Beaufort sedimentary rocks in the northeastern Free State is thus located stratigraphically between the (upper) Harrismith Member (correlates with the *Lystrosaurus - Procolophon* Assemblage Zone) and the (lower) Schoondraai Member (which correlates with the *Dicynodon - Theriognathus* Assemblage Zone). These members belong to the Normandien Formation.

The sedimentary profiles of the Schoondraai and Harrismith Members give useful information about the inferred sedimentation processes in the study area. The mudrocks indicate suspension settling of very fine material in a low energy environment. This fine material was probably deposited on a floodplain as a result of vertical accretion from overbank floods which carried the suspended, fine material. The presence of massive mudrocks may indicate rapid deposition of the sediments during sudden floods (Blatt, 1972). It can also have resulted from organic activity or bioturbation (Reineck and Singh, 1973). No burrows were observed, and therefore the former possibility is more likely. Alternatively, the massive mudrocks may reflect diagenesis.
The fine-grained sandstone interbedded with the mudrocks is evidence of fluctuation in the energy levels, traction sedimentation alternating with suspension settling. This fluctuation of energy levels was possibly due to seasonal control. The depositional palaeoenvironment was therefore not stagnant, but subject to change. The medium- to coarse-grained sandstones observed indicate a moderate to high energy depositional system. The planar cross-bedding which is present in these sandstone sequences, is evidence for the migration of straight-crested megaripple bedforms. Cross-bedding can also form in an aeolian setting, but the low angle of the cross-bedding, the moderate sorting and the upward-fining of most of the sandstones exclude wind as a depositional agent for these sediments. The sandstones were probably fluvial channel deposits, which tend typically to be upward-fining. The lack of large pebbles suggests that the river system was already

at a mature stage, where the rate of erosion was approximately equal to the rate of deposition. There is an inferred trend of declining energy levels from the lower Schoondraai Member through to the upper Harrismith Member. It is postulated that the palaeoenvironment also became more arid upwards in the succession studied, with an increase in associated oxidising conditions. The iron oxide most likely reflects diagenetic processes that include ageing and dehydration of brown, amorphous ferric oxide to goethite (limonite), and dehydration of the goethite to hematite. Warm climates promote this alteration of brown (limonite) to red (hematite) pigments on sand grains (Van Houten, 1968; Pettijohn *et al.*, 1973). According to Walker (1967) and Van Houten (1968) , most of the diagenetic hematite in sandstones owes its origin to *in situ* alteration of iron-rich minerals in hot, dry regions.

The palaeoenvironment was favourable for terrestrial life, as petrified wood, vertebrate fauna and leaf imprints are abundant in most of these Beaufort rocks. The presence of calcareous concretions is probably due to abundant organic material, such as carcasses (Dickson and Barber, 1976). Although the deposition of sediments in the Harrismith Member apparently took place in a more arid environment than those of the Schoondraai Member, the variation in depositional conditions was most likely small. No major fluctuations in inferred sedimentary processes could be detected, and therefore the transition across the Permian-Triassic boundary was only subject to small palaeoenvironmental variations.

The mineralogy of the clay fraction of the Schoondraai and Harrismith Members shows the presence of quartz, plagioclase and the clay minerals smectite, illite and chlorite. Trends of these minerals seem to be different near the Permian-Triassic boundary (Fig. 18). The reason for these trends is not clear. No potassium feldspar was detected. Illite is derived from continental weathering of micas, directly from solution at low and high temperatures, as well as by the conversion of smectite to illite/smectite during burial (Weaver, 1989). The source of illite is therefore considered to be commonly detrital, and terrestrial. A volcanic source for mudrocks is usually indicated by the presence of smectite (Weaver, 1959; Grim, 1968), cristobalite and laumontite.

No cristobalite, derived from the *in situ* weathering of volcanic ash (McLachlan and Jonker, 1990) and/or laumontite (diagenetic alteration of glassy volcanic debris)(Fuller, 1971; Elliot and Watts, 1974), were present. No volcanic glass shards were observed from the mudrock thin-sections. Glass shards are a definite indicator of volcanic ash (Martini, 1974). However, the shards could have been altered to clay minerals during weathering or burial diagenesis. The absence of these shards does, thus, not indicate without any doubt the absence of a volcanogenic component. Elliot and Watts (1974), Keyser (1983), Keyser and Zawada, (1988) and McLachlan and Jonker (1990) reported the presence of a volcanogenic component in the southeastern, southwestern and northeastern parts of the Beaufort Group in the Karoo basin. It is most unlikely that there exists a connection between volcanism and a global extinction event, but it is believed that acidic volcanic ash might have been the source of silica for silicification of the fossil tree trunks.The clay mineral smectite is present in the samples studied. This can indicate a volcanogenic component. However, the co-existence of plagioclase and smectite complicates the inference of a volcanic source. Smectite is stable diagenetically up to 100°C (Burst, 1959; Weaver, 1959; Dunoyer de Segonzac, 1969; Muffler and White, 1969; Browne and Ellis, 1970; Iijima, 1970; Perry and Hower, 1970; Van Moort, 1971 and Weaver and Beck, 1971). Plagioclase forms at a diagenetic temperature above 100°C (Dunoyer de Segonzac, 1970; Velde, 1985). At this temperature smectite will alter to chlorite or mica (Porrenga, 1967; Rex, 1967; Velde, 1985). The smectite in the present samples most probably formed after diagenesis, due to recent weathering in a temperate climate where the drainage was moderately good (Jackson, 1959).

The absence of potassium feldspar, which is stable in an acidic diagenetic environment (Velde, 1985) and the presence of plagioclase, indicates that the diagenetic environment was alkaline. From the clay mineralogy, it is evident that the shaly sediments were not partly volcanic ash layers, but rather detrital, terrestrial sediments.

The geochemistry of the major elements and trace elements also contributes to a more meaningful interpretation of the sedimentary rocks. The mudrocks of both the Schoondraai and the Harrismith Members are relatively consistent in chemical composition. The source rocks, as well as the depositional conditions would thus

probably have been the same for both members. This is consistent with the palaeoenvironment inferred from the sedimentary lithofacies. In spite of the colour difference of the two members, no abrupt change in the lithofacies occurred. Although SiO_2, Al_2O_3, TiO_2, CaO, K_2O and Na_2O show a slight enrichment, and MgO and Fe_2O_3 a slight depletion across the Permian-Triassic boundary, this observation is unlikely to reflect unusual or catastrophic conditions. The TiO_2/Al_2O_3 ratios for both the Schoondraai Member and the Harrismith Member show that the mudrocks are not altered volcanic ash layers, but ordinary or "typical shales" (Spears and Kanaris-Sotiriou, 1979). This is also consistent with the low energy, suspension settling depositional palaeoenvironment proposed for the mudrocks of both members. The trends observed in the clay mineralogy fraction near the Permian-Triassic boundary (Fig. 18) are not confirmed by the geochemical data.

The inferred weathering conditions of the mudrocks, reflected by the CIA, fall well within the range of "average shales" (Nesbitt and Young, 1982). The interpretation of the sedimentary profiles of the *Dicynodon - Theriognathus* Assemblage Zone (Schoondraai Member) and the *Lystrosaurus - Procolophon* Assemblage Zone (Harrismith Member), indicates a probable decline in energy levels upwards in the succession. The CIA-values of the corresponding samples show an increase of values from base to top. This information could be interpreted in the following way. As the energy levels declined, the exposure time of each mudrock lithofacies to synsedimentary weathering increased. In other words, each mudrock lithofacies weathered more than the one it succeeded. Nesbitt and Young (1982) also suggested that a decline in CIA-values indicated a cooling climatic trend. The CIA-values from the study area increase from the base to the top of the succession. These data could therefore suggest that the climatic trend was one of warming. The Cr/Zr ratios suggest granitic source rocks, with few or no contributions from ultramafic rocks, according to Wronkiewicz and Condie (1987). Palaeosalinity indicators such as the Rb/K ratios gave values that are difficult to interpret. The results point provisionally to a terrestrial palaeoenvironment rather than a marine one. From the sedimentological data no evidence of tidal activity, typically associated with marine sequences, was seen. The feldspathic sandstones are also atypical of a marine environment, unless the latter is situated in close proximity to a granitic source area. The observed fluctuation of energy levels in both members gave rise to a change in facies (mudrocks and sandstones), which is also more

gave rise to a change in facies (mudrocks and sandstones), which is also more typical of a terrestrial setting (McGowen *et al.*, 1979).

The macroscopic and microscopic study of the petrified wood gave useful information regarding the taxonomy, inferred palaeoclimatic conditions as well as the petrifying mineral. The fossil woods were all of the class Gymnospermae. No wood belonging to the class Angiospermae was found in the sedimentary rocks of the Beaufort Group in the study area. The reason for this is that the first evidence for flowering plants (angiosperm) only appears in the Lower Cretaceous (Doyle and Hickey, 1976; Hughes, 1976; Hickey and Doyle, 1977; Hughes, 1977; Doyle, 1978). Diversification of angiosperms in the Cretaceous occurred in a geologically short time. The petrified wood from both the Harrismith and Senekal areas was found in fine-grained sandstone or in *in situ* weathered soil. No wood was found in the mudrocks, except for some *in situ* petrified logs, of which the roots were embedded in a mudrock layer. Thin layers of interbedded mudrock and fine-grained sandstone occur around the tree trunks. This can be another indication of fluctuation in energy levels and therefore a probable seasonal control. The following is proposed as an explanation of this phenomenon. The trees grew on the flood-plains in clayey-muddy soil. With sudden floods, the tree trunks were transported by the water together with the fluvial channel sediments. When the energy level of the water decreased due to a decrease in the channel depth, the wood and the sediment were deposited. The trunks in the Senekal district are orientated in a northwest-southeast direction, indicating the direction of transport. The trunks were quickly covered by fine sediments, thereby preventing decay of the organic material. The environment was favourable for petrification and some of the trunks were preserved. The sediment was then lithified together with the trunks.

The presence of growth rings in all the specimens indicates a pronounced seasonality. Studies of the growth rings show that most of the mean sensitivity values of the specimens plot near the arbitrary value of 0.3, which indicates, that for most of the seasons, the climatic factors were limiting, but some seasons with favourable climatic factors also existed. The presence of very wide rings from both assemblage zones indicates that the growth rates of the trees were fast.
The observation that the ring-width of the *Dicynodon lacerticaps - Theriognathus* Assemblage Zone - woods are almost twice the width of the *Lystrosaurus* -

Procolophon Assemblage Zone - woods, indicates that the growth rates of the trees of the former zone were twice as fast. This can be interpreted as a possible gradual change or deterioration in climatic conditions from Late Permian to Early Triassic times (across the Permian-Triassic boundary). This can however not be proven without doubt.

The mineralogy of the petrified wood can also be linked to the Late-Permian and Early-Triassic palaeoenvironment. The petrifying mineral in all the petrified wood specimens is silica, but relatively high concentrations of zinc and iron also occur. In the *Dicynodon - Theriognathus* Assemblage Zone, the concentration of iron is low, but it increases significantly upwards in the succession into the *Lystrosaurus - Procolophon* Assemblage Zone (thus across the Permian-Triassic boundary). The oxidation of the iron was brought about by a palaeoenvironment that became more arid in time.

Change of life at the Permian-Triassic boundary was caused by a very hot climate at that time. The development of such changes over a considerable period of time is an important argument against an extra-terrestrial catastrophic event.

CHAPTER 5. SUMMARY AND CONCLUSIONS

Sedimentary rocks as well as the petrified wood across the Permian-Triassic boundary (situated in the Beaufort Group, Karoo Supergroup, South Africa), were studied. The information derived from these rocks and the petrified wood was used to give an indication of the palaeoenvironment in Late Permian - Early Triassic times, when a major mass extinction is thought to have occurred.

The timing and pattern of extinction, as studied by several workers, combined with the results from the present sedimentary studies, including petrography, clay mineralogy and geochemistry, and the fossil wood investigations, rule out the possibility of a catastrophic cause. There is evidence of volcanic activity in the Karoo basin, but the size and nature thereof was insufficient to cause a high level of terrestrial extinction.
The results of this study point to a gradual and not an abrupt change across the Permian-Triassic boundary, although small differences do occur. The palaeoclimatic information obtained from the growth rings of the petrified wood shows that the climate gradually became more arid. No major growth ring disruptions, which could indicate a sudden change in growing and climatic conditions, were observed. Permian-Triassic extinction may have resulted from several interrelated events, where climatic change was the driving force.

All these data indicate that the Permian-Triassic mass extinction was probably caused by a **gradual change** of the palaeoclimate, rather than an abrupt change due to volcanic activity or an asteroid impact.

CHAPTER 6. ACKNOWLEDGEMENTS

I wish to thank the Council for Geoscience for financial support.
I am grateful to Mr. Marco Claasen and the South African Society for Amateur Palaeontologists (SASAP) for their help in the sample collection.
Thanks are also due to the Palaeontological Section of the Council for Geoscience for their help and support.
I thank the following persons from the Council for Geoscience for their analytical and technical assistance: Mr. J.H. Elsenbroek, Mr. J.F. Bednarik, Mr. M Cloete, Mrs. H.C.C. Cloete, Mr. C.F. Janse van Vuuren, Dr. D. Bühmann, Mrs. M.T. Atanasova, Mrs. E. Hattingh, Mr. M.D. Kohler and Dr. D. de Bruin.
Dr. R.J. Hart of the Schonland Research Centre for Nuclear Physics, University of the Witwatersrand, for guidance and help with the platinum group element analyses.
Dr. M.K. Bamford of the Bernard Price Institute for Palaeontology, University of the Witwatersrand for help with the description of the fossil wood.
Valuable criticism and guidance were supplied by Professor C.P. Snyman and Professor P.G. Eriksson of the Geology Department, University of Pretoria and Dr. D. Bühmann of the Council for Geoscience.
Last, but not least, I thank my friends and family, especially my husband Derik, for their love and support throughout this study.

REFERENCES

Alekseev, A.S., Barsukova, L.D., Kolesov, G.M., Nazarov. M.A. and Grigoryan, A.G. (1983). The Permian-Triassic boundary event: geochemical investigation of the Transcaucasia section (abstract). *Lunar Planet. Sci.* ***14****, p. 3-4.*

Allen, J.R.L. (1963). The classification of cross-stratified units, with notes on their origin. *Sedimentology,* ***2****, p. 93-114.*

Alvarez, L.W., Alvarez, W., Asaro, F. and Michel, H.V. (1980). Extraterrestrial cause for the Cretaceous-Tertiary extinction. *Science* ***208****, p. 1905-1108.*

Arnold, C.A. (1947). *An introduction to palaeobotany.* McGraw-Hill Book Company, Inc. 433pp.

Asaro, F., Alvarez, L.W., Alvarez, W. and Michel, H.V. (1982). Geochemical anomalies near the Eocene/Oligocene and Permian/Triassic boundaries. *Geol. Soc. Am., Spec. Pap.* ***190****, p. 517-528.*

Bamford, M.K. and De Wit, M.C.J. (1993). Taxonomic description of fossil wood from Cainozoic Sak river terraces, near Brandvlei, Bushmanland, South Africa. *Palaeont. afr.,* ***30****, p. 71-80.*

Bars, H. (1973). *Structure and stratigraphy of an area south of Memel (O.F.S).* Soekor internal report. Open file no. 1973-0096, Geological Survey of South Africa 7pp.

Bars, H. and Guillebert, P. (1976). *Geological investigation of the Vrede-Memel-Volksrust area.* Soekor internal report. Open file no. 1976-0099, Geological Survey of South Africa 12pp.

Bars, H. and Roux, H. (1972). *Report on the geological investigations in the Verkykerskop South area, district Harrismith (O.F.S.).* Soekor internal report. Open file no. 1971-0108, Geological Survey of South Africa 16pp.

Bassham, J.H. (1971). Photosynthetic carbon metabolism. *Proc. Natl. Acad. Sci. USA.,* ***68****, p. 2877-2882.*

Berner, R.A. (1968a). Calcium carbonate concretion formed by the decomposition of organic matter. *Science* ***159****, p. 195-197.*

Berner, R.A. (1968b). Chemical changes affecting dissolved calcium during the bacterial decomposition of fish and clams in sea water. *Mar. Geol.* ***7****, p. 253-274.*

Berner, R.A. (1983). Sedimentary pyrite formation: An update. *Geochim. Cosmochim Acta, **48**, p. 605-615.*

Berner, R.A. and Raiswell, R. (1983). Burial of organic carbon and pyrite sulfur in sediments over Phanerozoic time: a new theory. *Geochim. Cosmochim Acta, **47**, p. 855-862.*

Blatt, H., Middleton G. and Murray, R. (1972). *Origin of sedimentary rocks.* Prentice-Hall, Inc., Englewood Cliffs, New Jersey. 634pp.

Botha, B.J. and Visser, J.N.J. (1970). Fossielboomstamme in die distrik Senekal. *Tydskr. Natuurwet., **10** (3), p. 201-212.*

Bowles,J.F.W. (1986). The development of platinum-group minerals in laterites. *Econ. Geol. **81**, p. 1278-1285.*

Brown, G. (1961). *The X-ray identification and crystal structures of clay minerals.* Mineralog. Soc. London, 544pp.

Browne, D.R.L. and Ellis, A.J. (1970). The Ohaki-Broadlands hydrothermal area, New Zealand: mineralogy and related geochemistry. *Amer. J. Sci. **269**, p. 97-131.*

Brush, L.M., Jr. (1965). Sediment sorting in alluvial channels, p. 25-33. In Middleton, G.V., Ed., *Primary sedimentary structures and their hydrodynamic interpretetion. Soc. Econ. Palaeontologists and Mineralogists, Spec. Pub. 12.*

Bühmann, D., Bühmann, C. and Von Brunn, V. (1989). Glaciogenic banded phosphorites from Permian sedimentary rocks. *Econ. Geol., **84**, p. 741-750*.

Burst, J.F. (1959). Postdiagenetic clay mineral environmental relationships in the Gulf Coast Eocene. *Clays Clay Min. **6**, p. 327-341.*

Cadle, A.B. and Proedrou, P. (1975). *A structural investigation of the Warden North area.* Soekor internal report. Open file no. 1975-0088, Geological Survey of South Africa 13pp.

Campbell, F.A. and Williams, G.D. (1965). Chemical composition of shales of the Mannville Group (Lower Cretaceous) of central Alberta, Canada. *Am. Assoc. Petrol. Geol., **49**, p. 81-87.*

Chaloner, W.G. and Creber G.T. (1973). Growth rings in fossil woods as evidence of past climates p.425-437. In Tarling, D.H. and Runcorn, S.K. (eds.) *Implications of continental drift to the earth science.* Academic Press, London.

Cheng, Z.W. (1980). Permo-Triassic continental deposits and vertebrate faunas of China. *In 5th International Gondwana Symposium, Wellington, New Zealand. p. 65-69.*

Clark, D.L., Wang, C., Orth, C.J. and Gilmore, J.S. (1986). Conodont survival and low iridium abundances across the Permian-Triassic boundary in South China. *Science **233**, p. 984-986.*

Clemens, W.A., Archibald, J.D. and Hickey, L.J. (1981). Out with a whimper not a bang. *Paleobiology **7**(3), p. 293-298.*

Cody, R.D. (1971). Adsorption and the reliability of trace elements as environmental indicators for shales. *J. Sedim. Petrol., **41**, p. 461-471.*

Conaghan, P.J. and Jones, J.G. (1975). The Hawkesbury Sandstone and the Brahmaputra: a depositional model for continental sheet sandstones. *J. Geol. Soc. Austr., **22**, p. 275-283.*

Cox, C.B. (1967). Changes in terrestrial vertebrate faunas during the Mesozoic. *In* W.B. Harland *et al*. (Eds). *The Fossil Record.* Geol. Soc., London, p. 77-89.

Creber, G.T. (1977). Tree rings: a natural data storage system. *Biol. Rev. **52**, p. 349-383.*

Creber, G.T. and Chaloner W.G. (1984). Climatic indications from growth rings in fossil woods p. 49-77. *In* Brenchley, P.J.(ed.) *Fossils and climate.* John Wiley, Chichester.

Crocket, J.H. and Kuo, H.Y. (1979). Sources of gold, palladium and iridium in deep-sea sediments. *Geochim. Cosmochim. Acta, **43**, p. 831-842.*

Crocket, J.H., MacDougall, J.D. and Harriss, R.C. (1973). Gold, palladium and iridium in marine sediments. *Geochim. Cosmochim. Acta, **37**, p. 2547-2556.*

Czaky, A.V and Wachsmuth, W. (1971). *Stratigraphy and hydrocarbon potential of the Dwyka, Ecca and Beaufort Groups in the Northern Karoo.* Soekor internal report. Open file no. 1977-0099, Geological Survey of South Africa 129pp.

Dapples, E.C. (1967). Diagenesis of sediments. In: G. Larson and G.V. Chilingar (Eds.), *Diagenesis of Sandstones.* Elsevier, Amsterdam.

Degens, E.T., Williams, E.G. and Keith, M.L. (1957). Environmental studies of Carboniferous sediments. Part I: Geochemical criteria for differentiating marine from fresh-water shales. *Am. Assoc. Petrol. Geol. Bull.,* ***41,*** *p. 2427-2455.*

Deines, P. (1980). The isotopic composition of reduced organic carbon. *In* Fritz, P. and Fontes, J.C. (Eds.), *Handbook of environmental isotope geology* (Vol. 1, part A). Amsterdam: Elsevier.

Denne, M.P. (1976). Effects of environmental change on wood production and wood structure in *Picea sitchensis* seedlings. *Ann. Bot., N.S.* ***40,*** *p. 1017-1028.*

Dickins, J.M. (1983). Permian to Triassic changes in life. *Mem. Ass. Australas. Palaeontols* ***1,*** *p. 297-303.*

Dickson, J.A.D and Barber, C. (1976). Petrography, chemistry and origin of early diagenetic concretions in the Lower Carboniferous of the Isle of Man. *Sedimentology,* ***23,*** *p. 189-211.*

Dott, R.H. (1964). Wacke, graywacke and matrix -what approach to immature sandstone classification? *J. Sed. Petrology vol.* ***34,*** *p. 625-632.*

Dunoyer de Segonzac, G. (1969). Les minéraux argileux dans la diagenèse. Passage au métamorphisme. *Mém. Serv. Carte Géol. Als. -Lorr.,* ***29,*** *320pp.*

Dunoyer de Segonzac, G. (1970). The transformation of clay minerals during diagenesis and low-grade metamorphism: A review. *Sedimentology,* ***15,*** *p. 281-346.*

Ehleringer, J.R., Sage, R.F., Flanagan, L.B. and Pearcy, R.W. (1991). Climate change and the evolution of C^4 photosynthesis. *Trends in Ecol. and Evoln.,* ***6,*** *no. 3, p. 95-99.*

Elliot, D.H. and Watts, D.R. (1974). The Nature and origin of volcaniclastic material in some Karroo and Beacon rocks. *Trans. Geol. Soc. S. Afr. 77(2), p. 109-111.*

Erasmus, T. (1976a). On the anatomy of *Dadoxylon arberi* Seward with some remarks on the phylogenetical tendencies of its tracheid pits. *Palaeont. afr.,* ***19,*** *p. 127-133.*

Erasmus, T. (1976b). A new species of *Dammaroxylon* Schultze-Motel, *D. natalense* sp. nov. from the Cretaceous of Natal, South Africa. *Palaeont. afr.,* ***19,*** *p. 135-139.*

Esau, K. (1977). *Anatomy of seed Plants.* Second edition. John Wiley & Sons, Inc. 550pp.

Faure, K. (1993). *Mineralogy and geochemistry of the carbonaceous mudstones, and coal petrogenesis of the Grootegeluk Formation in the Waterberg Coalfield, South Africa.* PhD thesis (unpubl.) Univ. of Cape Town, 208pp.

Fenner, F.D. and Presley, B.J. (1984). Iridium in Mississippi River suspended matter and Gulf of Mexico sediment. *Nature **312**, p. 260-262.*

Francis, J.E. (1986). Growth rings in Cretaceous and Tertiary wood from Antarctica and their palaeoclimatic implications. *Palaeontology, **29**(4), p. 665-684.*

Fritts, H.C. (1966). Growth rings of trees: their correlation with climate. *Science **154**, p. 973-979.*

Fritts, H.C. (1976). *Tree rings and climate.* Academic Press, London, 576pp.

Fuller, A.O. (1970). The occurrence of laumontite in strata of the Karroo System, South Africa. p. 455-456. *In Second Gondwana Symposium, South Africa, 1970. Proceedings and papers.*

Galimov, E.M., Girin, V.P. and Vernadskiy, V.I. (1968). Variations in the isotopic composition of carbon during the formation of carbonate concretions. *Geochem. Int. **5**, p. 178-182.*

Ganapathy, R. (1980). A major meteorite impact on earth 65 million years ago: Evidence from the Cretaceous-Tertiary boundary clay. *Science **209**, p. 921-923.*

Goldschmidt, V.M. and Peters, D. (1932). Zur Geochemie des Bors, Teil I and II. *Nachr. Ges. Wiss. Gottingen, Math. Physik. **K1**, p. 402-407, 528-545.*

Gould, S.J. (1977). *Ever since Darwin - reflections in natural history.* Penguin Group, p. 134-138.

Gould, S.J. (1983). *Hen's teeth and horses toes - further reflections in natural history.* Penguin Books, p. 320-331.

Greguss, P. (1955). *Identification of living Gymnosperms on the basis of Xylotomy.* Budapest: Akadémiai Kiadó.

Greguss, P. (1967). *Fossil gymnosperm woods in Hungary from the Permian to the Pliocene.* Budapest: Akadémiai Kiadó, 136pp.

Grim, R.E. (1968). *Clay mineralogy, 2nd Ed.* McGraw-Hill, New York, 560pp.

Groenewald, G.H. (1984). *Stratigrafie en sedimentologie van die groep Beaufort in die Noordoos-Vrystaat.* M.Sc-thesis (ongepubl.) Rand Afrikaanse Universiteit 174pp.

Groenewald, G.H. (1990). Gebruik van paleontologie in litostratigrafiese korrelasie in die Beaufort Groep, Karoo Opeenvolging van Suid-Afrika. *Palaeontology africana* ***27****, p. 21-30.*

Harms, J.C. and Fahnestock, R.K. (1965). Stratification bedforms and flow phenomena (with an example from the Rio Grande), p. 84-115. *In* Middleton, G.V., Ed., *Primary sedimentary structures and their hydrodynamic interpretetion. Soc. Econ. Palaeontologists and Mineralogists, Spec. Pub. 12.*

Harms, J.C., Southard, J.B., Spearing, D.R. and Walker, R.G. (1975). Depositional environments as interpreted from primary sedimentary structures and stratification sequences. *Soc. Econ. Palaeontologists and Mineralogists, Short Course 2,* 159pp.

Harriss, R.C., Crocket, J.H. and Stainton, M. (1968). Palladium, iridium and gold in deep-sea manganese nodules. *Geochim. Cosmochim Acta,* ***32****, p. 1049-1056.*

Heinrich, K.F.J. (1986). Mass absorbtion coefficients for electronprobe microanalysis. *Proc 11th Int. Congress on X-ray Optics and Microanalysis, London, Canada. J.B. Brown and R.H. Packwood (eds)., p. 67-119.*

Hickey, L.J. (1981). Land plant evidence compatible with gradual, not catastrophic, change at the end of the Cretaceous. *Nature* ***292****, p. 529-531.*

Hiller, N. and Stavrakis, N. (1984). Permo-triassic fluvial systems in the southeastern Karoo Basin, South Africa. *Palaeogeography, Palaeoclimatology and Palaeoecology* ***45****, p. 1-21.*

Hobday, D.K. (1973). Middle Ecca deltaic deposits in the Muden-Tugela Ferry area of Natal. *Trans. geol. Soc. S. Afr.,* ***76****, p. 309-318.*

Hobday, D.K., Tavener-Smith, R. and Greenshields, H.D. (1978). A major fluviatile complex in the Middle Beaufort of the Transkei, southern Africa. *4th Gondwana Symp., India, Proc. and Pap.*

Hodgson, W.A. (1966). Carbon and isotope ratios in diagenetic carbonates from marine sediments. *Geochim. Cosmochim. Acta,* ***30****, p. 1223-1233.*

Hoefs, J. (1970). Kohlenstoff- und Sauerstoff-Isotopenuntersuchungen an Karbonatkonkretionen und umgebenden Gestein. *Contr. Miner. Petrol.**27,** p. 66-79.*

Hoefs, J. (1987). *Stable isotope geochemistry.* Berlin: Springer-Verlag.

Horstman, E.L. (1957). The distribution of lithium, rubidium and caesium in igneous and sedimentary rocks. *Geochim. Cosmochim. Acta, **12**, p. 1-28.*

Ho Tun, E. (1979). Volcanoclastic material in Lower Beaufort Group, Karoo Rocks. *Geocongr. 79, Geol. Soc. S. Afr., p. 197-199.*

Iijima, A. (1970). Present day zeolitic diagenesis of the Neogene geosynclinal deposits in the Niigata Oil field, Japan. *Amer. Chem. Soc. 2nd Int. Zeolite Conf., p. 540-546.*

Jackson, M.L. (1959). Frequency distribution of clay minerals in major soil groups as related to factors of soil formation. *Clays Clay Min., **6**, p. 133-143.*

Johnson, M.R. and Keyser A.W. (1976). *Explanatory notes on Geological Map 3226, King William's Town.* Sheet, 1:250 000 Geological Series, Goverment Printer, Pretoria.

Joint Committee on Powder Diffraction Standards. (1986). *Mineral powder diffraction file data book.* International Centre for diffraction data, Swarthmore, USA, 1390pp.

Keays, R.R., Gostin, V.A. and Wallace, M.W. (1981). Mobilization of platinum metals by diagenetic fluids along the lake Acraman meteorite ejecta horizon, South Australia (abs). *Internat. Platinum Symposium, 3rd, Pretoria, Abstracts, p. 49.*

Keyser, A.W. (1979). A Review of the biostratigraphy of the Beaufort Group in the Karoo basin of South Africa. *In Geocongres 1979 Abstr. Part 2, Geol. Soc. S. Afr., Johannesburg. p. 13-29.*

Keyser, N. (1983). *The geology of areas 2728A, C and D in the north-eastern Orange Free State.* Unpubl. rep. Geological Survey of South Africa, 14pp.

Keyser, N. and Zawada, P.K. (1988). Two occurrences of ash-flow tuff from the lower Beaufort Group in the Heilbron-Frankfort area, northern Orange Free State. *S. Afr. J. Geol., **91**(4), p. 502-521.*

Kitching, J.W. (1970). A Short Review of the Beaufort zoning in South Africa. *Proc. 2nd Gondwana Symp., S. Afr., p. 309- 312.*

Koeberl, C. (1989). Iridium enrichment in volcanic dust from the blue ice fields, Antartica, and possible relevance to the K/T boundary event. *Earth Planet. Sci. Lett.* ***92****, p. 317-322.*

Krausel, R. (1919). Die fossile Koniferen-Höizer. (Unter Ausschluss von *Araucarioxylon* Kraus). *Palaeontographica,* ***62****, p. 185-285.*

Kyte, F.T., Zhou, Z. and Wason, J.T. (1980). Siderophile enriched sediments from the Cretaceous-Tertiary boundary. *Nature* ***288****, p. 651-656.*

Larson, P.R. (1964). Some indirect effect on wood formation. p. 345-365. *In* Zimmerman, M.H. (ed). *The Formation of wood in forest trees.* Academic Press, New York.

Lepekhina, V.G. and Yatsenko-Khmelevsky, A.A. (1966). Classification and nomenclature of woods of Palaeozoic pycnoxylic plants. *Taxon,* ***15****(2), p. 66-70.*

Lock, B.E. and Johnson, M.R. (1975). Discussion on "The nature and origin of volcaniclastic material in some Karroo and Beacon rocks". *Trans. Geol. Soc. S. Afr.,* ***78****, p. 171.*

Martini, J.E.J. (1974). On the presence of ash beds and volcanic fragments in the graywackes of the Karroo System in the southern Cape Province (South Africa). *Trans. Geol. Soc. S. Afr.,* ***77****, p. 113-116.*

Mason, T.R. (1992). Beaufort Group ichnofossils: trace fossils in woody substrates. *Palaeontological Society of Southern Africa, 7th Biennial Conference Abstracts, University of the Witwatersrand, Afr, p. 31.*

Maxwell, W.D. (1992). Permian and Early Triassic extinction of non-marine tetrapods. *Palaeontology,* ***35****(3), p. 571-583.*

McDonald, I. (1993). *The analysis of the platinum-group elements by neutron activation analysis and their behaviour in fire-assay and natural igneous melts in the presence of a carbonaceous volatile phase.* PhD thesis (unpubl.) Univ. of Cape Town, 294 pp.

McLachlan, I.R. and Jonker, J.P. (1990). Tuff beds in the norhtwestern part of the Karoo basin. *S. Afr. J. Geol.* ***93****(2), p.329-338.*

McLaren, D.J. (1970). Presidential adress: time, life and boundaries. *J. Palaeontology* ***44****, p. 801-815.*

McLennan, S.M., Fryer, B.J. and Young, G.M. (1979). Rare earth elements in Huronian (Lower Proterozoic) sedimentary rocks: composition and evolution of the post-Kenoran upper crust. *Geochim. Cosmochim. Acta, **43**, p. 375-388.*

Mountain, B.W. and Wood, S.A. (1988). Solubility and transport of platinum-group elements in hydrothermal solutions: thermodynamic and physical chemical constraints. In: *Geoplatinum 87* (Eds. H.M. Pricard, P.J. Potts, J.F.W. Bowles and S.J. Cribb), Elsevier Scientific Publications, London, p. 57-82.

Muffler, L.J.P. and White, D.E. (1969). Active metamorphism of Upper Cenozoic sediments in the Salton Sea geothermal field and the Salton Trough, Southeastern California. *Geol. Soc. Am. Bull. **80**, p. 157-182.*

Müller-Stoll, W.R. and Mädel, E. (1962). Fossil wood of Monimiaceae and Euphorbiaceae from the Upper Cretaceous Umzamba beds of East Pondoland, Cape Province. *Trans. Geol. Soc. S. Afr. **62**(1), p. 93-104.*

Murata, K.J. (1940). Volcanic ash as a source of silica for the silification of wood. *Am. J. Sci. **238**, p. 586-596.*

Murata, K.J. and Norman, M.B. (1976). An index of crystallinity for quartz. *Am. J. Sci. **276**, p. 1120-1130.*

Naldrett, A.J. and Campbell, I.H. (1982). Physical and chemical constraints on genetic models for komatiite-related Ni-sulphide deposits. In Arndt, N.T. and Nesbitt, E.G. (eds.) *Komatiites.* Geogre Allen and Unwin, London, p. 423-434.

Nesbitt, H.W. and Young, G.M. (1982). Early Proterozoic climates and plate motions inferred from major element chemistry of lutites. *Nature, **299**, p. 715-717.*

Norrish, K. and Hutton, J.T. (1969). An accurate X-ray spectrographic method for the analysis of a wide range of geological samples. *Geochim. Cosmochim. Acta, **33**, p. 431-453.*

Oberthur, T. (1986). Delineation of different mineral facies in the carbon leader reef placer, Carletonville goldfield, Witwatersrand, and their relation to sedimentology and gold distribution. *Extd. Abstr. Geocongress '86, Geol. Soc. S. Afr., p. 161-165.*

Panshin, A.J. and De Zeeuw, C. (1970). *Textbook of wood technology. Volume 1, 3th Ed.* McGraw-Hill Book Company. 705pp.

Perry, E.A. and Hower, J. (1970). Burial diagenesis in Gulf Coast pelitic sediments. *Clays Clay Min.* ***18****, p. 165-178.*

Pettijohn, F.R., Potter, P.E. and Siever, R., (1972). *Sand and sandstone.* Springer-Verlag Berlin, Heidelberg, New York, 618pp.

Plimer, I.R. and Williams, P.A. (1988). New mechanics for the mobilization of the platinum-group elements in the supergene zone. In: *Geoplatinum 87* (Eds. H.M. Pricard, P.J. Potts, J.F.W. Bowles and S.J. Cribb), Elsevier Scientific Publications, London, p. 83-92.

Porrenga, D.H. (1967). *Clay mineralogy ang geochemistry of recent marine sediments in tropical areas.* Thesis, Univ. Amsterdam.

Rampino, M.R. (1982). A non-catastrophist explanation for the iridium anomaly at the Cretaceous/Tertiary boundary. *Geol. Soc. Am. Spec. Pap.* ***190****, p. 455-460.*

Rampino, M.R. and Reynolds, R.C. (1983). Clay mineralogy of the Cretaceous-Tertiary boundary clay. *Science, vol.* ***219,*** p. 495-498.

Raup, D.M. (1979). Size of the Permo-Triassic bottleneck and its evolutionary implications. *Science* ***206****, p. 217-218.*

Raup, D.M. and Sepkoski, J.J. (1982). Mass extinctions in the marine fossil record. *Science* ***215****, p. 1501-1503.*

Reineck, H.E. and Singh, J.B. (1975). *Depositional sedimentary environments.* Springer-Verlag, Berlin, Heidelberg, New York, 439pp.

Rex, R.W. (1967). Authigenic silicates formed from basaltic glass by more than 60 million years contact with sea water, Synvania Guyot Marshall Islands. *Clays Clay Min.,* ***15****, p. 195-203.*

Sass, E. and Kolodny, Y. (1972). Stable isotopes, Chemistry and petrology of carbonate concretions (Mishash Formation, Israel). *Chem. Geol.* ***10****, p. 261-286.*

Scurfield, G. and Segnit, E.R. (1983). Petrification of wood by silica minerals. *Sedimentary Geology,* ***39****, p. 149-167.*

Sieswerda, T.A. (1974). *Geological well completed report of OM 1/73 Northern Karoo.* Soekor internal report. Open file no. 1973-0105, Geological Survey of South Africa 19pp.

Simons, D.B., Richardson, E.V. and Nordin, C.F., Jr. (1965). Sedimentary structures generated by flow in alluvial channels, p. 34-52. *In* Middleton, G.V., Ed., Primary sedimentary structures and their hydrodynamic interpretation. *Soc. Econ. Palaeontologists and Mineralogists, Spec. Pub. 12.*

Smit, J. and Hertogen, J. (1980). An extraterrestrial event at the Cretaceous/Tertiary boundary. *Nature, **285**, p. 198-200.*

Smith, R.M.H. (1990). Alluvial paleosols and pedofacies sequences in the Permian lower Beaufort of the south-western Karoo Basin, South Africa. *J. of Sedimentary Petrology, **60**, p. 258-276.*

Snyman, J.E.W. (1991). *Groeiringe - Die biologiese sleutel tot die verlede?* Honors project (unpubl.) University of Pretoria 44pp.

South African Committee for Stratigraphy (SACS). (1980). Stratigraphy of South Africa. Part 1 (Comp. L.E. Kent). Lithostratigraphy of the Republic of South Africa, South West Africa/Namibia and the Republics of Bobhuthatswana, Transkei and Venda: *Handb. Geol. Surv. S. Afr., **8**, 690pp.*

Spears, D.A. and Kanaris-Sotiriou, R. (1979). A geochemical and mineralogical investigation of some British and other European tonsteins. *Sedimentology **26**, p. 407-425.*

Stavrakis, N. (1980). Sedimentation of the Katberg Sandstone and adjacent formations in the south-eastern Karoo basin. *Trans. Geol. Soc. S. Afr., **83**, p. 361-374.*

Steele, T.W., Levin, J. and Copelowitz, I. (1975). *The preparation and certification of a precious metal ore.* N.I.M. report 1696, Council for Mineral Technology, Randburg, South Africa, 50pp.

Stein, C.L. (1982). Silica recrystallization in petrified wood. *J. of Sedimentary Petrology, **52**(4), p. 1277-1282.*

Sun, Y., Chai, Z., Ma, S., Mao, X., Xu, D., Zhang, Q., Yang, Z., Sheng, J., Chen, C., Rui, L., Liang, X., Zhao, J. and He, J. (1984). The discovery of iridium anomaly in the Permian-Triassic boundary clay in Chingxing, Zhejiang, China and its significance, *In Contributions to 27th Int. Geol. Congr., G. Tu, Ed., Science Press, Beijing, p. 235-245.*

Tan, F.C. and Hudson, J.D. (1974). Isotopic studies on the palaeoecology and diagenesis of the Great Estuarine Series (Jurassic of Scotland.). *Scott. J. Geol.* ***10****, p. 91-128.*

Theron, J.C. (1973). Sedimentological evidence for the extension of the African Continent southwards during Late Permian - Early Triassic times. *3rd Gondwana Symp., Canberra, Australia, p. 61-77.*

Tieszen, L.J. (1991). Natural variations in the carbon isotope values in plants. Implications for archaeology, ecology, and paleoecology. *J. of Archaeological Sci.,* ***18****, p. 227-248.*

Tredoux, M., De Wit, M.J., Hart, R.J., Lindsay, N.M., Verhagen, B. and Sellschop, J.P.F. (1989). Chemostratigraphy across the Cretaceous-Tertiary boundary and a critical assessment of the iridium anomaly. *J. of Geology, vol.* ***97****, p. 585-605.*

Tredoux, M. (1990). *The platinum group elements: Nuclear methods for their analysis and their behaviour in terrestrial rocks and meteorites.* PhD. thesis (unpubl.) University of the Witwatersrand.

Turner, J.R. (1977). *Palaeoenvironmental study of the lower Beaufort in the northeast Karoo Basin.* M.Sc-thesis (unpubl.) University of Natal 138pp.

Van Houten, F.B. (1968). Iron oxides in red beds. *Geol. Soc. Am. Bull.* ***79****, p. 399-416.*

Van Moort, J.C. (1971). A comparative study of the diagenetic alteration of clay minerals in Mesozoic shales from Louisiana, U.S.A. *Clays Clay Min.,* ***19****, p. 1-20.*

Velde, B. (1985). *Clay minerals: A physico-chemical explanation of their occurrence.* Developments in sedimentology 40. Elsevier Science Publishers B.V. 427pp.

Velde, B. and Bystrom-Bruzewitz, A.M. (1972). Transformation of natural clay minerals at elevated temperatures and pressures. *Geol. For. Forsh.,* ***94****, p. 450-458.1*

Walker, T.R. (1967). Formation of red beds in modern and ancient deserts. *Geol. Soc. Am. Bull.* ***78****, p. 353-368.*

Walton, J. (1925). On some South African fossil woods. *Ann. S. Afr. Mus.,* ***22****, p. 1-24.*

Warren, E. (1912). On some specimens of fossil wood in the Natal Museum. *Ann. Natal Mus.,* ***2/3****, p. 345-480.*

Weaver, C.E. (1959). The clay petrology of sediments. *Clays Clay Min.,* ***6****, p. 154-187.*

Weaver, C.E. (1989). *Clays, Muds, and Shales.* Developments in sedimentology 44. Elsevier Science Publishers B.V. 819pp.

Weaver, C.E. and Beck, K.C. (1971). Clay-water diagenesis during burial: how much mud becomes gneiss. *Geol. Soc. Am. Spes. Pap., **134**, 155pp.*

Wedepohl, K.H. (1978). *Handbook of Geochemistry.* Springer-Verlag, Heidelberg.

Weeks, L.G. (1957). Origin of carbonate concretions in shales, Magdalena Valley, Columbia. *Bull. geol. Soc. Am. **66**, p. 95-102.*

Wronkiewicz, D.J. and Condie, K.C. (1987). Geochemistry of Archean shales from the Witwatersrand Supergroup, South Africa: source-area weathering and provenance. *Geochim. Cosmochim. Acta, **51**, p. 2401-2416.*

Xu, D., Ma, S., Chai, Z., Mao, X., Sun, Y., Zhang, Q. and Yang, Z. (1985). Abundance variation of iridium and trace elements at the Permian/Triassic boundary at Shangsi in China. *Nature **314**, p. 154-156.*

Zangerl, R., Woodland, B.G., Richardson, E.S.Jr. and Zachary, K.L.Hr. (1969). Early diagenetic phenomena in the Fayetteville Black Shale (Mississippian) of Arkansas. *Sedim. Geol. **3**, p. 87-119.*

Zawada, P.K. (1987). Trace elements as possible palaeosalinity indicators of the Ecca and Beaufort Group mudrocks in the southwestern Orange Free State. *S. Afr. J. Geol., **91**(1), p. 18-26.*

Zhou, L. and Kyte, F.T. (1988). The Permian-Triassic boundary event: a geochemical study of three Chinese sections. *Earth and Planetary Letters, **90**, p. 411-421.*

Zoller, W.H., Parrington, J.R. and Phelan-Kotra, J.M. (1983). Iridium enrichment in airborne particles from Kilauea volcano, January 1983. *Science, **222**, p. 1118-1121.*